

Response to reviewers: Quantification of the Greenland ice sheet contribution to Last Interglacial sea-level rise

Firstly, many thanks to the editor for the handling of this manuscript, and the two reviewers Patrick Applegate and Alex Robinson, for their detailed constructive comments and suggestions on our paper: “Quantification of the Greenland ice sheet contribution to Last Interglacial sea-level rise.” We have addressed all their comments, and the following pages detail our responses. Where significant modifications/insertions are made to the text, line numbers refer to the tracked changes version of the original manuscript attached at the bottom of this response.

The main changes made to the paper in response to the specific comments are as follows:

- 1) An enhanced discussion on the implications from non-equilibration of the climate model.
- 2) An explanation of the statistical methodology used and the criteria of modern day ice volume in calculating the skill-score.
- 3) A section has been inserted on the methods of spinning up the ice-sheet model.
- 4) A discussion has now been included on the implications of using the PDD scheme in the ice sheet model.
- 5) An explanation of the climate-ice sheet model coupling methodology chosen has been included.
- 6) The layout of the paper has been modified and the number of figures reduced by combining various figures.

Response to comments by Reviewer 1, Patrick Applegate:

1) Climate model equilibration

“The authors use a 200-yr period to spin up their GCM. The first 100 yr is based on orbital parameters, greenhouse gas concentrations, and Greenland ice sheet topography appropriate for the preindustrial period (perhaps 1850). The second century of each GCM run is based on conditions appropriate for different times during the Eemian warm period. My concern about this spinup method stems from a recently-published study on GCM equilibration by Brandefelt and Otto-Bliesner (2009, Equilibration and variability in a Last Glacial Maximum climate simulation with CCSM3, Geophysical Research Letters 36, L19712). These authors discovered that an apparently-equilibrated Last Glacial Maximum simulation with the AOGCM CCSM3 was actually far from equilibrium. Their results suggest that about a thousand years of model evaluation was required to reach a “true” equilibrium. The long equilibration time was associated with the response time of the model ocean. The difference in Greenland summit temperatures between the apparently-equilibrated and fully-equilibrated model states is 6-10 deg C. This earlier study suggests that a century of Eemian spinup might not be sufficient to achieve a good climate model state to feed into the ice sheet model, and that the temperature errors involved could be substantial. Naturally, the Eemian is a lot closer to the present-day state than the Last Glacial Maximum, so the errors are likely to be smaller than those noted by Brandefelt and Otto-Bliesner (2009). But, I think some demonstration that the GCM runs really are equilibrated, or that the errors associated with poor equilibration are likely small, is absolutely needed for the paper. One way of partly addressing this concern would be to adjust the y-axes on Figure 3. This figure is clearly important, because it shows the temperature trajectories of the GCM runs, but it doesn’t allow a reader to determine whether the runs have properly equilibrated. A lack of equilibration would be indicated by a consistent, nonzero slope in global mean temperature near the end of the run. Please rescale all the y-axes so that they conform more closely to the y-extent of the temperature results in each panel. In column 1, I suggest using a y-extent of -23 to -20 deg C; in column 2, -22 to -17 degC; and in column 3, -19 to -12 deg C. Also in Figure 3, fit a straight line through the temperature values for the last 30 yr of each climate model run (the part of the run that is actually used for ice sheet model forcing). Plot these lines on the figure, and report the slopes in a table (or on the figure). The authors should also look at the abyssal ocean temperature trajectories, as did Brandefelt and Otto-Bliesner (2009). Including these trajectories in Figure 3, in separate panels, would be most helpful.”

We agree that 100 years is insufficient to fully spin-up the coupled atmosphere-ocean system which takes on the order of >1000 years. However, the simulations show that the multi-year model average trends in near-surface Greenland temperature in response to the changed orbits are close to equilibrium compared with the Greenland

temperature inter-annual variability. It is unlikely that for a 30 year average a best fit line with a slope of zero will be achieved due to decadal variability. However, for information we have included on Figure R1 the best-fit lines requested by the reviewer for the final 30 years of the simulations with the gradient of the slopes also quoted. Note the different y-axis scales.

A similar LIG simulation at 125ka using HadCM3 (see Lunt et al. 2012, CPD) has been run for 500 model years. Below Table R1 illustrates the near-surface Greenland temperature for 30-year average time-slices throughout the 500 years of the simulation. There is no clear trend evident in average Greenland near-surface temperature implying natural variability, and certainly not a 6 to 10°C difference seen by Brandefelt & Otto-Bliesner (2009). Furthermore, in some respect using fully equilibrated climatologies is somewhat artificial since inherently the LIG climate was transient in nature.

70-100 model years	170-200 model years	270-300 model years	370-400 model years	470-500 years
-20.55	-20.76	-20.26	-20.22	-20.0152

Table R1: 30-year averages of Greenland temperature taken at various points in a 500 model year HadCM3 125ka simulation.

However, we do acknowledge the uncertainties introduced in the climate model spin-up time in the text by including (page 11, line 337-342):

“The spin-up time in large-scale atmosphere-ocean models is governed by the slow processes in the deep ocean and is usually on the order of several thousand years. However, due to computational expense this is not easily achievable. As such the ocean component of HadCM3 does not fully represent changes in ocean circulation, but does fully interact thermodynamically with the atmosphere in our modelling framework.”

We have altered the y-axis to conform more closely to the data (-24 to -12°C instead of -26 to -10°C) on Figure 3 but wish to keep the same scale for all panels so it is possible to see the relative difference in Greenland temperature between different ice configurations and time periods. We have also represented the average temperature on Figure 3 for the 30-year forcing used in Glimmer with a horizontal thick black line.

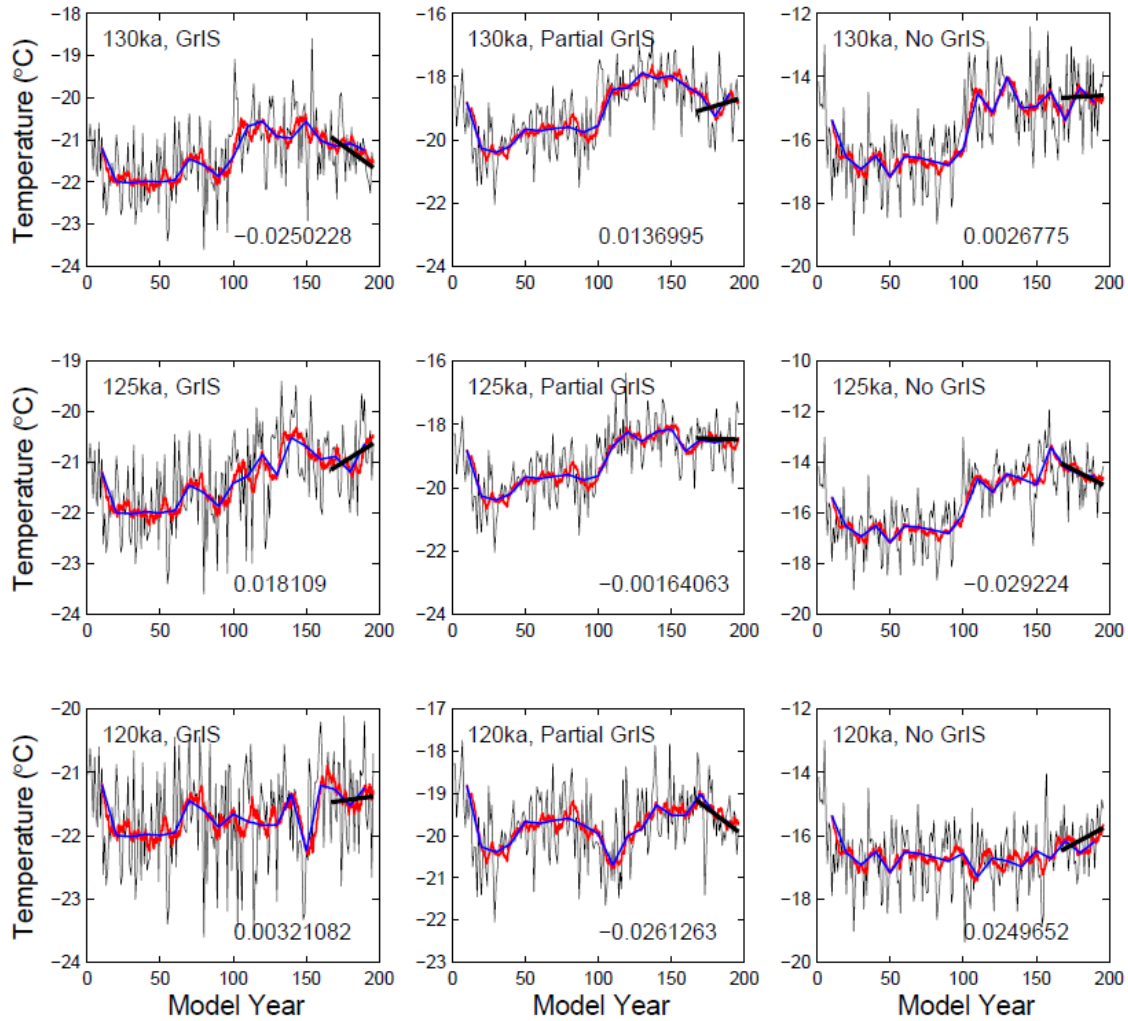


Figure R1: Near-surface Greenland temperature time-series for the three LIG snapshots with a GrIS, partial GrIS and without a GrIS included. The first 100 years represent pre-industrial greenhouse and orbital conditions. The last 100 years are the temperature response to changed orbital parameters. The black line is the annual mean, red line is the 10 year running average and the blue line is the 10 year mean. The thick black line represents the best fit line for the final 30 years of the simulations. The gradient of the slope is also included.

2) Ice sheet model spinup

“Rogozhina et al. (2011), On the long-term memory of the Greenland Ice Sheet, Journal of Geophysical Research 116, F01011) have recently published a study on different ways of spinning up ice sheet models. It is a bit difficult to establish from Rogozhina et al. (2011) what are "right" and "wrong" ways to spin up ice sheet models, but Stone et al. should provide some discussion of the paper and its possible implications for their own results. Figure 4 seems especially relevant in this context; here, Rogozhina et al. (2011) begin their simulation with an equilibration run under constant climate, then apply a time-dependent forcing. This method is at least broadly similar to that used in the present ms. One crucial difference is that Rogozhina et al. (2011) spin up to a glacial state, whereas Stone et al. spin up using interglacial conditions. From my own work, my sense is that ice sheet simulations tend to converge rather quickly during warm periods, regardless of initial state.”

We agree that more discussion on ice sheet spin-up is required and have inserted the following text into the manuscript accordingly (page 12, line 356-372). Note, that we actually spin-up the ice sheet using a GCM derived climatology representing 136ka.

“The correct method of reconstructing the initial state of the GrIS under past climate forcings is unclear but two main methods have been adopted in previous studies: (1) steady state simulations driven by present day or past climatic conditions (Ritz et al.

1997; Stone et al. 2010) and (2) transient simulations driven by palaeoclimatic reconstructions (e.g. Applegate et al. 2012). Each method has its own caveats which have been investigated recently by Rogozhina et al. (2011). For example, they show that initialising from an ice-free state under glacial forcings is not a good choice for ice sheet simulations that start under colder-than-modern conditions. Because it is not practically possible to spin-up an ensemble of coupled HadCM3 ice sheet model configurations for several glacial-interglacial cycles, we use an approach that assumes the ice sheet is in equilibrium at the start of the transient ice sheet model simulations. We adopt a similar methodology to Rogozhina et al. (2011) by initialising from a modern GrIS spun-up with a constant glacial climate forcing from HadCM3 then apply a time-dependent forcing into the interglacial period. We do not use palaeoclimatic reconstructions to obtain an initial state for the GrIS because prior to the onset of the LIG processes occurring in deeper parts of ice cores makes them somewhat unreliable and extending beyond the LIG is, therefore, unrealistic (Grootes et al., 1993; Johnsen et al., 1997).”

3) Statistical methods, bias, and overconfidence

“This study has the laudable goal of making probabilistic estimates of Greenland contributions to Eemian sea level change. Many probabilistic estimates, of any quantity, neglect important factors that make the inferred pdf too narrow (that is, overconfident) and shift it to one side relative to the “true” answer (bias). This study likely has similar problems. The ms needs a fuller accounting of sources of bias and overconfidence in the results, particularly in the abstract, but also in the discussion. Here are some potential sources of bias and uncertainty in the results.

– Eemian summer temperatures from the GCM. If I’m reading section 4 correctly, the simulated Greenland surface temperatures are about 1.5 deg C too cool. In that case, the simulated Greenland contributions will be biased toward too-small values.”

This is not the case because we use an anomaly coupling method and include changes in topographic height in response to changing temperatures. The temperatures quoted in this section refer to those from the GCM simulations where a modern day fixed GrIS is included in the climate model (i.e. not reduced in size). This temperature underestimate compared with palaeo-data indicates that to improve the match between model and data a smaller GrIS is needed. The positive temperature-elevation feedback mechanism can partially compensate for the mismatch. Because we use anomalies the temperature change from the GCM used to force the model occurs because of the insolation change during the LIG. The ice-sheet model then responds to this with the elevation changing accordingly and as a result the surface temperature over the ice sheet changes due to the lapse rate correction. To improve on this further the coupling methodology developed also allows the temperature-albedo feedback in response to a melting ice-sheet to be taken into account. You will see that that Figure 7 shows a better match between modelled temperature and data when ice-sheet changes are taken into account.

The text has been modified to make it clearer that it is the temperatures from the GCM simulation with a modern GrIS included that are compared with data (page 15, line 442-443):

“The GCM simulated annual average global temperature anomaly at 130 ka (*with a modern day fixed GrIS included*)...”

This coupling methodology ensures that the simulated Greenland ice sheets are, therefore, not biased toward too-small contributions to LIG sea-level because the GCM temperatures are too cool when a modern day ice-sheet is fixed in the climate model.

“– The model is naturally imperfect, leading to structural uncertainty. Stone et al. (2012) acknowledge some of these problems very briefly, especially in the discussion. One possibly serious problem is related to a lack of basal sliding in the

ice sheet model. In a previous paper with some of the same authors (Stone et al., 2010, The Cryosphere), the ice sheet was "glued" to its bed. The authors don't mention basal sliding in the present paper, making it hard to determine whether this ensemble has the same problem. If present, this flaw will tend to lead to too-large ice volumes, and maybe to too-small Eemian sea level rise contributions. Please acknowledge the lack of basal sliding, and the fact that other models of the same class do include this process, in the text."

The reviewer is correct that we do not mention basal sliding. We have now included the following (page 7, line 213-223):

"One limitation of the experiments presented here is that they do not include the process of basal sliding which has implications for the amount of ice mass lost dynamically. An increase in the ice velocity, by incorporating the basal sliding velocity, would result in more ice transferred from the accumulation zone to the ablation zone and, therefore, reduce the volume of the ice-sheet under a warm climate. Inclusion of this missing process could lead to a smaller GrIS during the Eemian. Indeed, the study by Parizek and Alley (2004) showed an increase in GrIS sensitivity to various warming scenarios due to surface meltwater lubrication of flow. However, previous studies (Robinson et al. 2011; Ritz et al. 1997) have shown that although the sliding coefficient parameter affects GrIS geometry, it was less significant compared with other parameters in determining the past evolution and present geometry of the modelled GrIS."

"– The use of root-mean-squared error on gridded modern ice thicknesses to evaluate the fidelity of model runs to the modern ice sheet conditions (Eqn. 7) will cause bias and overconfidence, because of spatially autocorrelated residuals due to model structural error. Because of the lack of certain processes in the ice sheet model (e.g., ice streams, basal sliding), the differences between the observed and modeled ice thicknesses in adjacent grid cells will be highly correlated with one another. For example, the real ice sheet has one very large ice stream, but the simulated ones won't, and the ice thicknesses of grid cells over this ice stream will be consistently in error. If this problem isn't accounted for in the choice of objective function, you effectively think you have more information than you have, and the results will be biased (wrong) and overconfident (you'll be very sure about your wrong answer). I would suggest using an aggregate metric, like ice volume, to assess the match to the modern ice sheet."

We have taken the reviewer's points into consideration by modifying Equation 1 such that $n=1$, x is the observed average ice thickness and $f(\theta)$ is the average ensemble member ice thickness over the whole ice-sheet. A plot has been included on Figure 11 to show the probability density functions that result using these two different methods of calculating the skill-score. As one can see from Fig.11e this makes little difference to the overall result. We include a comment in the discussion on sensitivities (page 23, line 697-699):

"In order to test the robustness of our skill-score on the resultant probability density function we modified Eq. 1 such that $n=1$ and used only the average ice-thickness as our metric. Figure 11e shows that this makes very little difference to the probability density function."

"– I don't fully understand how the information from the modern ice volume is being taken into account. I think it would be more standard to define some uncertainty about this modern ice volume estimate and use that to determine which runs are most consistent with the modern ice volume, perhaps using a normal distribution as a weighting function. What is the absolute difference in volume between the estimated modern ice volume and the model realization that produces the smallest ice sheet that is consistent with the Summit/NorthGRIP Eemian ice presence constraint?"

We use the distribution of modern day ice volume to account for the uncertainty caused by over-predicting the ice-sheet size by adjusting the kernel width. The kernel width is varied in the probability density function construction such that the modern-day observation lies within 1, 1.5 and 2 standard deviations of the mean of the modern-day ensemble (see Figure 9).

For information, the absolute difference in ice volume between the estimated modern ice volume and the model realisation that produces the smallest ice sheet is 7.85883×10^5 km³ (1.98 m) and can be seen in Figure 6b.

4) Sea level fingerprinting studies

“The authors cite Bob Kopp’s 2009 study that estimates Eemian sea level change. On p. 866, Kopp et al. write, “The posterior distribution suggests a 95% probability that both Northern Hemisphere ice sheets and Southern Hemisphere ice sheets reached minima at which they were at least 2.5m e.s.l. smaller than today, although not necessarily at the same point in time (Fig. 5, dotted line).” If applied to the present study, this constraint would wipe out about two-thirds of the allowed range of sea level rise contributions identified by Stone et al. At minimum, this point needs to be mentioned in the discussion, if the constraint is not actually included.”

We agree that if this constraint was applied to our study then it would alter our distribution of acceptable ice sheets considerably. Although we have included various palaeo-data to constrain our simulations for the LIG we argue that this is an independent study and we compare our results with Kopp et al. (2009) rather than constrain them with this data. Otherwise we have few results with which to make a comparison.

We have included the Kopp reference in the discussion where we state our GrIS sea-level contribution results without this constraint are lower than many previous estimates (page 26, line 802).

We have also included in Section 4 an additional plot on Figure 11 showing the probability density function that would result if we considered only simulations with a sea-level contribution greater than 2.5 m. The following text has been added (page 26, line 804-808):

“According to the global sea-level estimate for the LIG derived by Kopp et al. (2009) the distribution suggests a 95% probability that the GrIS reached a minimum at which it was at least 2.5 m of equivalent sea-level smaller than today. By including this constraint we show a shift in the probability density function with a peak contribution estimate of 3.2 m closer to the estimate of recent studies (Fig. 11f).”

5) Organization of the paper

“At present, the manuscript is divided into many sections that mix methods and results. This organization makes it difficult to find crucial details. I would prefer to see the classic introduction-methods-results-discussion, with the methods and results sections each divided into ice sheet modeling, climate modeling, and statistical methods subsections. As a side benefit, this reorganization might help make the paper shorter. The number of figures in the paper is very large; could the authors consolidate some figures and cut others? Figures 8 and 11; 10 and 14; and 12 and 13 could be combined.”

We have reorganised the manuscript so that it is the more traditional format of Introduction-Methods-Results-Discussion by reducing the number of sections. We outline the headings and sub-heading below:

1 Introduction

2 Model description and experimental design

2.1 The climate model

2.2 The ice sheet model

2.3 Experimental design and coupling methodology

2.3.1 LIG GCM simulations

2.3.2 Obtaining a 136ka GrIS

2.3.3 Coupling the climate and ice sheet models

3 Results

3.1 The modelled climate of the LIG

3.2 GrIS contribution to the LIG highstand

3.2.1 Probabilistic assessment of GrIS contribution to the LIG highstand
Probabilistic method
Probabilistic results and sensitivities

4 Discussion and conclusions

We have decided to keep the “Probabilistic Method” in Section 3 as some of the decisions made are based on the results obtained with the ice sheet and climate models and it would not be possible to report these results in the earlier methods sections. We have also consolidated the figures as suggested but do not wish to remove any as each one is important and discussed in the text.

6) Comparison to other methods of ice sheet model forcing

“Many other studies have used simple pattern scaling of modern climatology fields to estimate climate forcings for the past. I would be very interested in the authors’ ideas on what errors we should expect to see in Eemian simulations driven by ice core forcings, instead of results from GCMs. This material could easily go into a subsection of the discussion.”

We agree that a comment could be included in the text that reflects the differences that arise between simulations forced with ice core reconstructions compared with results from GCMs. This was actually discussed in a very recent paper by Born et al. (2012). We insert the following text to discuss the differences observed between our results and the previous methodologies citing Born et al. (2012) (page 25-26, line 775-795).

“We observe substantial retreat of the GrIS in the north while the ice sheet remains relatively stable in the south in contrast with many previous studies using a different forcing methodology (e.g. Cuffey & Marshall 2000; Tarasov & Peltier 2003; Lhomme et al. 2005) One fundamental difference between LIG ice sheets derived using climate forcings reconstructed from ice core records (e.g. Letreguilly et al. 1991; Cuffey & Marshall 2000; Lhomme et al. 2005) compared with a GCM is that the forcing fails to capture changes in atmospheric circulation patterns, precipitation changes and the heterogeneity of climate trends over Greenland. This failure to capture these processes is because the method uses the present day temperature pattern which is perturbed by a spatially homogenous anomaly of temperature derived from proxy data reconstructions (e.g. the GRIP ice core record). Precipitation anomalies are simply calculated using a standard relationship where precipitation is a function of temperature. Our method is similar to Born et al. (2012) who partly explain the preferential LIG warming and melting of northern Greenland in their results (which we also observe), but absent from most previous studies, as due to the impact of larger insolation changes in the north of Greenland not adequately captured using the proxy reconstruction forcing methods. Further differences between our study and previous work include the bedrock topography used (e.g. Cuffey & Marshall 2000; Otto-Bliesner et al. 2006), which has been previously shown to considerably affect simulated present day ice volume (Stone et al. 2010), and the use of the PDD scheme compared with a method which takes the impact of insolation on melt into account such as that used by Robinson et al. (2011 (see discussion above).”

Detailed comments

Page 2:

“Lines 1-18: Remove all inline (parenthetical) references from the abstract.”

Done.

“Lines 1-3: perhaps, "During the last interglacial period (130-115 thousand years ago, ka), Arctic climate was warmer than today, and global mean sea level was likely >6 m higher.””

Done.

“Lines 4-6: perhaps, "However, there are large discrepancies in the estimated contributions to this sea level change from various sources (the Greenland and Antarctic ice sheets, and smaller ice caps).””

Done.

“Line 9: what model(s) did you use?”

The text has been changed to include the climate and ice sheet model names (Glimmer and HadCM3) (page 2, line 43-44):

“Here, we determine probabilistically the likely contribution of Greenland ice sheet melt to Last Interglacial sea-level rise, taking into account ice sheet model parametric model uncertainty, by performing an ensemble of 500 Glimmer ice sheet model simulations forced with climatologies from the climate model HadCM3, and constrained by palaeo-data.”

“Line 11: what is meant by "model uncertainty?" do you mean parametric uncertainty (as in Stone et al., 2010, The Cryosphere), model structural uncertainty (differences among models or between models and the real world), stochastic uncertainty in the climate model, or all three?”

This has now been explicitly defined to refer to *ice sheet model* parametric uncertainty. For information, in order to assess the sensitivity of ice sheet model results to the climate model used we compared offline forcing of the ice sheet model with two different 125ka model climatologies (HadCM3 used here and the CCSM3 model). This comparison showed that, compared with the sensitivity to internal parameters (given in Table 1 and outlined in Stone et al. (2010)), the GrIS evolution is insensitive to the climate model used.

“Lines 9-14: change to, "Here, we perform an ensemble... to determine the likely contribution... Our results suggest a 90% probability that this contribution exceeded 3.5 msle...””

This text has been modified as suggested.

“Lines 9-14: your probabilistic estimates are likely to be overconfident and/or biased for one reason or another; mention any important sources of uncertainty or bias that you neglected here.”

We have inserted the following sentence into the abstract (page 2, line 55-57):

“Future work should assess additional uncertainty due to inclusion of basal sliding, the direct effect of insolation on surface melt, and the climate model used.”

“Line 14: can you say something about *why* your results are different? Is it because you used a coupled climate-ice sheet model, and other studies did not?”

We have expanded the following sentence to explain the main difference between this study and previous ones (page 2, line 47-52):

“Our results suggest a 90% probability that Greenland ice melt contributed at least 0.6 m but less than 10% probability it exceeded 3.5 m, a value which is lower than several recent estimates *which did not include a full general circulation climate model that can capture atmospheric circulation and precipitation changes in response to changes in insolation forcing.*”

“Line 20: avoid the use of "since" to mean "because," because "since" also means "after" and is sometimes ambiguous”
This word has been changed to “because”.

Page 3:

Line 9: the word "this" should always be followed by a specific noun; perhaps "this estimated temperature increase"
This text has been modified with the suggestion by the reviewer.

Line 14: should mention which of the Greenland ice cores contain Eemian ice and which do not (see Alley et al., Quaternary Science Reviews, 2010)

The text has been expanded to include the following (page 3, line 82-93):

“On Greenland itself, ice core measurements from the Summit region (NorthGRIP, GRIP and GISP2 ice cores) indicate ice was present during the LIG (Chappellaz et al., 1997; NorthGRIP, 2004; Suwa et al., 2006), with the surface elevation no more than a few hundred metres lower than present day based on the total gas content of the ice (Raynaud et al., 1997). In addition, basal ice from the northwestern ice core, Camp Century, has been proposed to be of LIG age and ice from the bottom section of a core from the Renland peninsula in eastern Greenland is dated older than 130ka (Johnsen et al., 2001) although there is uncertainty in the dating of these two ice cores (Alley et al., 2010). New results from the NEEM ice core project may indicate whether or not basal ice in this location is of LIG age. The dating of basal ice at Dye-3 in southern Greenland, however, remains highly uncertain (Koerner and Fischer, 2002; NorthGRIP, 2004).”

“Line 18-24: based on your abstract, comparison to previous studies is a crucial aspect of your work – please make this a separate paragraph and expand, explaining that some studies are "straight" ice sheet modeling studies (Letreguilly et al., 1991; Ritz et al., 1997; Cuffey and Marshall, 2000; Huybrechts, 2002), others are constrained by additional data (Tarasov and Peltier, 2003; Lhomme et al., 2005), and others are coupled climate-ice sheet modeling studies (you cover this point)”

The text has been changed to reflect this (page 3-4, line 95-103):

“Estimates of the Greenland ice sheet (GrIS) contribution to sea-level rise during the LIG range from 0.4 to 5.5 m based on a wide range of modelling techniques. These include palaeothermometry from ice cores coupled with thermo-dynamical ice sheet models (Huybrechts, 2002; Letréguiilly et al., 1991; Ritz et al., 1997; Cuffey and Marshall, 2000; Tarasov and Peltier, 2003; Lhomme et al., 2005; Greve, 2005) with similar studies also constraining their results by matching model predicted isotopic stratigraphy from ice cores with data (Tarasov and Peltier, 2003; Lhomme et al., 2005). Another method uses coupled climate-ice sheet models of varying complexity (Robinson et al., 2011; Fyke et al., 2011; Otto-Bliesner et al., 2006) to predict LIG Greenland ice-sheet geometry and sea-level contribution.”

“Line 18-24: also mention the 2.5 m lower bound constraint from Kopp et al. (2009), which is independent of ice sheet modeling.”

Please see our response to this comment above.

“Line 25-29: this sentence is extremely long; please break it into several sentences. Also provide some more details here: briefly describe why you chose this approach and what you hoped to learn from applying it.”

We have now expanded this paragraph and broken it down into two sentences (page 4, line 105-112):

“Here we assess the contribution of Greenland ice loss to global sea-level rise, derived from simulations of the LIG global climate and evolution of the GrIS from 130 to 120

ka using the general circulation model (GCM) HadCM3 ‘coupled’ to the ice sheet model Glimmer. We use an efficient offline coupling methodology to account for ice sheet-climate interactions (DeConto and Pollard, 2003) and estimate the range in GrIS contribution to LIG sea-level change by considering ice sheet model uncertainty in order to better understand the GrIS response under a warmer than present climate, critical for the assessment of future climate change.”

Under the methods section we have included an introductory paragraph which gives reasons for the methodological approach undertaken (see text to the reviewer’s comment concerning this below).

“Line 29: "ice sheet climate interactions" should probably be hyphenated: "ice sheet-climate interactions””

This has been changed.

Page 4:

“Section 2, 3...: please subsume the relevant sections into a Methods section, and lead this Methods section with a brief description of the relevant methods and how they help you solve your problem”

Please see our response to the reviewer’s comment about the organisation of the paper above. Sections 2 and 3 have now been combined. We have also inserted the following text at the beginning of the methods section for clarity (page 4, line 115-125):

“Here we outline the models used to estimate the GrIS contribution to LIG sea-level change. Due to computational expense we have developed a method to pseudo-couple our climate model to an ice-sheet model which takes into account the effect of the albedo feedback mechanism without the need to run fully coupled (two-way) climate-ice sheet simulations. We begin by describing the climate and ice sheet models followed by a detailed description of the experimental design and this coupling methodology. An ensemble is performed to take into account parametric uncertainty in the ice sheet model in order to estimate a range in GrIS contribution to LIG sea-level. We use palaeo-data in order to disregard simulations which do not satisfy these robust palaeo-data ice-sheet constraints (see Sect. 3.2). Finally, from the ensemble a probability density distribution of maximum sea-level contribution from the GrIS to LIG sea-level rise is constructed (see Sect. 3.2.1 for details of the probabilistic method).”

“Section 2.1: this section is made up of two very long paragraphs; please break them up and organize according to topic sentences that contain the most important points

– a reader should be able to glean all the important points just from reading the first sentence of each paragraph”

We hope that the reviewer will now find this section clearer as we have reduced the text accordingly with the first sentence describing the main features of the model components (see text below).

“Section 2.1: much of this detail seems unnecessary; can you simply indicate how the model is different from earlier and later versions of the same model and provide a reference?”

We have substantially reduced the text describing the climate model with the first paragraph referring to basic details of the atmosphere and land surface modules. The second paragraph describes briefly the ocean model and sea-ice model components. All include relevant references if the reader wishes to look at further details (page 5-6, line 126-169).

“The GCM simulations described in this paper are carried out using the UK Met Office coupled atmosphere-ocean GCM, HadCM3, version 4.5 (Gordon et al., 2000), which has been used in the third and fourth IPCC assessment reports. The atmosphere component

of HadCM3 is a global grid-point hydrostatic primitive equation model, with a horizontal grid-spacing of 2.5° (latitude) by 3.75° (longitude) and 19 levels in the vertical with a time step of 30 minutes. The performance of the atmosphere component has been shown to agree well with observations (Pope et al., 2000). The land surface scheme (MOSES 2.1) includes representation of the freezing and melting of soil moisture and the formulation of evaporation. Within this land surface scheme ice sheets are prescribed and are fixed.

The resolution of the ocean model is 1.25° by 1.25° with 20 levels in the vertical. The ocean model uses the mixing scheme of Gent and McWilliams (1990) with no explicit horizontal tracer diffusion. The sea-ice model uses a simple thermodynamic scheme and contains parameterisations of ice concentration (Hibler, 1979) and ice drift and leads (Cattle and Crossley, 1995). In simulations of the present-day climate, the ocean model has been shown to simulate sea surface temperatures in good agreement with modern observations, without the need for flux corrections (Gregory and Mitchell, 1997)."

Page 5:

"Section 2.2: for a reader who is not familiar with ice sheet models, this description might be a bit too technical; can you reconfigure this text with a non-ice sheet modeller in mind, or refer to general texts on/introductions to ice sheet modeling?"

We have simplified this section and explained briefly what the Shallow Ice Approximation (SIA) approach is including a discussion on the merits/disadvantages of the SIA (see below). We have also clarified what we mean by the isostatic response of the lithosphere. We feel the discussion on the PDD scheme is understandable so remains.

"A higher-order ice sheet modeler (I am not one) would probably insist on a boilerplate description of the disadvantages of shallow-ice approximation models here. For their benefit, could you include some text on this issue here? Some explanation of why shallow-ice models are still useful would also help. Clearly, one cannot run a full-Stokes model 500 times over thousands of years"

We have addressed this comment by including the following (page 6, line 177-185):

"The principle advantage of using the SIA for modelling the GrIS on palaeo-timescales is that it is computationally cheap allowing large multi-millennial ensembles to be easily performed. Although the method is accurate for the interior of a large ice sheet such as Greenland this is not the case at the margins where streams of fast flowing ice and coupling to ice shelves complicate the ice dynamics such that the SIA is unable to capture the observed changes in ice sheet geometry and velocity occurring on short timescales. The lack of higher order physics has resulted in the majority of ice sheet models overestimating the present day ice sheet volume and extent (e.g. Ritz et al. 1997; Stone et al. 2010; Greve et al. 2011; Robinson et al. 2011)."

"In Stone et al. (2010), the ice sheet model did not include basal sliding; is this process represented in the model version used here? (The string "basal sliding" doesn't seem to be anywhere in the paper.)"

Please see our response to the reviewer's comment about basal sliding above.

Page 6:

"line 25: again, follow "these" with a specific noun"

The word "parameter" has been inserted.

“lines 27 and ff, "Here we generate..." please move this key methodological detail to the first sentence of a paragraph; also, this information seems much more likely to be unfamiliar to a reader than how a climate or ice sheet model works – I would suggest deemphasizing sections 2.1 and 2.2 in favor of providing more detail here”

We disagree that this should be moved. We think it is important to explain first why and what we want to sample then explain what we did rather than the other way around.

We have, however, included more discussion on the method of Latin Hypercube Sampling (page 8, line 239-246):

“Here we generate an ensemble of 500 simulations using the statistical method of Latin Hypercube Sampling (LHS) in order to efficiently sample the five dimensional parameter space. This method generates a distribution of plausible parameter sets within a prescribed set of ranges (McKay et al., 1979) by using a stratified-random procedure where values are sampled from the prescribed distribution of each variable and paired randomly with the other variables assuming that the variables are independent of one another (which is the case here). The LHS distribution is given in Fig. 1. For more details on parameter choices refer to Stone et al. (2010).”

Page 7:

“line 4: "130, 125, and 120 ka:" as you point out in the abstract, the Eemian lasted until about 115 ka; why did you choose not to do a set of runs at 115 ka? I don't insist that you do these runs, but some explanation of this choice would be helpful.”

These time slices were chosen because they cover the timing of peak interglacial warmth, and sea-level highstand during the LIG. A sentence has now been inserted to reflect this (page 9, line 262-263):

“These time slices were chosen because they cover the interval of peak LIG warmth as well as the maximum sea-level highstand (Kopp et al., 2009; Petit et al., 1999; Lisiecki and Raymo, 2005).”

“lines 13-14: see comments on climate model spinup above. Was parametric uncertainty in the GCM considered, or was this source of uncertainty only treated in the ice sheet model?”

Only parametric uncertainty in the ice-sheet model was considered. To run a large ensemble of HadCM3 simulations would be very computationally expensive. However, we note that this is a major area of uncertainty which is discussed in Section 4, paragraph 2, and should be addressed in future work.

line 19, "this:" "this procedure"

Done.

Page 8:

“19, what does "perihelion 2.6 (day of the year)" mean? does this phrase indicate that the perihelion is 2.6* the Julian date?”

This has been reworded. This phrase refers to the fact that perihelion occurs on day 2.6 of the year.

19, "range of climate:" perhaps "range of climate states" (missing a word here?)

We agree and the word “states” has been inserted.

Page 9:

“11-20: parts of this paragraph about isostatic rebound seem redundant with material on pp. 7 and 8; consider combining/rewriting”

We agree that there is repetition and as a result lines 329-332 have been removed on page 11.

“21: "appropriated:" delete the "d"”

Done.

Page 10:

21 and following: because this material explains *why* the GCM simulations were done in the way you describe, it should probably be moved to the beginning of this section

We agree and this text has been to the beginning of Section 2.3.

Page 12

20-24: if your simulated summer temperature anomalies are too small, won't that make your estimated GIS contributions to Eemian sea level change also too small?

Please see our response to the reviewer's comment with regard to this point under the response to statistical methods section above.

Page 15:

“1-15: I looked for an answer to this question in the text, but did not find it easily. Where do your modern simulations come from? Did you run the simulations to equilibrium under a modern climatology, as in Stone et al. (2010)? Are the modern simulated ice volumes shown somewhere in the paper? The volumes in Stone et al. (2010) were all bigger than the "real" volume, if I remember correctly.”

The modern simulations are similar to those in Stone et al. (2010) but an ensemble of 500 is generated (rather than 250) and the climate coupling methodology developed here is also used to be consistent with the LIG simulations. The simulations are run to equilibrium where the vast majority are very close to or larger than the “real” volume. They are shown on Figure 6a and b on the righthand axis so that the evolution of the LIG simulations can be directly compared with their “modern” simulated volume. We have now also included the spin-up of the modern simulations on Figure 6a.

We have included the following text on page 17, line 506-506:

“Figure 6a shows the evolution of absolute ice volume throughout the 16,000 year ice sheet simulations. Also shown is the spin-up for the modern day GrIS for each ensemble member and subsequent spin-up using the 136ka climatology to give an approximation of the initial GrIS state at 136ka.”

Page 16:

“17: "Probabilisite" is misspelled”

Corrected.

Page 22:

“24: Colville et al. (2011, Science) inferred contributions as low as 1.6 m”

The text has been modified as follows and includes a reference to the Colville study (page 26-27, line 800-804).

“However, it is very likely that the GrIS contributed between 0.3 and 3.6 m to LIG sea-level rise, lower than the range of many recent estimates of 2.7 to 4.5 m (Tarasov and Peltier, 2003; Robinson et al., 2011; Cuffey and Marshall, 2000; Kopp et al., 2009) but similar to the lower bound of Robinson et al. (2011) and the estimate of 1.6 m from Colville et al. (2011)”

Figures

“For each figure, please include one sentence at the end of the caption that tells a reader what they should take away from the figure.”

We have not included these extra sentences because this is not standard procedure for Climate of the Past and we feel that the figure captions satisfactorily explain what the figures represent.

“Figure 1: I think this figure is a bit uninformative – it shows that the points are distributed through the five-dimensional space, but I can’t easily see if there are any gaps in the Latin hypercube (which can occur, depending on the number of points). Please replot as 10 different x-y plots, similar to Figure 1 of Applegate et al. (2012).”

We have removed Figure 1 in its current form and replaced it in the format suggested. We have also highlighted those experiments which are accepted for the LIG in red.

“Figure 3: see comments above.”

See our response to the reviewer’s comments above.

“Figure 5: Please show these results as a scatter plot of estimated LIG Arctic summer temperatures from paleo-data on the x-axis vs. your model-inferred temperatures on the y-axis. Show also the 1:1 line; if the points lie close to this line, then the model is behaving well relative to the data.”

Since this new figure represents schematically what is in Table 3 we have included it in Supplementary Information and included the following in the text (page 15, line 449-450):

“Overall, the agreement is good with 65% of the data points coinciding (within the uncertainty) with the 1:1 line on Fig. S1...”

“Figure 6: please stack the three panels one on top of another and make them wider; also scale the y-axes to be consistent with the data. The skill-score color scale probably only needs to be shown once.”

We have stacked the three panels, one on top of the other as suggested, and made them wider. The y-axis on Fig.6b and c has been scaled consistent with the data. We prefer to keep the skill-score colour on Fig.6b and Fig 6c since one shows absolute ice volume and the other relative change in sea-level and it makes it clearer to see the best performing experiments for the two different metrics.

“Please show a histogram of the spinup ice volumes, with lines indicating the modern ice volume and ensemble mean.”

This clearly seen in Figure 9 (grey line) and shows the real modern ice volume (now represented by a red line) as well as the ensemble mean.

“In this figure, time runs from right to left, which isn’t consistent with Figure 3. Please make the time values on the x-axis negative and switch the x-axes from left to right. This “switching” should also be done for the other figures with time dimensions.”

There is no set convention yet in palaeoclimatology in terms of which way the axes run for time. As a result we wish to keep ours in the convention shown. Also the axis title says ka which denotes thousands of years ago. Therefore, making the numbers negative is redundant and may also clutter the figure. As for Figure 3 this is model time rather than actual time so we feel it is justified to keep the axis running from 0 to 200.

“Please show the ice volume trajectories during the spin-up period in all the panels. Compressing them so that they don’t take up the whole x extent of each panel is OK.”

We have included the spin-up on Figure 6a (see comments above) but do not think it is necessary on Figure 6b. In order to compare the simulated modern day ice volume with the LIG ice volume trajectories we wish to keep Figure 6b in the form currently shown. Note on Figure 6a we have inserted a red dashed line which separates spin-up initially with a modern day climate followed by spin-up with a 136ka climate. The caption has been modified to reflect this.

“Figure 9: Please show another panel which is the same as this figure, but including only the runs shown in black on Figure 6.”

We do not feel this is necessary because it does not add any significant information that is not already displayed in Figure 6a. For example, it is clear that those ensemble members that are acceptable for the LIG tend to have the higher simulated modern ice sheet volumes than those rejected when compared with the observation.

“The small star is hard to see, and may be even less visible on the final typeset manuscript. Please replace this star with a vertical red line.”

We have removed the red star and replaced it with a vertical red line.

Response to comments by Reviewer 2, Alex Robinson:

1. GCM Climatic forcing

“Overall, by interpolating between different time slices and topographies, the approach for producing more realistic transient climates for the ice sheet is clever. However, I am not so convinced by the use of the “cl_pice” (partially melted) state. In the discussion, the authors mention also running simulations that only interpolate between ice-free and ice-covered states, and producing similar results. To me, this seems like a better and cleaner approach, since it could be argued that the method as it is now would impose a deglaciation pattern similar to that of the future warming scenarios of Stone et al. (2010). Although not a requirement, I would suggest using the alternative simulations instead (only interpolating between ice-free and ice covered states).”

We originally submitted this article to another journal where one reviewer suggested that we change our methodology from interpolating between an ice-covered and ice-free state to one where an intermediate ice sheet was also included. We agreed with this suggestion for the following reasons. It was argued that implementing no Greenland ice at all in the GCM was overly extreme because all the accepted runs simulated GrIS retreats which did not go beyond that shown in Figure 8b . They suggested it would be better to include an ice sheet in the GCM that looked similar to that in Figure 8b (approximately half the ice volume of the modern day ice sheet) in the coupling methodology, a suggestion with which we agreed. Furthermore, this would considerably reduce spurious weighting for intermediate-sized ice-sheets, whose orographic precipitation on their flanks cannot be captured by a linear weighting of those for full ice and no ice.

It is true that by using an ice sheet geometry from a future warming experiment described in Stone et al. (2010) that it could impose a deglaciation pattern similar to that of future warming. However, the ice sheet pattern chosen is similar to that derived for the LIG using the coupling methodology with only two GrIS states. We also wanted to choose an ice sheet geometry that was independent of the LIG coupling methodology to ensure no bias was introduced. Furthermore, the climate parameters imposed in the GCM with this partial ice-sheet are still consistent with a LIG climate not a future climate. As such for these reasons we prefer to keep the coupling methodology and results as described in the current manuscript.

For information, we found by modifying the coupling methodology 97 more simulations were inconsistent with the LIG palaeo-data but that the overall probability density function was not greatly changed and the maximum predicted sea-level contribution range only slightly reduced. We have now included this information in a Supplementary Figure (Fig. S3).

2. PDD

“The authors, while aware of the issues of using PDD forcing during the Eemian, justify its use here with the following sentence: “However, although the mass balance scheme used in this study does not take into account directly the radiative forcing, it does indirectly because the GCM sees the full insolation change, which then modifies the seasonality of the surface temperature which drives the PDD scheme.”

Unfortunately, this justification is incorrect. For example, as stated by van de Berg et al. (2011), “Our sensitivity experiments show that only about 55% of this change in surface mass balance can be attributed to higher ambient temperatures, with the remaining 45% caused by higher insolation and associated nonlinear feedbacks”. Through sensitivity analyses, they show that “the PDD method significantly underestimates melt for the experiments with Eemian insolation conditions”. Thus, although the GCM climate shows higher temperatures or different seasonality, the PDD melt scheme as applied still cannot account for a fundamentally different ratio between the absorption of shortwave and longwave radiation. In principle, this could perhaps still be done using the PDD method by increasing the PDD factors as a function of the insolation anomaly. At a minimum, I think this point needs to be discussed in more detail. However, I would also strongly recommend that the authors consider if their method could be improved somewhat to account for the insolation change. In principle, the suggestion above would only require rerunning the rather short Eemian simulations, which should certainly be computationally feasible.”

We agree that our justification is incorrect and thank the reviewer for clarifying this section. As a result we have now changed the text to reflect the problems with using the PDD scheme for the LIG. Although it is beyond the scope of this paper to modify the PDD scheme we have also indicated that future improvements could include the PDD factors as a function of insolation anomaly (page 24, line 728-741).

“Thirdly, the PDD scheme used in calculating the surface mass balance, although efficient, as it only needs temperature as an input and does not require the use of regional climate models, has been shown by van de Berg et al. (2011) to significantly underestimate melt for simulations which include LIG insolation forcing compared with an approach which takes insolation and albedo explicitly into account (Robinson et al., 2010). Van de Berg et al. (2011) show that surface melt is affected not only by higher ambient temperatures but also directly through stronger summertime insolation and associated non-linear feedbacks (melting snow absorbs twice as much solar radiation as dry snow). Temperature-melt relationships assume a fixed relation between near-surface air temperature and melt-rate but this relation is also dependent on insolation and, therefore, changes in orbital forcing parameters and the latitude. In essence, the PDD scheme fails to capture north-south melt gradients driven by insolation gradients. As a result, inclusion of this process could melt the GrIS further back during the LIG. Future improvements to the PDD scheme could be to use PDD factors which are function of insolation change.”

3. Model skill score

“The following statement is very problematic for me and highlights a larger issue with the manuscript: “Our estimate is more reliable because it derives from a full probabilistic analysis, taking into account ice sheet model and data uncertainties.” The probabilistic methods applied here certainly improve the interpretation of the modeling results and provide more information than only performing one simulation, for example. However, the skill score that has been applied is based only on consideration of how well the model reproduces the present-day distribution of ice. This is a rather dubious criterion, however, especially given that the shallow-ice approximation ice sheet model is unable to account for fast flow and consistently produces too large ice sheets for the present day. Figure 9 should already serve as a warning in this respect, since the entire range of simulated ice volumes are well above that of the data. Using ice volume as the sole evaluative criterion thus gives higher skill to model versions that likely compensate for this lack of physics with higher melt rates,

which doesn't necessarily make these model versions more realistic and could dramatically impact the pattern of ice loss simulated during the Eemian. I would therefore strongly urge the authors to consider additional criteria in their assessment of the performance of the different model versions”

We agree that Figure 9 shows that the majority of the modern day GrIS volumes are above the modern day observed value, likely due to the inability of the model physics to capture fast flow processes. However, for a number of reasons we feel our approach is justified.

Firstly, we do not only use the simulated modern day GrIS skill-score to constrain the LIG probability density function of maximum sea-level contribution but also include LIG palaeo-data constraints. We agree that those simulations with higher skill likely have model versions that compensate for the lack of higher order physics and have associated higher melt rates making them unrealistic. However, our ensemble shows that those simulations with ice volumes closest to the real volume (Fig 6a) indeed melt away during the LIG due to unrealistic high melt rates and, therefore, are rejected. This can also be observed in the new version of Figure 1 where the accepted LIG simulations all fall within the region of smaller PDD ice values within the LHS (coloured red). As a result the accepted LIG simulations are the best possible simulations from our ensemble (with the shallow ice approximation model used) that are consistent with the LIG and modern day. Note also that the simulations which are accepted have relatively similar skill-scores compared with those that are rejected and, therefore, the skill does not have as large an effect on the upper tail of the sea-level contribution as might be expected (see Figure 11 in the revised manuscript).

Secondly, in response to Reviewer 1 we also modified the skill-score formulation but found that it did not make a notable difference to the resultant probability density function.

Thirdly, as we mention in the discussion and conclusions section our over-prediction of modern day ice-sheets is partly due to the observation only including the contiguous ice-sheet –a new dataset for Greenland is currently being produced that separates the contiguous ice-sheet from isolated ice caps but this is not yet available for use. The discrepancy is also due to uncertainties in the lack of certain physical processes. We do not include basal sliding for instance, which would likely melt the ice-sheet back further. See our response to Reviewer 1 regarding this. We have now included a sentence in the discussion to reflect this point (page 25, line 766-768):

“The omission of the basal sliding process may also result in simulations being biased toward higher values for modern day ice volume since it is likely this would result in the ice sheet melting back further.”

Finally, we have now also included a comment about the uncertainties in the boundary conditions used. Stone et al. (2010) showed that changing the bedrock alone can make a difference to ice volume by more than 14%.

Minor comments

“Abstract: Please consider rephrasing the term “coupled climate – ice sheet model simulations”, as I think this a bit misleading. The simulations performed here do attempt to account for potential coupling effects between the climate (GCM) and the ice sheet and this should be acknowledged. But to me, the term “coupled” implies something more interactive.”

We agree that this is misleading and have changed the text to the following (page 2, line 40-41):

“...by performing an ensemble of 500 Glimmer ice sheet model simulations forced with climatologies from the climate model HadCM3...”

“Please move the description of the probabilistic method (section 5.1.1) to an Appendix.

It is important to show the statistical methodology used, but such a detailed description of arguably well-documented statistical methods in the paper itself distracts from the main message of the paper.”

We wish to keep the probabilistic methods section where it currently is. The reason for this is because much of the method description contains text that refers to specific modifications we have made to the Bayesian analysis e.g. the logistic function. If this were included in the Appendix it may become very opaque to the reader, especially with regard to the discussion on sensitivity to the various parameters included in the methods.

“Page 2740, line 29: “The monthly average climate: : :”. This wording is a bit unclear. By climate, I suppose the authors mean temperature and precipitation fields? This might be more clearly reformulated as “The monthly average variables of temperature and precipitation, here denoted as CL(t),: : :”.

We agree that this is not clear and the text has been changed (page 13, line 401-402).

“Climate interpolation equations: The equations were somewhat hard to follow because of the symbols used and the mixed sub/superscripts. For example, “CL” could be represented more concisely by one letter, like “C”, and “vol” could be “V”. Furthermore, I don’t see the need to switch between lower and uppercase letters CL or cl, as they are the same variable. Also note that right now, “ice” and “pice” appear as subscripts for “vol”, but superscripts for “cl”, which seems inconsistent. Finally, instead of putting the time in subscripts for the GCM climate fields, this could be in parentheses, like (t) is elsewhere. This would leave the only subscripts to be “ice”, “pice” and “0”, which are enough to indicate that these are the GCM derived fields. These are only suggestions, but I think the equations would be much easier to follow.”

We agree that the equations can be made easier to follow by the reviewer’s helpful suggestion (see modified equations below).

$$C(t) = \frac{C^{ice}(130) - C^{ice}(136)}{t_1} t + C^{ice}(136)$$

$$(1) C^{ice}(t) = \frac{C^{ice}(125) - C^{ice}(130)}{t_2} t + C^{ice}(130)$$

$$(2) C^{pice}(t) = \frac{C^{pice}(125) - C^{pice}(130)}{t_2} t + C^{pice}(130) \quad (3)$$

$$C^0(t) = \frac{C^0(125) - C^0(130)}{t_2} t + C^0(130) \quad (4)$$

$$C(t) = \left(\frac{V(t) - V^{ice}(130)}{V^{ice}(130) - V^{pice}(130)} \right) (C^{ice}(t) - C^{pice}(t)) + C^{ice}(t) \quad (5)$$

$$C(t) = \frac{V(t)}{V(130)} (C^{pice}(t) - C^0(t)) + C^0(t) . \quad (6)$$

“Page 2751, line 25: In this context, the proper reference concerning temperature-melt relationships and insolation is Robinson et al., The Cryosphere, 2010.”

This is correct. Thank you for spotting this.

“Table 1: The units given for the PDD factors are mm / d / degC. Is this mm water equivalent or mm ice? Please clarify.”

This is mm water equivalent. The text has been modified.

“Table 2: Perhaps it would be useful to add a column with the 65 N maximum summer insolation anomalies as well.”

We have now included the 65°N June maximum insolation anomalies in Table 2 for reference.

“Table 3, caption: please change “brackets” to “parentheses””

Done.

“Figures: It seems that some of the figures concerning statistical uncertainty could be condensed. Perhaps Fig. 10 and Fig. 14 could go together as four panels, which would also facilitate their comparison. Fig. 12 and Fig. 13 could also be combined.”

We agree and have combined the figures as suggested. See our response to Reviewer 1.

“It would also be very interesting to see the 2D climatic forcing fields that were applied to the ice sheet during the Eemian. For example, for the highest skill score simulation, it would be informative to see the temperature (summer) and precipitation anomalies applied at the time of the maximum temperature anomaly and at the time of minimum ice volume.”

We have now included the plots requested in Supplementary information and have included the following text (page 18, line 547-553):

“The associated precipitation and temperature forcings for the simulation with the highest skill-score, derived from HadCM3 according to the coupling methodology, are shown in Figure S2 in Supplementary Information. The cases where minimum ice volume and maximum temperature anomaly are reached are given and illustrate the latitudinal gradient in temperature from the enhanced insolation forcing and the change in topographic height in response to the warming.”

1 **Quantification of the Greenland ice sheet contribution to**
2 **Last Interglacial sea-level rise**

3 **Emma J. Stone¹, Daniel J. Lunt¹, James D. Annan² and Julia C. Hargreaves²**

4 | [1] {BRIDGE, School of Geographical Sciences, University of Bristol, Bristol, [BS8 1SS](#),
5 UK}

6 [2] {Research Institute for Global Change, JAMSTEC, Yokohama, Japan}

7 Correspondence to: Emma J. Stone (emma.j.stone@bristol.ac.uk)

8
9
10
11
12
13
14
15
16
17
18
19
20
21
22
23
24
25
26
27
28
29
30
31

32 **Abstract**

33 ~~The Last Interglaciation~~ During the Last Interglacial period (~130-115 thousand years ago)
34 ~~was a time when the a~~Arctic climate was warmer than today,~~(Anderson et al., 2006; Kaspar et~~
35 ~~al., 2005)~~ and global mean sea-level was extremely likely at least probably more than 6
36 ~~metres higher~~ ~~(Kopp et al., 2009)~~. However, there ~~are~~is large discrepancies uncertainty in
37 the estimated relative contributions to this sea-level changerise from various sources (the
38 Greenland and Antarctic ice sheets and smaller ice caps)~~fields~~ ~~(Otto-Bliesner et al., 2006;~~
39 ~~Huybrechts, 2002; Letréguilly et al., 1991; Ritz et al., 1997; Cuffey and Marshall, 2000;~~
40 ~~Tarasov and Peltier, 2003; Lhomme et al., 2005; Greve, 2005; Robinson et al., 2011; Fyke et~~
41 ~~al., 2011)~~. Here, we determine probabilistically the likely contribution of Greenland ice sheet
42 melt to Last Interglacial sea-level rise, taking into account ice sheet model parametric model
43 uncertainty, by ~~By~~ performing an ensemble of 500 Glimmer ice sheet model simulations
44 forced with climatologies from the climate model HadCM3~~coupled climate ice sheet~~
45 ~~model simulations, and~~ constrained by palaeo-data, ~~we determine probabilistically the likely~~
46 ~~contribution of Greenland ice sheet melt to Last Interglacial sea level rise, taking into account~~
47 ~~model uncertainty.~~ Here we show Our results suggest a 90% probability that Greenland ice
48 melt contributed at least 0.6 m but less than 10% probability it exceeded 3.5 m, a value which
49 is lower than several recent- estimates. These previous ~~(Cuffey and Marshall, 2000; Tarasov~~
50 ~~and Peltier, 2003; Lhomme et al., 2005; Robinson et al., 2011)~~ estimates did not include a full
51 general circulation climate model that can capture atmospheric circulation and precipitation
52 changes in response to changes in insolation forcing. Our combined modelling and palaeo-
53 data approach suggests that the Greenland ice sheet is less sensitive to orbital forcing than
54 previously thought, and implicates Antarctic melt as providing a substantial contribution to
55 Last Interglacial sea-level rise. Future work should assess additional uncertainty due to
56 inclusion of basal sliding, the direct effect of insolation on surface melt, and the climate
57 model used.

58

59 **1 Introduction**

60 Past time periods provide important case studies for evaluating the performance of Earth
61 system models, ~~since~~ because model results can be compared with geological records. In
62 particular, warm climates of the past are useful as they can also provide an analogue for

63 | possible future warming. The Last Interglaciation (LIG) provides such a case study as
64 | globally averaged sea-level was thought to be several metres higher than today, and high
65 | latitude temperatures warmer. Estimates of maximum sea-level increase, derived from
66 | sedimentary deposits and coral sequences, typically range from 4 to 6 m (Rostami et al.,
67 | 2000; Muhs et al., 2002). A recent sea-level data synthesis shows that sea-level ~~was~~ likely
68 | ~~exceeded up to~~ 8 m higher than today with the highstand extremely likely (95% probability)
69 | greater than 6 m (Kopp et al., 2009), consistent with less glacial ice on Earth during the LIG.
70 | The likely contributors to the sea-level rise are ice losses from the Greenland and Antarctic
71 | ice sheets along with high latitude Arctic icefields such as those in the Canadian Arctic,
72 | together with thermal expansion of sea-water.

73 |
74 | Further evidence from proxy data located in the Arctic and European regions suggests the
75 | LIG climate featured temperatures, at least regionally, several degrees warmer than today
76 | (Kaspar et al., 2005; Anderson et al., 2006). This estimated temperature increase is supported
77 | by climate model simulations indicating summer ~~a~~Arctic warming was as much as 5°C
78 | relative to modern, with the greatest warming over Eurasia and in the Baffin
79 | Island/Greenland region (Montoya et al., 2000; Kaspar et al., 2005; Otto-Bliesner et al.,
80 | 2006). Palaeo pollen, macrofossil and soil records suggest the expansion of boreal forests
81 | northwards into areas now occupied by tundra in Russia, Siberia and Alaska during peak LIG
82 | warmth (Muhs et al., 2001; Kienast et al., 2008). On Greenland itself, ice core
83 | measurements from the Summit region (NorthGRIP, GRIP and GISP2 ice cores) indicate ice
84 | was present ~~during throughout~~ the LIG (Chappellaz et al., 1997; NorthGRIP, 2004; Suwa et
85 | al., 2006), with the surface elevation no more than a few hundred metres lower than present
86 | day based on the total gas content of the ice (Raynaud et al., 1997). In addition, basal ice
87 | from the northwestern ice core, Camp Century, has been proposed to be of LIG age and ice
88 | from the bottom section of a core from the Renland peninsula in eastern Greenland is dated
89 | older than 130ka (Johnsen et al., 2001) although there is uncertainty in the dating of these
90 | two ice cores (Alley et al., 2010). New results from the NEEM ice core project may indicate
91 | whether or not basal ice in this location is of LIG age. The dating of basal ice at Dye-3 in
92 | southern Greenland, however, remains highly uncertain (Koerner and Fischer, 2002;
93 | NorthGRIP, 2004).

94 |
95 | Estimates of the Greenland ice sheet (GrIS) contribution to sea-level rise during the LIG
96 | range from 0.4 to 5.5 m based on a wide range of modelling techniques. These include

97 palaeothermometry from ice cores coupled with thermo-dynamical ice sheet models
98 (Letréguilly et al., 1991; Ritz et al., 1997; Cuffey and Marshall, 2000; Huybrechts, 2002;
99 Greve, 2005) with similar methodological studies also constraining their results by matching
100 model-predicted isotopic stratigraphy from ice cores with data (Tarasov and Peltier, 2003;
101 Lhomme et al., 2005).~~and~~ Another method uses coupled climate-ice sheet models of varying
102 complexity (Otto-Bliesner et al., 2006; Fyke et al., 2011; Robinson et al., 2011; Born and
103 Nisancioglu, 2012) to predict LIG Greenland ice sheet geometry and sea-level contribution.

104
105 Here we assess the contribution of Greenland ice loss to global sea-level rise, derived from
106 simulations of the LIG global climate and evolution of the GrIS from 130 to 120-ka using the
107 general circulation model (GCM) HadCM3 'coupled' to the ice sheet model Glimmer. ~~over~~
108 ~~the Greenland region~~ We ~~using~~ an efficient offline coupling methodology to account for ice
109 sheet-climate interactions (DeConto and Pollard, 2003), ~~and estimate the range in GrIS~~
110 contribution to LIG sea-level change by considering ice sheet model uncertainty in order to
111 better understand the GrIS response under a warmer than present climate- critical for the
112 assessment of future climate change.

114 **2 Model description and experimental design**

115 Here we outline the models used to estimate the GrIS contribution to LIG sea-level change.
116 Due to computational expense we have developed a method to pseudo-couple our climate
117 model to an ice sheet model which takes into account the effect of the albedo feedback
118 mechanism without the need to run fully coupled (two-way) climate-ice sheet simulations.
119 We begin by describing the climate and ice sheet models followed by a detailed description
120 of the experimental design and this coupling methodology. An ensemble is performed to take
121 into account parametric uncertainty in the ice sheet model in order to estimate a range in GrIS
122 contribution to LIG sea-level. We use palaeo-data in order to disregard simulations which do
123 not satisfy these robust palaeo-data ice sheet constraints (see Sect. 3.2). Finally, from the
124 ensemble a probability density distribution of maximum sea-level contribution from the GrIS
125 to LIG sea-level rise is constructed (see Sect. 3.2.1 for details of the probabilistic method).

126

1.4.2.1 The climate model

The GCM simulations described in this paper are carried out using the UK Met Office coupled atmosphere-ocean GCM, HadCM3, version 4.5 (Gordon et al., 2000) which has been used in the third and fourth IPCC assessment reports. The atmosphere component of HadCM3 is a global grid-point hydrostatic primitive equation model, with a horizontal grid-spacing of 2.5° (latitude) by 3.75° (longitude) (~~73 by 96 grid points~~) and 19 levels in the vertical with a time step of 30 minutes. The performance of the atmosphere component ~~is described in Pope et al. (2000) where HadAM3 (the atmosphere only version of the Hadley Centre Model) is run with observed sea surface temperatures. It~~ has been shown to agree well with observations (Pope et al., 2000). The land surface scheme (MOSES 2.1), ~~which includes representation of the freezing and melting of soil moisture and the formulation of evaporation process, incorporates the dependence of stomatal resistance on temperature, vapour pressure and CO₂. In addition, it treats sub-grid land cover explicitly.~~ Within this land surface scheme ice sheets are prescribed and are fixed.

~~The radiation scheme is that of Edwards and Slingo (1996) with six and eight spectral bands in the shortwave and longwave respectively. The convective scheme is based on Gregory and Rowntree (1990) with an additional parameterisation of the direct impact of convection on momentum (Gregory et al., 1997). The cloud scheme employed is a prognostic one that diagnoses cloud amount, cloud ice and cloud water based on the total moisture and the liquid water potential temperature. The orography of Greenland is particularly important when considering the deglaciation and reglaciation of the GrIS since previous work has shown it can have profound effects on atmospheric circulation patterns if the ice sheet were removed (Petersen et al., 2004; Junge et al., 2005) since orographic gravity waves represent a major sink of momentum flux in the atmosphere. In order to include the effect of orographic forcing on atmospheric circulation, HadCM3 also includes a parameterisation of orographic drag (Milton and Wilson, 1996) and a gravity wave drag scheme in order to represent the mechanisms of sub-grid scale orographic forcing in stable and turbulent atmospheric flow. The scheme includes anisotropy of orography, high drag states and flow blocking as well as trapped lee waves (Gregory et al., 1998).~~

The resolution of the ocean model is 1.25° by 1.25° with 20 levels in the vertical. The ocean model uses the mixing scheme of Gent and McWilliams (1990) with no explicit horizontal tracer diffusion. ~~The horizontal resolution allows the use of a smaller coefficient of horizontal~~

160 ~~momentum viscosity leading to an improved simulation of ocean velocities.~~ The sea-ice
161 model uses a simple thermodynamic scheme and contains parameterisations of ice
162 concentration (Hibler, 1979) and ice drift and leads (Cattle and Crossley, 1995). ~~Surface~~
163 ~~temperatures and fluxes over the sea ice and leads fractions of gridboxes are calculated~~
164 ~~separately in the atmosphere component of HadCM3. The surface albedo of sea ice is 0.8 at~~
165 ~~temperatures less than 10°C and decreases linearly to 0.5 between 10 and 0°C. This is to~~
166 ~~account for the aging of snow, formation of melt ponds and the relatively low albedo of bare~~
167 ~~ice.~~ ~~For~~ In simulations of the present-day climate, the ocean model has been shown to
168 simulate sea surface temperatures in good agreement with modern observations, without the
169 need for flux corrections (Gregory and Mitchell, 1997).

170 4.22.2 **The ice sheet model**

171 We also use the three dimensional thermomechanical ice sheet model Glimmer version 1.0.4
172 (Payne, 1999; Rutt et al., 2009), ~~which is forced with monthly temperature and precipitation~~
173 ~~from HadCM3. The core of the model is based on the ice sheet model described by Payne~~
174 ~~(1999). T~~ The horizontal resolution of the model is 20 km with 11 vertical layers. The -ice
175 dynamics are represented with the widely-used shallow-ice approximation (SIA) approach,
176 which neglects longitudinal stresses in the ice sheet. This simplification is appropriate for ice
177 masses that are thin compared with their horizontal extent. The principle advantage of using
178 the SIA for modelling the GrIS on palaeo-timescales is that it is computationally cheap,
179 allowing large multi-millennial ensembles to be easily performed. Although the method is
180 accurate for the interior of a large ice sheet such as Greenland this is not the case at the
181 margins where streams of fast flowing ice and coupling to ice shelves complicate the ice
182 dynamics such that the SIA is unable to capture the currently observed changes in ice sheet
183 geometry and velocity occurring on short timescales. The lack of higher order physics has
184 resulted in the majority of ice sheet models overestimating the present day ice sheet volume
185 and extent (e.g. Ritz et al. 1997; Stone et al. 2010; Greve et al. 2011; Robinson et al. 2011).
186 ~~and a full three dimensional thermodynamic model is used to determine the ice flow law~~
187 ~~parameter. The model is formulated on a Cartesian grid, and takes as input the surface mass-~~
188 ~~balance and air temperature at each time step. In the present work, the ice dynamics time step~~
189 ~~is one year.~~

190

191 The surface mass-balance is simulated using the positive degree day (PDD) approach
192 described by Reeh (1991). The basis of the PDD method is the assumption that the melt that
193 takes place at the surface of the ice sheet is proportional to the time-integrated temperature
194 above freezing point, known as the positive degree day. ~~The method described by Reeh~~
195 ~~(1991) and implemented here is somewhat more sophisticated, in that Two wo~~-PDD factors
196 are used, one each for snow and ice, to take account of the different albedos and densities of
197 these materials. The use of PDD mass-balance models is well-established in coupled
198 atmosphere-ice sheet palaeoclimate modelling studies (DeConto and Pollard, 2003; Lunt et
199 al., 2008; Lunt et al., 2009). Limitations of using the PDD scheme are discussed in Sect. 4.

200

201 -Glimmer also includes a representation of the isostatic response of the lithosphere to a
202 change in ice mass. The response of the lithosphere, ~~which~~ is assumed to behave elastically,
203 based on the isostasy model of Lambeck and Nakiboglu (1980).

204

205 The forcing data from HadCM3 are transformed onto the ice model grid using bilinear
206 interpolation, which ensures that precipitation is conserved in the atmosphere-ice sheet
207 coupling. In the case of the surface air temperature field, ~~a~~ a spatially homogenous vertical
208 lapse-rate correction is used to take account of the difference between the high-resolution
209 topography seen within Glimmer, and that represented within HadCM3. The use of a lapse-
210 rate correction to better represent the local temperature is established in previous work
211 (Pollard and Thompson, 1997; Vizcaíno et al., 2008).

212

213 One limitation of the experiments presented here is that they do not include the process of
214 basal sliding which has implications for the amount of ice mass lost dynamically. An
215 increase in the ice velocity, by incorporating the basal sliding velocity, would result in more
216 ice transferred from the accumulation zone to the ablation zone and, therefore, would likely
217 reduce the volume of the ice sheet under a warm climate. Inclusion of this missing process
218 could lead to a smaller GrIS during the LIG. Indeed, the study by Parizek and Alley (2004)
219 showed an increase in GrIS sensitivity to various warming scenarios due to surface meltwater
220 lubrication of flow. However, previous studies (Ritz et al., 1997; Robinson et al., 2011) have
221 shown that although the sliding coefficient parameter affects GrIS geometry, it is less
222 significant compared with other parameters in determining the past evolution and present
223 geometry of the modelled GrIS.

224

225 For the baseline climate to which the GCM temperature and precipitation anomalies are
226 applied we use those described in Stone et al. (2010). The temperature climatology ~~are is~~
227 derived from ERA-40 observations (Hanna et al., 2005) and precipitation also from ERA-40
228 reanalysis (Uppala et al., 2005). ~~The Glimmer ice sheet model uses a single value for the~~
229 ~~lapse rate correction which is a tuneable parameter.~~ We use the Greenland bedrock
230 topography of Bamber et al. (2001) on a 20 km resolution grid.

231
232 Several parameters in large-scale ice sheet modelling are still poorly constrained, resulting in
233 highly variable ice sheet volume and extent depending on the values prescribed in the model
234 (Ritz et al., 1997). Previous work (Stone et al., 2010) investigated the sensitivity of ice sheet
235 evolution for the modern GrIS to five tuneable parameters which affect the ice sheet
236 dynamics and surface mass balance. These parameters are the PDD factors for ice and snow,
237 near-surface lapse rate, flow enhancing factor and the geothermal heat flux (see Table 1).

238
239 Here we generate an ensemble of 500 simulations using the statistical method of Latin
240 Hypercube Sampling (LHS) in order to efficiently sample the five dimensional parameter
241 space. This method generates a distribution of plausible parameter sets within a prescribed set
242 of ranges (McKay et al., 1979) by using a stratified-random procedure where values are
243 sampled from the prescribed distribution of each variable and paired randomly with the other
244 variables assuming that the variables are independent of one another (which is the case here).
245 The LHS distribution is given is is illustrated in Figure 1. For more details on parameter
246 choices refer to Stone et al. (2010).

247

248 **4.32.3 Experimental design and coupling methodology**

249 Computationally, it is not yet feasible to run HadCM3 fully coupled (two-way) with Glimmer
250 for the timescales of thousands of years, such as through the LIG. A methodology is
251 developed based on that of Deconto and Pollard (2003) in order to account for a transient
252 climate which evolves as the ice sheet volume evolves, whilst minimising computational
253 expense. It takes into account a changing climate as a result of the change in ice sheet
254 geometry by including the elevation-temperature feedback and an approximation to the
255 albedo feedback. We outline (1) the GCM simulations performed, (2) the ice sheet model

256 spin-up procedure and (3) details of the coupling method used between climate and ice sheet
257 model.

259 2.3.1 LIG GCM simulations

260 GCM simulations representing 130, 125 and 120-ka, are forced with insolation anomalies
261 resulting from changes in the Earth's orbital parameters for the early to mid part of the LIG.
262 These time-slices were chosen because they cover the interval of peak LIG warmth as well as
263 the maximum sea-level highstand (Petit et al., 1999; Lisiecki and Raymo, 2005; Kopp et al.,
264 2009). Compared with pre-industrial, larger eccentricity and obliquity and Northern
265 Hemisphere summer (as opposed to winter) occurring at perihelion (see Table 2), results in
266 greater seasonality, leading to pronounced high northern latitude summer insolation,
267 consistent with warming observed in the geological record (NorthGRIP, 2004; Kaspar et al.,
268 2005; Anderson et al., 2006) (see Fig. 2). This seasonal variation in insolation is important
269 because ice sheet surface mass balance is particularly sensitive to summer warming.

270
271 The three LIG snapshot time-slices are run for 100 model years (70 years spin-up and 30
272 years for averaging) with the following Greenland boundary conditions:

- 273 1. Modern day GrIS present
- 274 2. Partial GrIS present derived from a tuned ice model experiment forced with a
275 560 ppmv climate (Stone et al., 2010)
- 276 3. No GrIS present with bedrock in isostatic equilibrium

277 This procedure gives a range of climate states between which the 'expected' climate over a
278 partially melted GrIS during the LIG might lie. One caveat of these climate simulations
279 concerns the use of ~~anisostatic~~isostatic equilibrium for the orography in the ice-free state.
280 Obviously, if there was a substantial ice sheet present before the start of the LIG, as inferred
281 from the eustatic sea-level curve (Siddall et al., 2007), there would likely have been
282 insufficient time for all the ice to melt, the bedrock to rebound fully and soil to develop on
283 the bare rock surface. However, this provides the most contrasting climate scenario to a fully
284 glaciated Greenland being present throughout the LIG (which is also unlikely). Another
285 limitation of this approach (which was required for computational efficiency) is that as
286 described in Sect. 2.3.3, the climate state is constrained to linearly interpolate between these
287 states.

288

289 For the LIG the changed forcings from present day are: the modified trace gas concentrations
290 and the seasonal and latitudinal insolation changes at the top of the atmosphere associated
291 with the Milankovitch orbital forcing (Milankovitch, 1941) consistent with the perturbed
292 forcings in the standard PMIP LIG simulations. Figure 2a shows the variation in insolation
293 from 140 to 110-ka for the spring and summer months at three latitudes over Greenland:
294 65°N, 74°N and 80°N. Insolation anomalies over Greenland relative to present day (Fig. ~~ure~~
295 2b) are at a maximum at ~130 ka for May and June and decrease toward 120-ka. Smaller
296 anomalies for July and August peak from ~120 to 125-ka. Orbital parameters are taken from
297 Berger and Loutre (1991) for the three ~~time~~ snapshots at 130, 125 and 120-ka. Table 2 shows
298 the obliquity, eccentricity and perihelion for these three scenarios. A further HadCM3
299 experiment at 136-ka is also included in order to spin-up the ice sheet model sufficiently but
300 differs slightly by including a MOSES 1- land surface scheme (Cox et al., 1999). This
301 simulation is run for 500 model years with an averaging time of 30 years.

302

303 An additional simulation, the pre-industrial control, includes trace gas concentrations (280
304 ppmv for CO₂, 760 ppbv for CH₄ and 270 ppbv for N₂O) and orbital parameters (obliquity
305 23.45°, perihelion ~~occurs on day 2.6 of the year~~(~~day of the year~~) and eccentricity 0.01724)
306 appropriate for 1850A.D.

307

308 Also shown in Fig. ~~ure~~ 2 is the atmospheric CO₂ concentration, reconstructed from ice cores,
309 from 140 to 110 ka based on Lüthi et al. (2008). All CO₂ values are on the EDC3 gas age
310 scale (Louergue et al., 2007). There is a sharp rise in CO₂ concentration between 140-ka and
311 130-ka from ~200 to 260 ppmv. Thereafter, this trace gas concentration stabilises between
312 260 and 290 ppmv. Since the greenhouse gases do not markedly vary from pre-industrial
313 during the LIG (Lüthi et al., 2008) and it has been shown that climate perturbations were
314 predominantly orbitally driven at this time (Slowey et al., 1996; Loutre et al., 2007; Yin and
315 Berger, 2012), gas concentrations are held constant and unchanged from the values used in
316 the pre-industrial simulations. In this way any changes in LIG climate from the pre-industrial
317 are due to changes in the orbital parameters of the Earth. CO₂ is, therefore, held constant at
318 280 ppmv for all experiments performed using HadCM3 between 130-~~ka~~ and 120-ka. All
319 other trace gases are equivalent to pre-industrial values. The exception is for the simulation at
320 136 ka where CO₂, methane (CH₄) and nitrous oxide (N₂O) are lower compared with pre-
321 industrial at 200 ppmv, 413 ppbv and 229 ppbv respectively. This is because differences in

322 the trace gases compared with pre-industrial are the driving mechanism for this earlier
323 perturbed climate rather than changes in the orbital parameters compared with pre-industrial
324 (see Fig. 2b where summer high latitude insolation anomalies are small at 136-ka).

325

326 Outside of Greenland, global vegetation coverage is prescribed at present-day distributions.
327 The simulations where the GrIS is removed/partially melted are prescribed bare soil coverage
328 in place of Greenland ice while the simulations with a full GrIS included use the present-day
329 ice sheet mask with bare soil in ice-free regions. ~~For the LIG simulations with the ice sheet
330 removed, the bedrock is rebounded and in isostatic equilibrium. Likewise, the simulations
331 with the GrIS included use modern day topography and those with a partial ice sheet use their
332 associated topography. Finally,~~ The land-sea mask remains unchanged from modern since
333 there were no significant tectonic changes to the continents between 130-ka and present and
334 the estimated sea-level change would result in negligible land-sea mask changes.

335

336 All GCM simulations were continued from pre-industrial simulations of 100 model years
337 with the appropriate bedrock and ice coverage. ~~The spin-up time in large-scale atmosphere-
338 ocean models is governed by the slow processes in the deep ocean and is usually on the order
339 of several thousand years. However, due to computational expense this is not easily
340 achievable. As such the ocean component of HadCM3 does not fully represent changes in
341 ocean circulation, but does fully interact thermodynamically with the atmosphere in our
342 modelling framework.~~ Figure 3 shows the average temperature evolution over Greenland
343 (one of the inputs into the Glimmer ice sheet model) including this pre-industrial spin-up. A
344 10-year ~~running average (red) and~~ 10-year mean trend (~~red~~blue) ~~are is~~ shown and indicates
345 sufficient spin-up of the model near-surface temperature in response to the changed orbits.
346 ~~This trend shows~~ that compared with inter-annual variability the ~~mutli-year average
347 temperature response of the~~ simulations ~~is are~~ close to equilibrium.

348

349 4.3.12.3.2 Obtaining a 136ka GrIS

350 It is not known exactly how big the GrIS was at 130-ka (or at any other point during the LIG),
351 although sea-level was similar to present day (Siddall et al., 2007; Kopp et al., 2009)
352 implying a substantial amount of ice must have been present at high northern and southern
353 latitudes. ~~Since it is not practically possible to spin-up an ensemble of coupled HadCM3 ice
354 sheet model configurations for several glacial interglacial cycles, an approach is used that~~

~~assumes the ice sheet is in equilibrium at the start of the transient ice sheet model simulations. The correct method of reconstructing the initial state of the GrIS under past climate forcings is unclear but two main methods have been adopted in previous studies: (1) steady state simulations driven by present day or past climatic conditions (e.g. Ritz et al. 1997; Stone et al. 2010) and (2) transient simulations driven by palaeoclimatic reconstructions (e.g. Applegate et al., 2012). Each method has its own caveats which have been investigated recently by Rogozhina et al. (2011). For example, they show that initialising from an ice-free state under glacial forcings is not a good choice for simulations that start under colder-than-modern conditions. Because it is not practically possible to spin-up an ensemble of coupled HadCM3 ice sheet model configurations for several glacial-interglacial cycles, we use an approach that assumes the ice sheet is in equilibrium at the start of the transient ice sheet model simulations. We adopt a similar methodology to Rogozhina et al. (2011) by initialising from a modern GrIS spun-up with a constant glacial climate forcing from HadCM3 then apply a time-dependent forcing into the interglacial period. We do not use palaeoclimatic reconstructions to obtain an initial state for the GrIS because prior to the onset of the LIG processes occurring in deeper parts of ice cores makes them somewhat unreliable and extending beyond the LIG is, therefore, unrealistic (Grootes et al., 1993; Johnsen et al., 1997).~~

In order that changes in the ice sheet response to climate at 130-ka are not a result of inadequate spin-up of the ice sheet model, simulations begin at 136 ka when the climate was substantially colder. As a result, the ice sheet model is initiated with an ice sheet in equilibrium with the 136-ka climate. The ice sheet model is spun-up for 50,000 years in anomaly mode using the 136-ka climatology. This method requires GCM monthly mean changes in precipitation and near-surface temperature (defined relative to a pre-industrial climate) to be superimposed onto a present day reference climatology (see Sect. 2.1) used by the surface mass balance model in Glimmer. Anomaly coupling is used to reduce climate model bias both for precipitation and temperature which affects the ice sheet model output, as in previous studies (Lunt et al., 2008; Lunt et al., 2009).

~~In order to assess the sensitivity of ice sheet model results to the climate model used we compared offline forcing of the ice sheet model with two different 125ka model climatologies (HadCM3 used here and the CCSM3 model). This comparison showed that, compared with~~

388 ~~the sensitivity to internal parameters (given in Table 1 and outlined in Stone et al. (2010)), the~~
389 ~~GrIS evolution is insensitive to the climate model used.~~

390
391 ~~Computationally, it is not yet feasible to run HadCM3 fully coupled (two-way) with Glimmer~~
392 ~~for the timescales of thousands of years, such as through the LIG. A methodology is~~
393 ~~developed based on that of Deconto and Pollard (2003) in order to account for a transient~~
394 ~~climate which evolves as the ice sheet volume evolves, whilst minimising computational~~
395 ~~expense. It takes into account a changing climate as a result of the change in ice sheet~~
396 ~~geometry by including the elevation temperature feedback and an approximation to the~~
397 ~~albedo feedback.~~

398 2.3.3 Coupling the climate and ice sheet models

399 ~~We model a~~ A total of 16,000 years ~~are modelled~~, representing the time period from 136 to
400 120-ka. Figure 4 shows a diagram of the coupling process, which is outlined in detail below.
401 The monthly average variables of temperature and precipitation, here denoted as climate,
402 $CCL(t)$, is linearly interpolated along the time-axis from 136 to 130-ka where the
403 notation $C^{\text{state of Greenland}}$ is used (i.e. state of Greenland in HadCM3 is either ice covered: ice,
404 partial ice: pice or ice-free: 0),

$$406 \quad C(t) = \frac{C^{ice}(130) - C^{ice}(136)}{t_1} t + C^{ice}(136). \quad (1)$$

407 The interpolation is between the 136-ka climate, $C^{ice}(136)$, and the 130-ka climate, $C^{ice}(130)$,
408 where t_1 is 6,000 model years. Glimmer is initiated with the equilibrated ice sheet geometry
409 which was obtained by forcing Glimmer offline with the constant 136 ka climate. At 130-ka
410 the climate is allowed to evolve each year between the three climate scenarios (with a GrIS, a
411 partial GrIS and without a GrIS) according to a weighting function defined by the ratio of the
412 ice volume ($V_{vol}(t)$) at time t and the ice volume predicted at 130-ka ($V_{vol}(130)$) by the ice
413 sheet model. Between 130 and 125-ka the following linear interpolations are performed
414 (represented by the solid blue, orange and red arrows respectively in Fig. 4) similar to
415 Eq.equation (1)

417
$$C^{ice}(t) = \frac{C^{ice}(125) - C^{ice}(130)}{t_2} t + C^{ice}(130), \quad (2)$$

418

419
$$C^{pice}(t) = \frac{C^{pice}(125) - C^{pice}(130)}{t_2} t + C^{pice}(130), \quad (3)$$

420 and

421
$$C^0(t) = \frac{C^0(125) - C^0(130)}{t_2} t + C^0(130), \quad (4)$$

422

423 where $C^{ice}(125)$ is the 125-ka climate with the GrIS present, $C^{pice}(125)$ and $C^{pice}(130)$ are the
 424 125 and 130-ka climates respectively with a partial GrIS, $C^0(125)$ and $C^0(130)$ are the 125
 425 and 130-ka climates respectively with the GrIS removed and t_2 is 5,000 years. Likewise,
 426 similar linear interpolations are also performed from 125 to 120-ka.

427

428 If the ice volume, $V_{vol}(t)$, is greater than the partial ice volume (defined as: $V_{vol}^{pice} =$
 429 $0.46 V_{vol}^{ice}(130)$), then the climate, $C_L(t)$, at each year is now also weighted either towards
 430 the climate with a partial GrIS, $C^{pice}(t)$, or the GrIS climate, $C^{ice}(t)$, according to

431

432
$$C(t) = \left(\frac{V(t) - V^{ice}(130)}{V^{ice}(130) - V^{pice}(130)} \right) (C^{ice}(t) - C^{pice}(t)) + C^{ice}(t) \quad (5)$$

433

434 Alternatively, if the ice volume is less than the partial ice volume then the climate, $C_L(t)$, at
 435 each year is weighted either towards the climate with no GrIS, $C^0(t)$, or the partial GrIS
 436 climate, $C^{pice}(t)$, according to

437

438
$$C(t) = \frac{V(t)}{V(130)} (C^{pice}(t) - C^0(t)) + C^0(t) \quad (6)$$

439

23 Results

2.43.1 The modelled climate of the Last Interglaciation

The GCM simulated annual average global temperature anomaly at 130-ka (with a modern day fixed GrIS included) is only 0.13°C relative to pre-industrial, consistent with the small mean annual forcing associated with the orbital configuration for the LIG. However, the seasonal temperature anomaly is -1.6°C and 2.0°C in the Northern Hemisphere for winter/summer respectively. Figure 5 shows a comparison of the LIG simulated Northern Hemisphere maximum summer warming with reconstructed terrestrial temperature anomalies derived from ice cores, pollen and microfossils (Kaspar et al., 2005; Anderson et al., 2006). Overall, the agreement at high Northern Hemisphere latitudes is ~~very~~ good with 65% of the data points coinciding (within the uncertainty) with the 1:1 line on Fig. S1 (see also Table 3). However, during the summer months the maximum LIG average temperature anomaly over Greenland is 3.5°C, cooler than values inferred (4 to 5°C) from the temperature reconstructions over this region (Anderson et al., 2006). This implies that the GrIS during the LIG was likely smaller than today and represents a minimum temperature anomaly estimate. Simulated LIG warmth in Greenland is sustained under a 130 and 125-ka climate but with significant cooling by 120-ka consistent with the change in summer insolation distribution (see Fig. 2). These changes are amplified by sea-ice feedbacks discussed below. -However, comparisons with proxy derived estimates of temperature at the location of the NorthGRIP ice core show a simulated summer temperature of 4.2°C ±1.3°C, and an annual precipitation-weighted temperature of 3.3°C, lower than the 5°C estimate obtained from the ice core oxygen isotope record (NorthGRIP, 2004) . Over much of the Greenland region predicted annual precipitation rate changes throughout the LIG are small.

Since the ice sheet climate coupling requires a set of GCM simulations where the GrIS is removed and replaced with bare soil we can assess the climate of the extreme scenario of an ice-free Greenland under LIG climate conditions. At the location of the NGRIP ice core, simulated maximum annual precipitation weighted temperature anomalies relative to pre-industrial are in excess of 20°C and the average maximum summer Greenland anomaly ranges from 14 to 16°C for the time period 125 to 130 ka. These are clearly greater than the annual proxy palaeo-data estimate of 5°C (Anderson et al., 2006), which supports the ice core evidence that the GrIS did not completely disappear during the LIG (NorthGRIP, 2004).

472

473 The increased insolation relative to pre-industrial during the early part of the LIG results in
474 spring/summer melting of Arctic sea-ice with reduced concentrations compared with pre-
475 industrial throughout the summer months. At 130-ka sea-ice concentration is reduced by up to
476 40% compared with the pre-industrial in the central part of the Arctic Ocean, similar to
477 results from Otto-Bliesner et al. (2006). This reduction of summer sea-ice around the margins
478 of Greenland results in a positive sea-ice-albedo feedback and contributes to the observed
479 warming in this region, particularly in the Labrador Sea. At 125-ka there is still a reduction in
480 sea-ice in the Arctic compared with the pre-industrial but only up to 20% over the majority of
481 the region. By 120-ka the summer sea-ice concentration is similar if not greater than the pre-
482 industrial with over 50% sea-ice present again in the vicinity of the Labrador Sea. This
483 increase in sea-ice is attributed to the cooler climate as a result of reduced summer insolation
484 forcings toward the termination of the LIG. Although this reduction in average sea-ice over
485 the Arctic Ocean implies a significant temperature difference relative to pre-industrial, the
486 inter-annual variability over the averaging period of the simulations ranges from ~ 0 to $+1^{\circ}\text{C}$
487 and, therefore, results in the regional temperature differences being statistically insignificant
488 (see Fig. 5).

489

490

491 GrIS contribution to the LIG highstand

492 3.2

493 ~~GrIS contribution to the Last Interglacial highstand~~

494 In order to estimate the contribution of the GrIS to LIG sea-level change we drive 500
495 realisations of ~~thean~~ ice sheet model with the GCM-predicted evolving climate from 136 to
496 120ka. Consequently, ice sheet geometry is predicted throughout the LIG and compared with
497 reconstructed ice-surface extent data as implied from various ice cores on Greenland. The
498 impact of ice sheet model parametric uncertainty (Stone et al., 2010) on the evolution of the
499 GrIS through the LIG is used to derive a probability density function of the Greenland
500 contribution to LIG sea-level rise contingent on our modelling choices. This also takes into
501 account the mismatch between present-day observed and modelled ice sheets, most likely
502 due to missing higher order physical ice dynamics and the inclusion of a parameterised
503 surface mass balance scheme.

504

505 All 500 ice sheet model simulations show contraction of the ice sheet in response to peak LIG
506 warming. Figure 6a shows the evolution of absolute ice volume throughout the 16,000 year
507 ice sheet simulations. Also shown is the spin-up for the modern day GrIS for each ensemble
508 member and subsequent spin-up using the 136ka climatology to give an approximation of the
509 initial GrIS state at 136ka. It is possible to reject a number of the GrIS LHS experiments
510 using proxy palaeo data from the LIG. We use the criteria of the presence of ice persisting ~~It~~
511 ~~has been shown that~~ at the Summit (Raynaud et al., 1997) and NorthGRIP (NorthGRIP,
512 2004) ice cores on Greenland, ~~ice very likely persisted~~ throughout most of the LIG ~~at these~~
513 ~~locations~~. The Dye-3, Camp Century and Renland ice cores are not, however, used to
514 reject/accept simulations, as the evidence for the presence of ice there is more equivocal. In
515 addition, simulations which make a negative contribution to sea-level change are also
516 rejected. As a result a subset of 73 simulations are selected according to this evidence from
517 the ice core data; that is simulations where ice is absent at the NorthGRIP and Summit ice
518 cores are rejected. The selected simulations are shown in Fig. ~~ure~~ 6b, including a
519 representation of their ability to reproduce the modern day GrIS according to a skill-score
520 (for a given set of input parameters θ) given by

521

$$522 \quad s(\theta) = -\frac{1}{2n} \sum_{i=1}^n \frac{(x_i - f_i(\theta))^2}{\sigma^2 + \tau^2}, \quad (7)$$

523

524 where n is the number of grid-points, x_i is the observational ice thickness at each grid-point i ,
525 $f_i(\theta)$ is the experimental ice thickness at each grid-point for each ensemble member, σ is the
526 ice thickness Root Mean Squared Error (RMSE) of the median parameter set experiment in
527 terms of the LHS shown in Fig. ~~ure~~ 1- and τ^2 is the observational error variance at each grid-
528 point. The observational error is assumed to be constant across all grid-points. This skill-
529 score for modern ice thickness measures the spatial fit over the model domain assuming the
530 differences between model and observation at each grid-point location are independent and
531 normally distributed. We calculate the differences with respect to the digital elevation model
532 derived by Bamber et al. (2001), interpolated to a 20 km resolution.

533

534 The ice sheet retreats in all selected cases compared with the pre-industrial, in response to the
535 orbitally induced warming, with minimum ice sheet volume reached between 125-ka and

536 | 120.5-ka. All simulations show recovery towards the end of the LIG in response to the
537 | reduction in summer insolation. This is also shown by the average temperature anomaly over
538 | the Greenland region which peaks at around 2 to 5°C for the selected members of the
539 | ensemble (see Fig. 7). Maximum GrIS contribution to LIG sea-level rise ranges between 0.4
540 | and 3.8 m (Fig. 6c). None of the accepted simulations show an absence of ice in the vicinity
541 | of the Dye-3 ice core in accordance with some evidence that ice persisted through the LIG at
542 | this location (NorthGRIP, 2004; Willerslev et al., 2007). However, there is large uncertainty
543 | in the dating of basal ice at this location (Willerslev et al., 2007) which is why it is not
544 | appropriate to use this data as a direct constraint on GrIS extent. Figure 8a-c shows the GrIS
545 | geometries for parameter sets resulting in the maximum, most likely and minimum ~~and most~~
546 | ~~likely~~ (according to the skill-score) contribution to LIG sea-level change. Also shown is the
547 | respective ensemble member modern day GrIS geometry (Fig. 8e-g). The associated
548 | precipitation and temperature forcings for the simulation with the highest skill-score, derived
549 | from HadCM3 according to the coupling methodology, are shown in Fig. S2 in
550 | Supplementary Information. The cases where minimum ice volume and maximum
551 | temperature anomaly are reached are given and illustrate the latitudinal gradient in
552 | temperature from the enhanced insolation forcing and the change in topographic height in
553 | response to the warming. The most likely extent of the GrIS shows retreat from the northern
554 | margins but ice is still present over central and southern Greenland (Fig. 8b). This contrasts
555 | with several previous studies (Cuffey and Marshall, 2000; Tarasov and Peltier, 2003;
556 | Lhomme et al., 2005; Otto-Bliesner et al., 2006) where ice sheet retreat is sensitive in the
557 | south but not the north. However, this sensitivity of the northern margin agrees with other
558 | recent GrIS simulations (Fyke et al., 2011; Greve et al., 2011; Born and Nisancioglu, 2012;
559 | Quiquet et al., 2012). An isolated cap remains in the vicinity of the Camp Century and
560 | Renland ice core locations for all simulations where ice also persists in the Summit region, in
561 | agreement with evidence suggesting ice also persisted here (Johnsen et al., 2001). The
562 | drawdown of the ice surface at the Summit core location in Fig. 8a and Fig. 8b is ~450 m and
563 | ~60 m respectively, consistent with ice core data (Raynaud et al., 1997). In contrast, Fig. 8c
564 | shows little change from the modern day ice sheet extent with an increase of ~50 m at the
565 | location of Summit.

3.2.1 Probabilistic assessment of GrIS contribution to the LIG highstand

It is possible to derive a probabilistic assessment of GrIS contribution to LIG sea-level rise by considering the LIG palaeo-evidence of the GrIS geometry, uncertainty in ice sheet model parameterisation and the ability of the ice sheet model to reproduce the modern day ice sheet. In this section we outline our probabilistic method followed by an assessment of the likely contribution of the GrIS to LIG sea-level rise including a sensitivity analysis to the method used.

Probabilistic method

From Bayes' Theorem for a continuous distribution:

$$P[\theta|Y] \propto P[\theta]P[Y|\theta], \quad (8)$$

the posterior probability distribution ($P[\theta|Y]$) is proportional to the prior probability distribution ($P[\theta]$) multiplied by the likelihood function ($P[Y|\theta]$). The likelihood function, $P[Y|\theta]$, is calculated for each member of the ensemble from the skill-score given in [Eq. equation \(7\)](#).

$$P[Y|\theta] = A \cdot e^{s(\theta)} \cdot l(\theta), \quad (9)$$

where A is a normalising constant such that the $\sum P[Y|\theta] = 1$ and the logistic function, $l(\theta)$ accounts for the uncertainty as to where the simulated ice sheet margin lies relative to the ice core locations at the resolution of the ice sheet model domain

$$l(\theta) = \frac{1}{2} \left[1 - \tanh \left(\frac{Y(\theta) - Y_{max}}{2l_w} \right) \right]. \quad (10)$$

$Y(\theta)$ is the maximum sea-level change for each member of the ensemble, Y_{max} is the maximum contribution to LIG sea-level rise from the accepted simulations (in this case 3.8 m) and l_w is the logistic width.

595 The prior probability distribution, $P[\theta]$, weights each ensemble member according to its
 596 parameter set probability. ~~The most basic is that each parameter is uniformly distributed such~~
 597 ~~that each ensemble member is equally weighted. However,~~ According to Stone et al. (2010)
 598 the parameter sets can reasonably be weighted as Gaussian 2-sigma ranges such that the
 599 extreme parameter choices are penalised. Hence, we model the prior probability distribution
 600 as a multivariate Gaussian distribution

601

$$602 \quad P[\theta] = \frac{1}{(2\pi)^{\frac{5}{2}} \cdot 2 \cdot \prod_{j=1}^5 \sigma_j} \times \exp\left\{-\frac{1}{2} \sum_{j=1}^5 \left(\frac{\theta_j - \mu_j}{2\sigma_j}\right)^2\right\}, \quad (11)$$

603

604 where θ_j is the value of each parameter j , σ_j is the standard deviation for each parameter and μ_j
 605 is the mean for each parameter range (see Table 1). A comparison of the derived probability
 606 density function between Gaussian and uniform prior probability distributions indicates the
 607 choice of prior probability distribution does not have a notable affect on the outcome of the
 608 overall probability density function.

609

610 Subsequently, the posterior probability distribution of the ensemble and the associated
 611 maximum LIG sea-level contribution are used to construct a probability density function
 612 using a Kkernel density estimator (Wand and Jones, 1995; Bowman and Azzalini, 1997). A
 613 probability density function is a function that describes the relative likelihood of a variable
 614 (in this case maximum sea-level change) to take on a particular given value. The probability
 615 for the variable to fall within a particular region is given by the integral of this variable's
 616 density over the region. ~~This integral must add up to one.~~ A Kkernel estimator is a non-
 617 parametric way of estimating the probability density function of a particular variable and is
 618 closely related to a histogram. Unlike a histogram, a smooth kKernel function rather than a
 619 discrete box is used and each of these is centred directly over each model output in order to
 620 remove the dependence of end points of bins which occurs using a histogram method (Wand
 621 and Jones, 1995). In this way the kKernel estimator smoothes out the contribution of each
 622 observed data point over a local neighbourhood to that data point. The kKernel density
 623 estimator at any point Y , $\hat{g}(Y)$, is of the form

624

$$625 \quad \hat{g}(Y) = \frac{1}{n} \sum_{i=1}^n K\left(\frac{Y - Y_i}{h}\right), \quad (12)$$

626

627 where n is the number of ensemble members, K is a function satisfying $\int K(Y)dY = 1$, the
628 kKernel, whose variance is controlled by the parameter, h (usually known as the window
629 width or smoothing parameter). K is chosen to be a unimodal probability density function that
630 is symmetric about zero. In this case we implement a normal density
631 function $\left(K(Y) = \frac{1}{\sqrt{2\pi}} e^{-\frac{1}{2}Y^2} \right)$.

632

633 The choice of h is important since structure in the data can be lost by over-smoothing. Scott
634 (1992) shows that the reference rule bandwidth with a normal kernel is

635

$$636 \quad h = (4/3)^{1/5} \hat{\sigma} n^{-1/5} \approx 1.06 \hat{\sigma} n^{-1/5}, \quad (13)$$

637

638 where $\hat{\sigma}$ is the sample standard deviation, in this case for maximum LIG sea level, and n is
639 the sample number. Alternatively, we can choose a kKernel width based on the modern ice
640 sheet volume ensemble distribution. Figure 9 shows kKernel widths that result in the
641 measured ice volume lying 1, 1.5 and 2 standard deviations away from the mean of the
642 ensemble. In this way the smoothing parameter accounts for the additional uncertainty in the
643 ice sheet model resulting in overestimation of the modern day GrIS volume (see Fig. 6a).

644

645 **4 Probabilistic rResults and sensitiviitiessensitivities**

646 From the ensemble of 500 simulations we have derived a probabilistic assessment of the
647 likely contribution from the GrIS to LIG sea-level change (Fig. 10) with the uncertainty in the
648 ice model parameter distributions, modern day GrIS observations and the location of the
649 palaeo-data constraints taken into account. Although the maximum contribution from all the
650 selected simulations is 3.8 m, Fig. 10a shows the most likely maximum GrIS contribution to
651 LIG sea-level change is 1.5 m with a 90% probability that the maximum contribution falls
652 between 0.3 and 3.6 m. Figure 8d44 shows the predicted ice extent that results in a sea-level
653 contribution of 1.5 m for the LIG (Fig. 11b) derived from this probability density function.
654 This shows a similar pattern of retreat from the north and south-west as the ensemble member
655 with the highest skill-score (Fig. 8c). We further show that the maximum contribution range
656 varies from a maximum of 0.2 to 4.7 m to a minimum between 0.5 to 2.4 m depending on the

657 parameters chosen in the formulation of the density function which takes into account ice
658 sheet model uncertainty. There is a 90% probability of the GrIS contribution exceeding 0.6
659 m during the LIG and a 67% probability of exceeding 1.3 m. However, it is unlikely (<33%
660 probability) the contribution exceeded 2.2 m and very unlikely (<10%) that it exceeded 3.2 m
661 (Fig. 10b). Compared with estimates of the LIG sea-level highstand (Rostami et al., 2000;
662 Muhs et al., 2002; Kopp et al., 2009; Dutton and Lambeck, 2012) exceeding 4 m, we find that
663 sources other than the GrIS are required to account for this high sea-level, such as the West
664 Antarctic Ice Sheet (Scherer et al., 1998; Huybrechts, 2002) and/or the Canadian icefields
665 (Otto-Bliesner et al., 2006).

666

667 In order to assess the sensitivity of our probability density function to various uncertainties in
668 its construction we first examined the effect of varying the kernel width. Figure- 11a42
669 shows the case where the kernel width is applied to the LIG for the optimal width (0.40 m
670 according to Eq. equation (13)), and the modern day observation lying one ($h=1.50$ m) and
671 two ($h=0.75$ m) standard deviations away from the modern modelled ensemble mean.
672 Although the peak of the probability density function does not change, the upper tail is
673 sensitive to the kernel width with a very likely sea-level contribution exceedance ranging
674 between 3.1 and 4.1 m. The case with the optimal kernel width assumes the anomaly in ice
675 volume between the LIG and present day being biased in a consistent way. The alternative
676 extreme scenario is the case where the uncertainty in the anomaly is equivalent to the model
677 error such that the modern day ensemble lies only one standard deviation away from the
678 observation ($h=1.50$ m). We choose a kernel width of half this width, 0.75 m, as our most
679 plausible case, described above and shown in Fig. 10.

680

681 In order to further address the sensitivity of the probability density function to uncertainty we
682 also varied σ (Fig. 113ba), the observational error on modern day ice thickness (τ) (Fig.
683 113cb) (both given as input in equation-Eq. (7)) and the width of the logistic function (Fig.
684 113de). Figure 113ba shows when σ is equal to zero, the peak of the probability density
685 function coincides closely with the simulation with the highest skill-score. The spread shown
686 is a result of the kernel smoothing method used. When all simulations have equal skill
687 (equal weighting) the probability density function shows a similar response to when σ is
688 equal to the RMSE of the median experiment. The vertical accuracy of observational ice
689 thickness is between 10 and 100 m (Bamber et al., 2001; Layberry and Bamber, 2001) while
690 Bogorodskiy (1985) reports that a typical radar-sounding survey has an inherent uncertainty

691 | of about 15 m for ice depth measurements. Figure 113cb shows that the observation error
692 | between 10 and 100 m makes no noticeable change to the overall probability density
693 | function. Therefore, we use a value of 15 m. Figure 113de ~~indicates~~ shows that the choice of
694 | the logistic width parameter does show some sensitivity for the upper tail of the probability
695 | density function. In this case a value of 0.2_m is selected.

696 |
697 | In order to test the robustness of our skill-score on the resultant probability density function
698 | we modified Eq. (1) such that $n=1$ and used only the average ice-thickness as our metric.
699 | Figure 11e shows that this makes very little difference to the probability density function.

700 |
701 | ~~W~~We also tested the robustness of the coupling methodology by performing ~~ing~~ an ensemble
702 | of simulations where only two modelled climates (with and without the GrIS) were used in
703 | the coupling method illustrated in Fig. 4. We found that although this increased the number
704 | of accepted simulations it did not result in a notable difference in the overall structure of the
705 | probabilistic distribution of GrIS contribution to LIG sea-level (see Fig. S3).

706 |
707 | Finally, if the recent NEEM ice core drilling project reveals that ice persisted throughout the
708 | LIG at this location, then the GrIS contribution to LIG sea-level rise can be constrained
709 | further (61 accepted simulations compared with 73 when NEEM is not included) with values
710 | very likely (>90% probability) greater than 0.5 m but very unlikely (<10% probability)
711 | greater than 2.8 m (see Fig. 10c-d14).

713 | **34 Discussion and Conclusions**

714 | There are several caveats that should be discussed in the context of this study. Firstly, the
715 | uncertainty in dating basal ice limits to an extent the usefulness of this binary criterion. With
716 | the advent of new improved ice cores in the future (such as NEEM) it may be possible to
717 | preferentially weight the skill toward these improved ice cores. In the future other aspects of
718 | the new ice-cores could also be used for model evaluation, e.g. down-core temperature
719 | profiles. However, uncertainties associated with these observations are currently quite large.

720 |
721 | Secondly, these results, of course, are somewhat limited by the absence of climate model
722 | uncertainty. We use only one model where we linearly interpolate between ~~three~~ possible
723 | ~~extreme~~ LIG climate states. It is difficult to estimate the uncertainty in the LIG climate since

724 there is only limited data for this time. Future work could assess the impact of structural
725 climate model error on LIG sea-level change as part of the ~~palaeo-model inter-comparison~~
726 ~~project~~ PMIP 3 (PMIP3).

727
728 Thirdly, the PDD scheme used in calculating the surface mass balance, although efficient, as
729 it only needs temperature as an input and does ~~does~~ not requiree the use of regional climate
730 models, has been shown by van de Berg et al. (2011) to significantly underestimate melt for
731 simulations which include LIG insolation forcing compared with an approach which takes
732 insolation and albedo explicitly into account (Robinson et al., 2010). Van de Berg et al.
733 (2011) show that surface melt is affected not only by higher ambient temperatures but also
734 directly through stronger summertime insolation and associated non-linear feedbacks
735 (melting snow absorbs twice as much solar radiation as dry snow). Temperature-melt
736 relationships assume a fixed relation between near-surface air temperature and melt-rate but
737 this relation is also dependent on insolation and, therefore, changes in orbital forcing
738 parameters and the latitude. In essence, the PDD scheme fails to capture north-south melt
739 gradients driven by insolation gradients. As a result, inclusion of this process could melt the
740 GrIS further back during the LIG. Future improvements to the PDD scheme could be to use
741 PDD factors which are function of insolation change.

742 ~~Thirdly, recent work (Robinson et al., 2010; van de Berg et al., 2011) has shown that~~
743 ~~temperature-melt relationships are dependent on insolation and as such the PDD method for~~
744 ~~predicting surface mass balance change during the LIG may not be suitable due to its~~
745 ~~different insolation forcing compared with today. However, although the mass balance~~
746 ~~scheme used in this study does not take into account directly the radiative forcing, it does~~
747 ~~indirectly because the GCM sees the full insolation change, which then modifies the~~
748 ~~seasonality of the surface temperature which drives the PDD scheme.~~

749
750 Fourthly, our climate model simulations did not include interactive vegetation. Inclusion of
751 this feedback could partially explain the mismatch between data and model in terms of Arctic
752 temperature response to enhanced solar insolation because previous work with HadCM3 has
753 shown that vegetation feedbacks can have a significant impact on the evolution of the
754 Greenland ice-sheet (Stone and Lunt, 2012). In addition, other previous modelling studies
755 have highlighted the positive feedback from vegetation changes in response to increased solar
756 insolation during the Holocene and LIG (e.g. Foley et al., 1994; Harrison et al., 1995).

758 ~~Fourthly~~Fifthly, and perhaps most critically, the majority of the ensemble have an associated
759 modern ice sheet which is too large (Fig. 6a~~;~~-b), a feature of many ice sheet models (Ritz et
760 al., 1997; Ridley et al., 2005; Robinson et al., 2011). This is partly due to additional ice at the
761 margins not captured in the ice surface extent observation (Bamber et al., 2001) which
762 includes only the contiguous ice sheet. In common with many other studies (Lhomme et al.,
763 2005; Robinson et al., 2011), we assume that the predicted LIG volume anomaly with respect
764 to the predicted modern is more robust. This is because the overestimation of volume, which
765 is thought to result from the lack of higher-order terms in the ice-flow equations, is likely to
766 affect both modern and LIG ice sheets in a consistent manner. The omission of the basal
767 sliding process may also result in simulations being biased toward higher values for modern
768 day ice volume since it is likely this would result in the ice sheet melting back further. In
769 order, to account for potential bias, however, we choose a plausible probability density
770 function that takes into account this uncertainty. The skill-score used to generate the
771 probability density function (~~Eq.equation~~ (7)) does also ensure that the simulations which
772 have the best representation of the modern ice sheet contribute most to the probability density
773 function.

774
775 We observe substantial retreat of the GrIS in the north while the ice sheet remains relatively
776 stable in the south in contrast with many previous studies using a different forcing
777 methodology (e.g. Cuffey and Marshall 2000; Tarasov & Peltier 2003; Lhomme et al. 2005).
778 One fundamental difference between LIG ice sheets derived using climate forcings
779 reconstructed from ice core records (e.g. Letreguilly et al. 1991; Cuffey and Marshall 2000;
780 Lhomme et al. 2005) compared with a GCM is that the forcing fails to capture changes in
781 atmospheric circulation patterns, precipitation changes and the heterogeneity of climate
782 trends over Greenland. This failure to capture these processes is because the method uses the
783 present day temperature pattern which is perturbed by a spatially homogenous anomaly of
784 temperature derived from proxy data reconstructions (e.g. the GRIP ice core record).
785 Precipitation anomalies are simply calculated using a standard relationship where
786 precipitation is a function of temperature. Our method is similar to Born et al. (2012) who
787 partly explain the preferential LIG warming and melting of northern Greenland in their
788 results (which we also observe), but absent from most previous studies, as due to the impact
789 of larger insolation changes in the north of Greenland not adequately captured using the
790 proxy reconstruction forcing methods. Further differences between our study and previous
791 work include the bedrock topography used (e.g. Cuffey and Marshall 2000; Otto-Bliesner et

792 al. 2006), which has been previously shown to considerably affect simulated present day ice
793 volume (Stone et al. 2010), and the use of the PDD scheme compared with a method which
794 takes the impact of insolation on melt into account such as that used by Robinson et al.
795 (2011) (see discussion above).

796
797 Our climate model, when forced with LIG insolation anomalies, shows good agreement with
798 maximum summer warmth from LIG proxy temperature estimates in the Arctic region. We
799 show that the GrIS contribution to LIG sea-level change, consistent with ice core data, is
800 between 0.4 m and 3.8 m. However, it is very likely that the GrIS contributed between 0.3
801 and 3.6 m to LIG sea-level rise, lower than the range of ~~many previous~~ recent estimates, of
802 2.7 to 4.5 m (Cuffey and Marshall, 2000; Tarasov and Peltier, 2003; Kopp et al., 2009;
803 Robinson et al., 2011) but similar to the lower bound of Robinson et al. (2011) and the
804 estimate of 1.6 m from Colville et al. (2011). According to the global sea-level estimate for
805 the LIG derived by Kopp et al. (2009) the distribution suggests a 95% probability that the
806 GrIS reached a minimum at which it was at least 2.5 m of equivalent sea-level smaller than
807 today. By including this constraint we show a shift in the probability density function with a
808 peak contribution estimate of 3.2 m closer to the estimate of recent studies (Fig. 11f). ~~Our~~
809 estimate is more reliable because it derives from a full probabilistic analysis, taking into
810 account ice sheet model and data uncertainties. We also show that ice persists throughout the
811 LIG at the Dye-3 ice core for all accepted simulations consistent with the suggestion that ice
812 at the base of Dye-3 may predate the beginning of the LIG (Willerslev et al., 2007; Colville et
813 al., 2011) although dating of basal ice at this location is equivocal (Willerslev et al., 2007).

814
815 In conclusion, this study emphasises the importance of including ice sheet model parametric
816 uncertainty and palaeo-data as well as modern observations, in the context of a probabilistic
817 assessment when evaluating the impact of ~~the Arctic on~~ climate change on ice sheets.
818 Furthermore, we show that in order for a full probabilistic analysis to effectively take into
819 account robust skill-scores based on simulating the modern day GrIS, efforts should be
820 directed at improving the existing ice sheet model physics and representation of fast flowing
821 processes in models used by the palaeoclimate community whilst still minimising
822 computational costs.

826 **Acknowledgements**

827 This work was carried out with funding from a NERC studentship and the European
828 project [Ppast4Future](#). This is Past4Future contribution n° 28. The research leading to these
829 results has received funding from the European Union's Seventh Framework programme
830 (FP7/2007-2013) under grant agreement n° 243908, [“Past4Future. Climate change -
831 Learning from the past climate”](#). [This work is also partly associated with “iGlass”,
832 NE/I010874/1.](#)

833

834

835 **References**

836 [Alley, R. B., Andrews, J. T., Brigham-Grette, J., Clarke, G. K. C., Cuffey, K. M., Fitzpatrick,
837 J. J., Funder, S., Marshall, S. J., Miller, G. H., Mitrovica, J. X., Muhs, D. R., Otto-Bliesner,
838 B. L., Polyak, L., and White, J. W. C.: History of the Greenland Ice Sheet: paleoclimatic
839 insights, *Quat. Sci. Rev.*, 29, 1728-1756, \[10.1016/j.quascirev.2010.02.007\]\(#\), 2010.](#)

840

841 Anderson, P., Bermike, O., Bigelow, N., Brigham-Grette, J., Duvall, M., Edwards, M.,
842 Frechette, B., Funder, S., Johnsen, S., Knies, J., Koerner, R., Lozhkin, A., Marshall, S.,
843 Matthiessen, J., Macdonald, G., Miller, G., Montoya, M., Muhs, D., Otto-Bliesner, B.,
844 Overpeck, J., Reeh, N., Sejrup, H. P., Spielhagen, R., Turner, C., Velichko, A., and Members,
845 C.-L. I. P.: Last Interglacial Arctic warmth confirms polar amplification of climate change,
846 *Quat. Sci. Rev.*, 25, 1383-1400, 2006.

847

848 [Applegate, P. J., Kirchner, N., Stone, E. J., Keller, K., and Greve, R.: An assessment of key
849 model parametric uncertainties in projections of Greenland Ice Sheet behavior, *The
850 Cryosphere*, 6, 589-606, 2012.](#)

851

852 Bamber, J. L., Layberry, R. L., and Gogineni, P.: A new ice thickness and bed data set for the
853 Greenland ice sheet 1. Measurement, data reduction, and errors, *J. Geophys. Res.*, 106,
854 33773-33780, 2001.

855

856 Berger, A., and Loutre, M. F.: Insolation Values for the Climate of the Last 10 Million Years,
857 *Quat. Sci. Rev.*, 10, 297-317, 1991.

858

859 Bogorodskiy, V. V.: Radioglaciology, D. Reidel Publishing Company, Dordrecht, 1985.

860 Born, A., and Nisancioglu, K. H.: Melting of Northern Greenland during the last
861 interglaciation, *The Cryosphere*, 6, 1239-1250, 2012.

862

863 Bowman, A. W., and Azzalini, A.: *Applied Smoothing Techniques For Data Analysis: The*
864 *Kernel Approach with S-Plus Illustrations*, 18, Oxford Univ. Press, New York, 1997.

865 Cattle, H., and Crossley, J.: Modeling Arctic Climate-Change, *Philos. Trans. R. Soc. London*
866 *Ser. A*, 352, 201-213, 1995.

867

868 [Chappellaz, J., Brook, E., Blunier, T., and Malaize, B.: CH4 and delta O-18 of O-2 records](#)
869 [from Antarctic and Greenland ice: A clue for stratigraphic disturbance in the bottom part of](#)
870 [the Greenland Ice Core Project and the Greenland Ice Sheet Project 2 ice cores, *J Geophys*](#)
871 [Res-Oceans, 102, 26547-26557, 1997.](#)

872

873 Colville, E. J., Carlson, A. E., Beard, B. L., Hatfield, R. G., Stoner, J. S., Reyes, A. V., and
874 Ullman, D. J.: Sr-Nd-Pb Isotope Evidence for Ice-Sheet Presence on Southern Greenland
875 During the Last Interglacial, *Science*, 333, 620-623, 2011.

876

877 Cox, P. M., Betts, R. A., Bunton, C. B., Essery, R. L. H., Rowntree, P. R., and Smith, J.: The
878 impact of new land surface physics on the GCM simulation of climate and climate sensitivity,
879 *Clim. Dyn.*, 15, 183-203, 1999.

880

881 Cuffey, K. M., and Marshall, S. J.: Substantial contribution to sea-level rise during the last
882 interglacial from the Greenland ice sheet, *Nature*, 404, 591-594, 2000.

883

884 DeConto, R. M., and Pollard, D.: Rapid Cenozoic glaciation of Antarctica induced by
885 declining atmospheric CO₂, *Nature*, 421, 245-249, 2003.

886

887 [Dutton, A., and Lambeck, K.: Ice Volume and Sea Level During the Last Interglacial,](#)
888 [*Science*, 337, 216-219, 2012.](#)

889

890 [Foley, J. A., Kutzbach, J. E., Coe, M. T., and Levis, S.: Feedbacks between climate and](#)
891 [boreal forests during the Holocene epoch, *Nature*, 371, 52-54, 1994.](#)

892

893

894
895
896
897
898
899
900
901
902
903
904
905
906
907
908
909
910
911
912
913
914
915
916
917
918
919
920
921
922
923
924
925
926

Fyke, J. G., Weaver, A. J., Pollard, D., Eby, M., Carter, L., and Mackintosh, A.: A new coupled ice sheet/climate model: description and sensitivity to model physics under Eemian, Last Glacial Maximum, late Holocene and modern climate conditions, *Geosci. Model Dev.*, 4, 117-136, 2011.

Gent, P. R., and McWilliams, J. C.: Isopycnal Mixing in Ocean Circulation Models, *J Phys Oceanogr*, 20, 150-155, 1990.

Gordon, C., Cooper, C., Senior, C. A., Banks, H., Gregory, J. M., Johns, T. C., Mitchell, J. F. B., and Wood, R. A.: The simulation of SST, sea ice extents and ocean heat transports in a version of the Hadley Centre coupled model without flux adjustments, *Clim. Dyn.*, 16, 147-168, 2000.

Gregory, J. M., and Mitchell, J. F. B.: The climate response to CO₂ of the Hadley Centre coupled AOGCM with and without flux adjustment, *Geophys. Res. Lett.*, 24, 1943-1946, 1997.

Greve, R.: Relation of measured basal temperatures and the spatial distribution of the geothermal heat flux for the Greenland ice sheet, *Ann. Glaciol.*, 42, 424-432, 2005.

Greve, R., Saito, F., and Abe-Ouchi, A.: Initial results of the SeaRISE numerical experiments with the models SICOPOLIS and IcIES for the Greenland ice sheet, *Ann. Glaciol.*, 52, 23-30, 2011.

[Grootes, P. M., Stuiver, M., White, J. W. C., Johnsen, S., and Jouzel, J.: Comparison of Oxygen-Isotope Records from the GISP2 and GRIP Greenland Ice Cores, *Nature*, 366, 552-554, 1993.](#)

Hanna, E., Huybrechts, P., Janssens, I., Cappelen, J., Steffen, K., and Stephens, A.: Runoff and mass balance of the Greenland ice sheet: 1958-2003, *J. Geophys. Res.*, 110, doi:10.1029/2004JD005641, 2005.

927 [Harrison, S. P., Kutzbach, J. E., Prentice, I. C., Behling, P. J., and Sykes, M. T.: The](#)
928 [Response of Northern-Hemisphere Extratropical Climate and Vegetation to Orbitally Induced](#)
929 [Changes in Insolation during the Last Interglaciation, Quaternary Res., 43, 174-184, 1995.](#)
930

931 Hibler, W. D.: A Dynamic Thermodynamic Sea Ice Model, J Phys Oceanogr, 9, 815-846,
932 1979.
933

934 Huybrechts, P.: Sea-level changes at the LGM from ice-dynamic reconstructions of the
935 Greenland and Antarctic ice sheets during the glacial cycles, Quat. Sci. Rev., 21, 203-231,
936 2002.
937

938 [Johnsen, S. J., Clausen, H. B., Dansgaard, W., Gundestrup, N. S., Hammer, C. U., Andersen,](#)
939 [U., Andersen, K. K., Hvidberg, C. S., DahlJensen, D., Steffensen, J. P., Shoji, H.,](#)
940 [Sveinbjornsdottir, A. E., White, J., Jouzel, J., and Fisher, D.: The delta O-18 record along the](#)
941 [Greenland Ice Core Project deep ice core and the problem of possible Eemian climatic](#)
942 [instability, J Geophys Res-Oceans, 102, 26397-26410, 1997.](#)
943

944 Johnsen, S. J., DahlJensen, D., Gundestrup, N., Steffensen, J. P., Clausen, H. B., Miller, H.,
945 Masson-Delmotte, V., Sveinbjornsdottir, A. E., and White, J.: Oxygen isotope and
946 palaeotemperature records from six Greenland ice-core stations: Camp Century, Dye-3,
947 GRIP, GISP2, Renland and NorthGRIP, J. Quat. Sci., 16, 299-307, 2001.
948

949 Kaspar, F., Kuhl, N., Cubasch, U., and Litt, T.: A model-data comparison of European
950 temperatures in the Eemian interglacial, Geophys. Res. Lett., 32,
951 doi:10.1029/2005GL022456, 2005.
952

953 Kienast, F., Tarasov, P., Schirrmeister, L., Grosse, G., and Andreev, A. A.: Continental
954 climate in the East Siberian Arctic during the last interglacial: Implications from
955 palaeobotanical records, Global Planet. Change, 60, 535-562, 2008.
956

957 [Koerner, R., and Fischer, H.: Ice-core evidence for widespread Arctic glacier retreat in the](#)
958 [Last Interglacial and the early Holocene, Ann. Glaciol., 35, 19-24, 2002.](#)
959

960 Kopp, R. E., Simons, F. J., Mitrovica, J. X., Maloof, A. C., and Oppenheimer, M.:
961 Probabilistic assessment of sea level during the last interglacial stage, *Nature*, 462, 863-868,
962 2009.

963

964 Lambeck, K., and Nakiboglu, S. M.: Seamount Loading and Stress in the Ocean Lithosphere,
965 *J. Geophys. Res.*, 85, 6403-6418, 1980.

966

967 Laskar, J., Robutel, P., Joutel, F., Gastineau, M., Correia, A. C. M., and Levrard, B.: A long-
968 term numerical solution for the insolation quantities of the Earth, *Astron. Astrophys.*, 428,
969 261-285, 2004.

970

971 Layberry, R. L., and Bamber, J. L.: A new ice thickness and bed data set for the Greenland
972 ice sheet 2. Relationship between dynamics and basal topography, *J. Geophys. Res.*, 106,
973 33781-33788, 2001.

974

975 Letréguilly, A., Reeh, N., and Huybrechts, P.: The Greenland ice sheet through the last
976 glacial-interglacial cycle, *Global Planet. Change*, 90, 385-394, 1991.

977

978 Lhomme, N., Clarke, G. K. C., and Marshall, S. J.: Tracer transport in the Greenland Ice
979 Sheet: constraints on ice cores and glacial history, *Quat. Sci. Rev.*, 24, 173-194, 2005.

980

981 [Lisiecki, L. E., and Raymo, M. E.: A Pliocene-Pleistocene stack of 57 globally distributed](#)
982 [benthic delta O-18 records, *Paleoceanography*, 20, 10.1029/2004pa001071, 2005.](#)

983

984 Louergue, L., Parrenin, F., Blunier, T., Barnola, J. M., Spahni, R., Schilt, A., Raisbeck, G.,
985 and Chappellaz, J.: New constraints on the gas age-ice age difference along the EPICA ice
986 cores, 0-50 kyr, *Clim. Past*, 3, 527-540, 2007.

987

988 Loutre, M. F., Berger, A., Crucifix, M., Desprat, S., and Sánchez-Göni, M. F.: Interglacials as
989 Simulated by the LLN 2-D NH and MoBidiC Climate Models, in: *The Climate of Past*
990 *Interglacials*, 7, 1st ed., edited by: Sirocko, F., Claussen, M., Litt, T., and Sánchez-Göni, M.
991 F., *Development in Quaternary Science*, 7, Elsevier, Oxford, 547-561, 2007.

992

993 Lunt, D. J., Foster, G. L., Haywood, A. M., and Stone, E. J.: Late Pliocene Greenland
994 glaciation controlled by a decline in atmospheric CO₂ levels, *Nature*, 454, 1102-1105, 2008.
995

996 Lunt, D. J., Haywood, A. M., Foster, G. L., and Stone, E. J.: The Arctic cryosphere in the
997 Mid-Pliocene and the future, *Philos. Trans. R. Soc. London Ser. A*, 367, 49-67, 2009.
998

999 Lüthi, D., Le Floch, M., Bereiter, B., Blunier, T., Barnola, J. M., Siegenthaler, U., Raynaud,
1000 D., Jouzel, J., Fischer, H., Kawamura, K., and Stocker, T. F.: High-resolution carbon dioxide
1001 concentration record 650,000-800,000 years before present, *Nature*, 453, 379-382,
1002 10.1038/Nature06949, 2008.
1003

1004 [McKay, M. D., Beckman, R. J., and Conover, W. J.: A Comparison of Three Methods for](#)
1005 [Selecting Values of Input Variables in the Analysis of Output from a Computer Code,](#)
1006 [Technometrics, 21, 239-245, 1979.](#)
1007

1008 Milankovitch, M.: *Kanon der Erdbestrahlungen und seine Anwendung auf das*
1009 *Eiszeitenproblem* Belgrade. (English translation *Canon of Insolation and the Ice-Age*
1010 *Problem*), Israel Program for Scientific Translations, 1969, Jerusalem, 1941.
1011

1012 Montoya, M., von Storch, H., and Crowley, T. J.: Climate simulation for 125 kyr BP with a
1013 coupled ocean-atmosphere general circulation model, *J. Clim.*, 13, 1057-1072, 2000.
1014

1015 Muhs, D. R., Ager, T. A., and Begét, J. E.: Vegetation and paleoclimate of the last
1016 interglacial period, central Alaska, *Quat. Sci. Rev.*, 20, 41-61, 2001.
1017

1018 Muhs, D. R., Simmons, K. R., and Steinke, B.: Timing and warmth of the Last Interglacial
1019 period: new U-series evidence from Hawaii and Bermuda and a new fossil compilation for
1020 North America, *Quat. Sci. Rev.*, 21, 1355-1383, 2002.
1021

1022 NorthGRIP: High-resolution record of Northern Hemisphere climate extending into the last
1023 interglacial period, *Nature*, 431, 147-151, 2004.
1024

1025 Otto-Bliesner, B. L., Marsha, S. J., Overpeck, J. T., Miller, G. H., Hu, A. X., and CAPE:
1026 Simulating Arctic Climate Warmth and Icefield Retreat in the Last Interglaciation, *Science*,
1027 311, 1751-1753, 2006.

1028

1029 [Parizek, B. R., and Alley, R. B.: Implications of increased Greenland surface melt under](#)
1030 [global-warming scenarios: ice-sheet simulations, *Quaternary Science Reviews*, 23, 1013-](#)
1031 [1027, 2004.](#)

1032

1033 Payne, A. J.: A thermomechanical model of ice flow in West Antarctica, *Clim. Dyn.*, 15, 115-
1034 125, 1999.

1035

1036 Pépin, L., Raynaud, D., Barnola, J. M., and Loutre, M. F.: Hemispheric roles of climate
1037 forcings during glacial-interglacial transitions as deduced from the Vostok record and LLN-
1038 2D model experiments, *J. Geophys. Res.*, 106, 31885-31892, 2001.

1039

1040 Petit, J. R., Jouzel, J., Raynaud, D., Barkov, N. I., Barnola, J. M., Basile, I., Bender, M.,
1041 Chappellaz, J., Davis, M., Delaygue, G., Delmotte, M., Kotlyakov, V. M., Legrand, M.,
1042 Lipenkov, V. Y., Lorius, C., Pepin, L., Ritz, C., Saltzman, E., and Stievenard, M.: Climate
1043 and atmospheric history of the past 420,000 years from the Vostok ice core, Antarctica,
1044 *Nature*, 399, 429-436, 1999.

1045

1046 Pollard, D., and Thompson, S. L.: Driving a high-resolution dynamic ice sheet model with
1047 GCM climate: ice-sheet initiation at 116,000BP, *Ann. Glaciol.*, 25, 296-304, 1997.

1048

1049 Pope, V. D., Gallani, M. L., Rowntree, P. R., and Stratton, R. A.: The impact of new physical
1050 parametrizations in the Hadley Centre climate model: HadAM3, *Clim. Dyn.*, 16, 123-146,
1051 2000.

1052

1053 [Quiquet, A., Ritz, C., Punge, H. J., and Salas y Méliá, D.: Contribution of Greenland ice sheet](#)
1054 [melting to sea level rise during the last interglacial period: an approach combining ice sheet](#)
1055 [modelling and proxy data, *Clim. Past Discuss.*, 8, 3345-3377, 2012.](#)

1056

1057 Raynaud, D., Chappellaz, J., Ritz, C., and Martinerie, P.: Air content along the Greenland Ice
1058 Core Project core: A record of surface climatic parameters and elevation in central
1059 Greenland, *J. Geophys. Res.*, 102, 26607-26613, 1997.

1060

1061 Reeh, N.: Parameterization of melt rate and surface temperature on the Greenland ice sheet,
1062 *Polarforschung*, 59, 113-128, 1991.

1063

1064 Ridley, J. K., Huybrechts, P., Gregory, J. M., and Lowe, J. A.: Elimination of the Greenland
1065 ice sheet in a high CO₂ climate, *J. Clim.*, 18, 3409-3427, 2005.

1066

1067 Ritz, C., Fabre, A., and Letréguilly, A.: Sensitivity of a Greenland ice sheet model to ice flow
1068 and ablation parameters: Consequences for the evolution through the last climatic cycle,
1069 *Clim. Dyn.*, 13, 11-24, 1997.

1070

1071 [Robinson, A., Calov, R., and Ganopolski, A.: An efficient regional energy-moisture balance](#)
1072 [model for simulation of the Greenland Ice Sheet response to climate change, *The Cryosphere*,](#)
1073 [4, 129-144, 2010.](#)

1074

1075 Robinson, A., Calov, R., and Ganopolski, A.: Greenland ice sheet model parameters
1076 constrained using simulations of the Eemian Interglacial, *Clim. Past*, 7, 381-396, 2011.

1077

1078 Rogozhina, I., Martinec, Z., Hagedoorn, J. M., Thomas, M., and Fleming, K.: On the long-
1079 term memory of the Greenland Ice Sheet, *J. Geophys. Res.*, 116, doi: 10.1029/2010jf001787,
1080 2011.

1081

1082 Rostami, K., Peltier, W. R., and Mangini, A.: Quaternary marine terraces, sea-level changes
1083 and uplift history of Patagonia, Argentina: comparisons with predictions of the ICE-4G
1084 (VM2) model of the global process of glacial isostatic adjustment, *Quat. Sci. Rev.*, 19, 1495-
1085 1525, 2000.

1086

1087 Rutt, I. C., Hagdorn, M., Hulton, N. R. J., and Payne, A. J.: The Glimmer community ice
1088 sheet model, *J. Geophys. Res.*, 114, doi:10.1029/2008JF001015, 2009.

1089

1090 Scherer, R. P., Aldahan, A., Tulaczyk, S., Possnert, G., Engelhardt, H., and Kamb, B.:
1091 Pleistocene collapse of the West Antarctic Ice Sheet, *Science*, 281, 82-85, 1998.
1092
1093 Scott, C.: *Multivariate Density Estimation: theory, practice and Visualization*, John Wiley &
1094 Sons, New York, 1992.
1095
1096 Siddall, M., Chappell, J., and Potter, E.-K.: Eustatic Sea level During Past Interglacials, in:
1097 *The Climate of Past Interglacials*, 7, 1st ed., edited by: Sirocko, F., Claussen, M., Litt, T., and
1098 Sánchez-Göni, M. F., *Development in Quaternary Science*, 7, Elsevier, Oxford, 75-92, 2007.
1099 Slowey, N. C., Henderson, G. M., and Curry, W. B.: Direct U-Th dating of marine sediments
1100 from the two most recent interglacial periods, *Nature*, 383, 242-244, 1996.
1101
1102 Stone, E. J., Lunt, D. J., Rutt, I. C., and Hanna, E.: Investigating the sensitivity of numerical
1103 model simulations of the modern state of the Greenland ice-sheet and its future response to
1104 climate change, *The Cryosphere* 4, 397–417, 10.5194/tc-4-397-2010, 2010.
1105
1106 [Stone, E. J., and Lunt, D. J.: The role of vegetation feedbacks on Greenland glaciation, *Clim.*](#)
1107 [*Dyn.*, 10.1007/s00382-012-1390-4, 2012.](#)
1108
1109 Suwa, M., von Fischer, J. C., Bender, M. L., Landais, A., and Brook, E. J.: Chronology
1110 reconstruction for the disturbed bottom section of the GISP2 and the GRIP ice cores:
1111 Implications for Termination II in Greenland, *J. Geophys. Res.*, 111, 10.1029/2005jd006032,
1112 2006.
1113
1114 Tarasov, L., and Peltier, W. R.: Greenland glacial history, borehole constraints, and Eemian
1115 extent, *J. Geophys. Res.*, 108, doi:10.1029/2001JB001731, 2003.
1116
1117 Uppala, S. M., Kallberg, P. W., Simmons, A. J., Andrae, U., Da Costa Bechtold, V., Fiorino,
1118 M., Gibson, K., Haseler, J., Hernandez, A., Kelly, G. A., Li, X., Onogi, K., Saarinen, S.,
1119 Sokka, N., Allan, R. P., Andersson, E., Arpe, K., Balmaseda, M. A., Beljaars, A. C., Van de
1120 Berg, L., Bidlot, J., Bormann, N., Caires, S., Chevallier, F., Dethof, A., Dragosavac, M.,
1121 Fisher, M., Fuentes, M., Hagemann, S., Holm, E., Hoskins, B. J., Isaksen, L., Janssen, P. A.
1122 E. M., Jenne, R., McNally, A. P., Mahfouf, J.-F., Morcrette, J.-J., Rayner, N. A., Saunders, R.

1123 W., Simon, P., Sterl, A., Trenberth, K. E., Untch, A., Vasiljevic, D., Viterbo, P., and
1124 Woollen, J.: The ERA-40 re-analysis, *Q. J. R. Meteorol. Soc.*, 131, 2961-3013, 2005.
1125
1126 van de Berg, W. J., van den Broeke, M., Ettema, J., van Meijgaard, E., and Kaspar, F.:
1127 Significant contribution of insolation to Eemian melting of the Greenland ice sheet, *Nat*
1128 *Geosci*, 4, 679-683, 2011.
1129
1130 Vizcaíno, M., Milkolajewicz, U., Groger, M., Maier-reimer, E., Schurgers, G., and Winguth,
1131 A. M. E.: Long-term ice sheet-climate interactions under anthropogenic greenhouse forcing
1132 simulated with a complex Earth System Model, *Clim. Dyn.*, 31, 665–690, 2008.
1133
1134 Wand, M. P., and Jones, M. C.: *Kernel Smoothing*, 60, Chapman & Hall/CRC, Boca Raton,
1135 | 1995.
1136
1137 Willerslev, E., Cappellini, E., Boomsma, W., Nielsen, R., Hebsgaard, M. B., Brand, T. B.,
1138 Hofreiter, M., Bunce, M., Poinar, H. N., Dahl-Jensen, D., Johnsen, S., Steffensen, J. P.,
1139 Bennike, O., Schwenninger, J. L., Nathan, R., Armitage, S., de Hoog, C. J., Alfimov, V.,
1140 Christl, M., Beer, J., Muscheler, R., Barker, J., Sharp, M., Penkman, K. E. H., Haile, J.,
1141 Taberlet, P., Gilbert, M. T. P., Casoli, A., Campani, E., and Collins, M. J.: Ancient
1142 biomolecules from deep ice cores reveal a forested Southern Greenland, *Science*, 317, 111-
1143 114, 2007.
1144
1145 Yin, Q. Z., and Berger, A.: Individual contribution of insolation and CO₂ to the interglacial
1146 climates of the past 800,000 years, *Clim. Dyn.*, 38, 709-724, 2012
1147
1148
1149 |
1150 |
1151 |
1152 |
1153 |
1154 |
1155 |

1156 **Table 1.** List of five parameters varied according to ranges determined in the literature (Stone
 1157 et al., 2010). Also included are the mean and standard deviation for each parameter used in
 1158 [Eq. equation](#) (11).

Parameter	Range	Mean (μ)	Standard deviation (σ)
Positive degree day factor for snow, α_s (mm water d ⁻¹ °C ⁻¹)	3.0 to 5.0	4.0	±1.2
Positive degree day factor for ice, α_i (mm water d ⁻¹ °C ⁻¹)	8.0 to 20.0	14.0	±6.9
Enhancement flow factor, f	1.0 to 5.0	3.0	±2.3
Geothermal heat flux, G (mW m ⁻²)	-61.0 to -38.0	-49.5	±13.3
Near surface lapse rate, L_G (°C km ⁻¹)	-8.2 to -4.0	-6.1	±2.4

1159

1160

1161

1162

1163

1164

1165

1166 **Table 2.** The orbital parameters (from Milankovitch theory) for four time snapshots between
 1167 140 and 120 ka (Berger and Loutre, 1991). Also shown for comparison are the parameters for
 1168 pre-industrial.

Time (ka)	Obliquity (°)	Eccentricity	Perihelion (day of yr)	<u>Max. 65°N June insolation anomaly (Wm⁻²)</u>
136	23.97	0.0367	35.1	<u>6.7</u>
130	24.25	0.0401	121.8	<u>70.0</u>
125	23.82	0.0423	200.0	<u>50.6</u>
120	23.04	0.0436	287.6	<u>-28.0</u>
0	23.45	0.0172	2.6	<u>0.0</u>

1169
 1170
 1171
 1172
 1173
 1174
 1175
 1176
 1177
 1178
 1179
 1180
 1181
 1182
 1183

1184 **Table 3.** Comparison of LIG temperature anomalies (in °C) derived from palaeo-proxy
 1185 reconstructions (Anderson et al., 2006) with the simulated maximum LIG summer
 1186 temperature anomalies from HadCM3. All locations described are shown on Fig. 5. The
 1187 values in parentheses brackets for comparison with ice core data on Greenland (NGRIP &
 1188 Renland) refer to the warmest annual precipitation-weighted temperatures. Values derived
 1189 from HadCM3 include $\pm 2\sigma$.

Location	Observed ΔT	Modelled ΔT
Greenland		
Central Greenland, NGRIP (75.1°N, 42.3°W)	5	4.2±1.1 (3.3)
E Greenland, Renland (71.3°N, 26.7°W)	5	4.3±1.9 (4.9)
E Greenland, Jamesonland (72.0°N, 23.0°W)	5	2.2±1.4
NW Greenland, Thule (76.0°N 68.0°W)	4	3.5±1.4
Canada		
Robinson Lake, Baffin Is. (63.0°N, 64.0°W)	5	1.4±1.4
Brother of Fog Lake, Baffin Is. (67.0°N, 63.0°W)	4	1.9±1.6
Fog Lake, N. Baffin Is. (67.2°N 63.3°W)	3-4	1.9±1.6
Flitaway Beds, Baffin Is. (70.0°N 75.0°W)	4-5	5.1±1.0
Amarok Lake, Baffin Is. (66.3°N 65.8°W)	5-6	3.4±1.2
Russia		
NE Siberia (Chakota region) (68.0°N 177.0°E)	4-8	2.6±1.5
Siberia (73.3°N 141.5°E)	4-5	1.7±1.5
European Russia (White Sea) (63.0°N 35.0°E)	4	3.6±1.5
Alaska		
Interior Alaska, Eva Creek (64.9°N, 147.9°W)	0-2	2.8±1.6
NW Alaska, Squirrel Lake (67.4°N, 160.7°W)	1-2	1.9±1.7

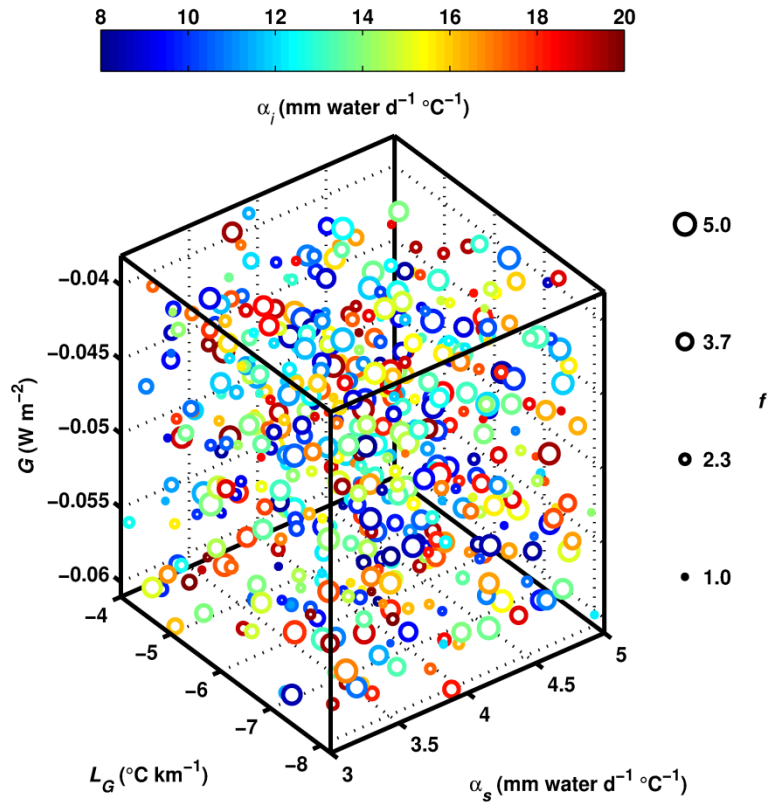
	NW Alaska, Ahaliorak Lake (68.0°N, 153.0°W)	1-2	2.7±1.7
	NW Alaska, Noatak Valley (68°N, 160°W)	0-2	1.9±1.7
	North Coast Alaska (70.0°N 150.0°W)	3	3.6±1.9
Norway	(60.2°N, 5°E)	2.9	1.3±1.2
Svalbard	78°N, 22°E	2-2.5	1.2±1.5
North Atlantic			
	JPC8 (61°N,28°W)	3-4	1.4±0.8
	NA87-25 (55.2°N,14.7°W)	1-2	0.9±1.3
	CH69-K9 (41°N, 47°W)	-1	1.9±1.3
	SU90-03 (40.5°N, 32.1°W)	0±1	1.8±1.1

1190

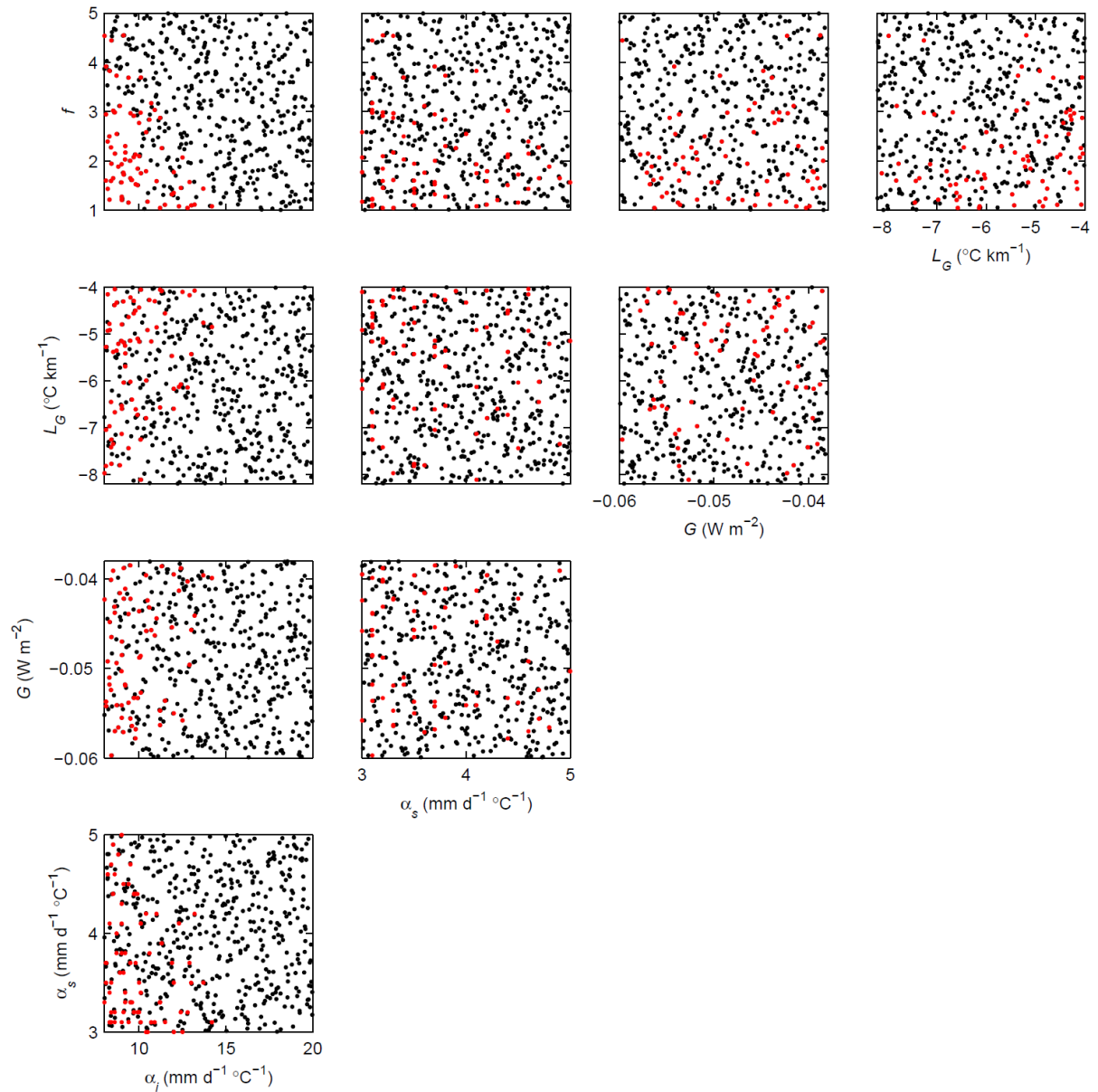
1191

1192

1193



1194



1195

1196

1197

1198

1199

1200

1201

1202

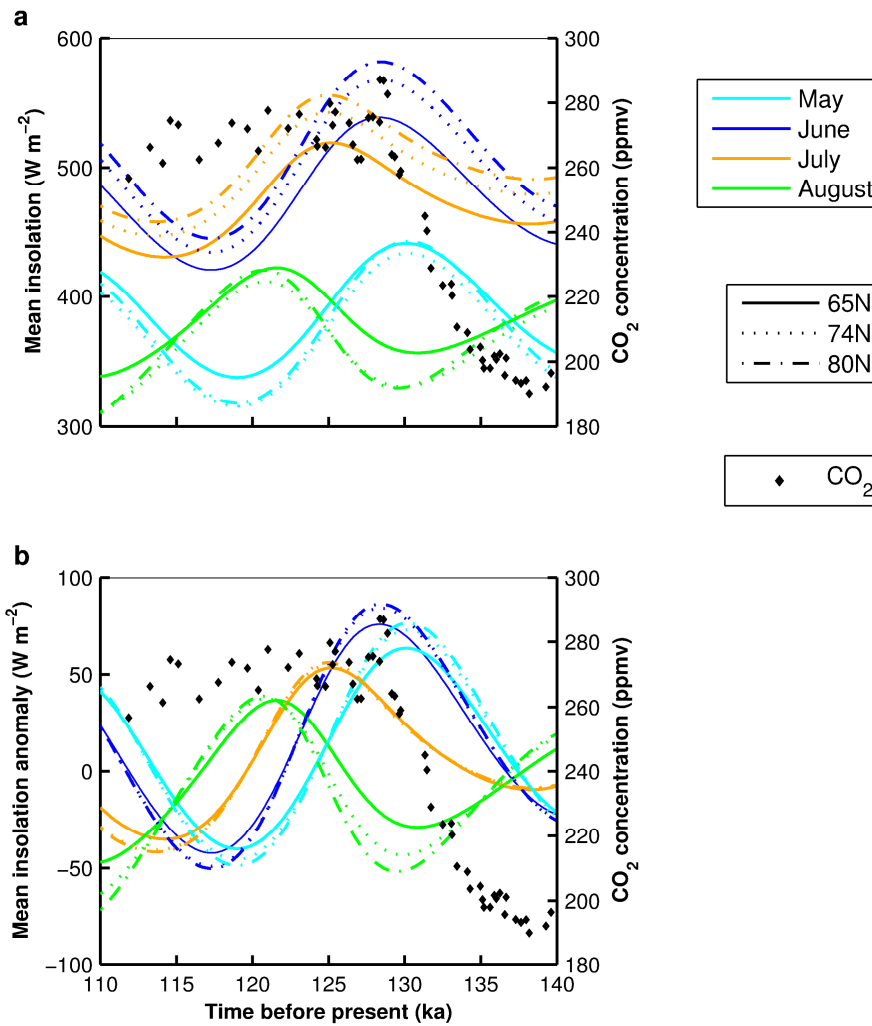
1203

1204

1205

1206

Figure 1. Distribution of 500 experiments produced by Latin-Hypercube Sampling. In three dimensions geothermal heat flux (G), Positive Degree Day (PDD) factor for snow (α_s) and atmospheric vertical lapse rate (L_G) are shown. In addition, for each experiment the PDD factor for ice (α_i) is shown in terms of the colour scale and the enhancement flow factor (f) in terms of the size of circle. Distribution of 500 Glimmer parameter experiments produced by Latin-Hypercube Sampling and projected onto two-dimensional slices through the five dimensional space. The parameters are as follows: geothermal heat flux (G), Positive Degree Day (PDD) factor for snow (α_s), the PDD factor for ice (α_i), the atmospheric vertical lapse rate (L_G) and the enhancement flow factor (f). The experiments highlighted in red are those which are valid for the LIG.



1207

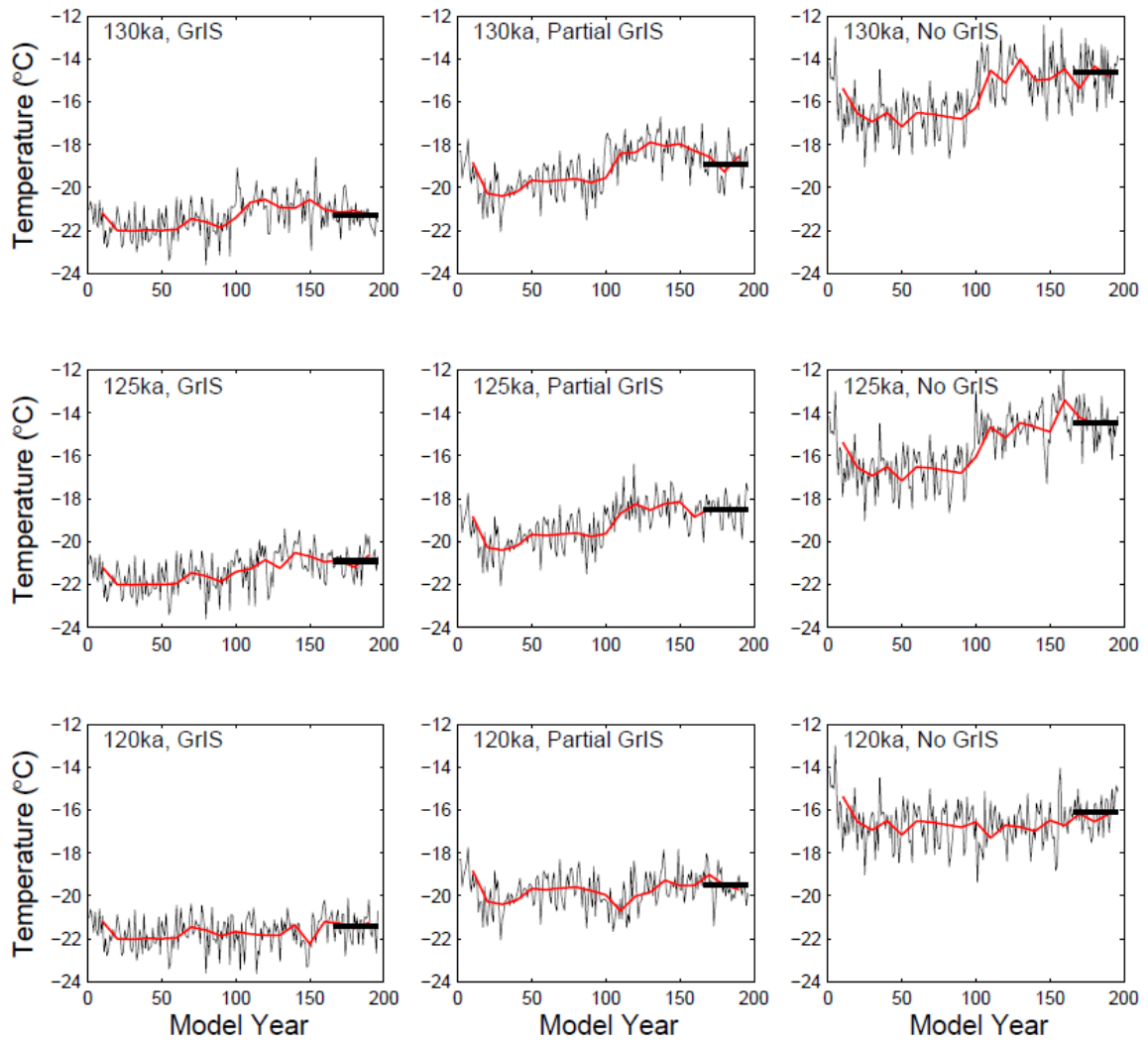
1208 **Figure 2.** Time series of LIG (a) insolation and (b) insolation anomaly relative to pre-
 1209 industrial over Greenland for the period 140 to 110ka. Insolation values are calculated using
 1210 the numerical solution of Laskar et al. (2004) [using the Julian calendar](#). Also overlain is CO₂
 1211 concentration (ppmv) from the composite record of Lüthi et al. (2008) based on data from
 1212 Petit et al. (1999) and Pépin et al. (2001) for the LIG (they are on the EDC3 gas age scale
 1213 (Loulergue et al., 2007)). The colours correspond to the following months: May (light blue),
 1214 June (blue), July (orange) and August (green). Line styles refer to different latitudes over
 1215 Greenland.

1216

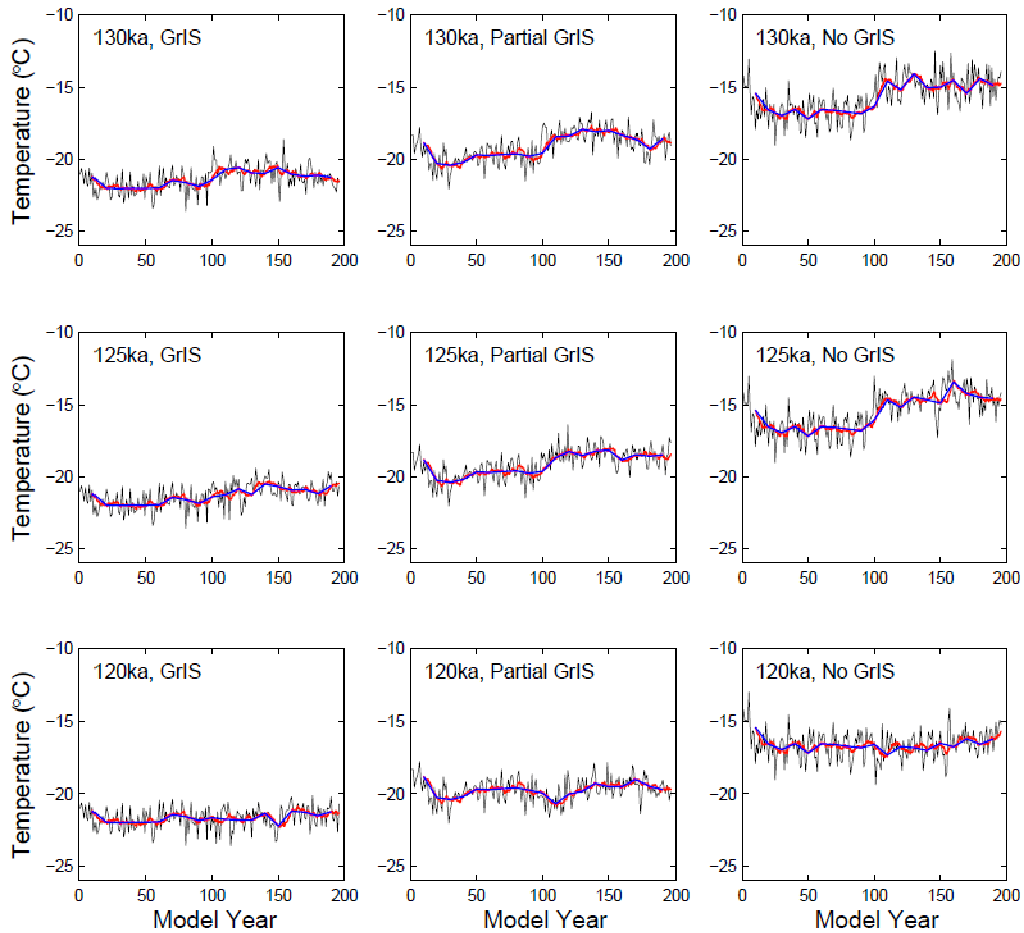
1217

1218

1219



1220



1221

1222 **Figure 3.** Near-surface Greenland temperature time-series for the three LIG snapshots with a
 1223 GrIS, partial GrIS and without a GrIS included. The first 100 years represent pre-industrial
 1224 greenhouse and orbital conditions. The last 100 years are the temperature response to
 1225 changed orbital parameters. The black line is the annual mean ~~and the~~; red line is the 10 year
 1226 ~~running average and the blue line is the~~ 10 year mean. The thick black horizontal line shows
 1227 the 30-year annual Greenland temperature average.

1228

1229

1230

1231

1232

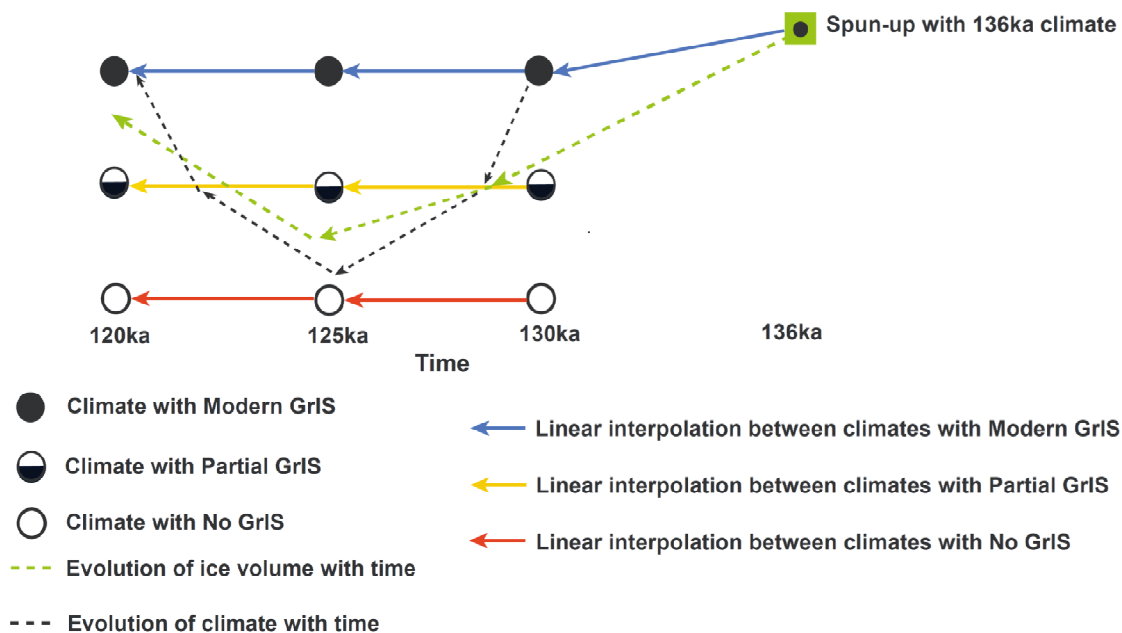
1233

1234

1235

1236

1237



1238

1239 **Figure 4.** Illustration of the coupling methodology between climate and ice sheet for the LIG.
 1240 Simulations are run for a total of 16,000 model years, initiated with a climate representative
 1241 of 136-ka (GrIS included). The transient climate evolves simultaneously with the ice sheet
 1242 model. The climate is linearly interpolated from 136 to 130-ka. From 130-ka to 120-ka the
 1243 climate evolves (black dashed arrow shows an example) according to a weighting towards
 1244 either a transient climate where there is a modern day GrIS (black filled circles), one where
 1245 there is a partial GrIS (black half filled circles) and where the GrIS is removed (black open
 1246 circles). The weighting is based on the ratio of the previous years' ice volume relative to the
 1247 ice volume at 130-ka. The green dashed arrow shows schematically the evolution of the ice
 1248 sheet volume. See text for more details and equations.

1249

1250

1251

1252

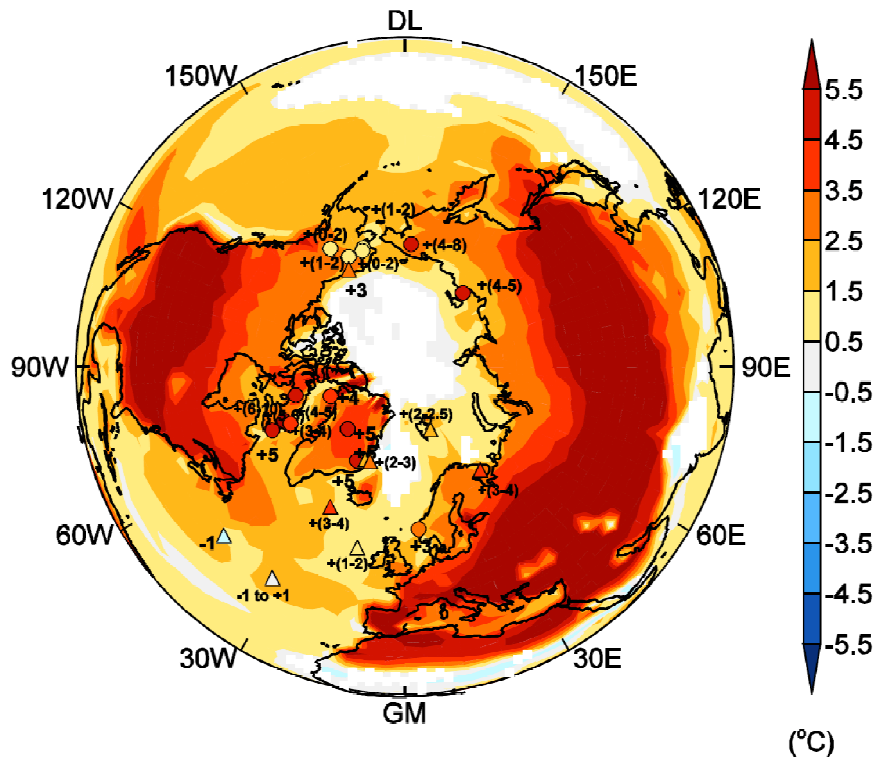
1253

1254

1255

1256

1257



1258

1259 **Figure 5.** Simulated maximum LIG Arctic summer (June, July, August) temperature anomaly
 1260 relative to pre-industrial. Overlain is the maximum observed LIG summer temperature
 1261 anomalies from palaeo temperature proxies (terrestrial [circles] and marine [triangles])
 1262 (Anderson et al., 2006; Kaspar et al., 2005). White regions are not statistically significant (at
 1263 the 95% confidence interval).

1264

1265

1266

1267

1268

1269

1270

1271

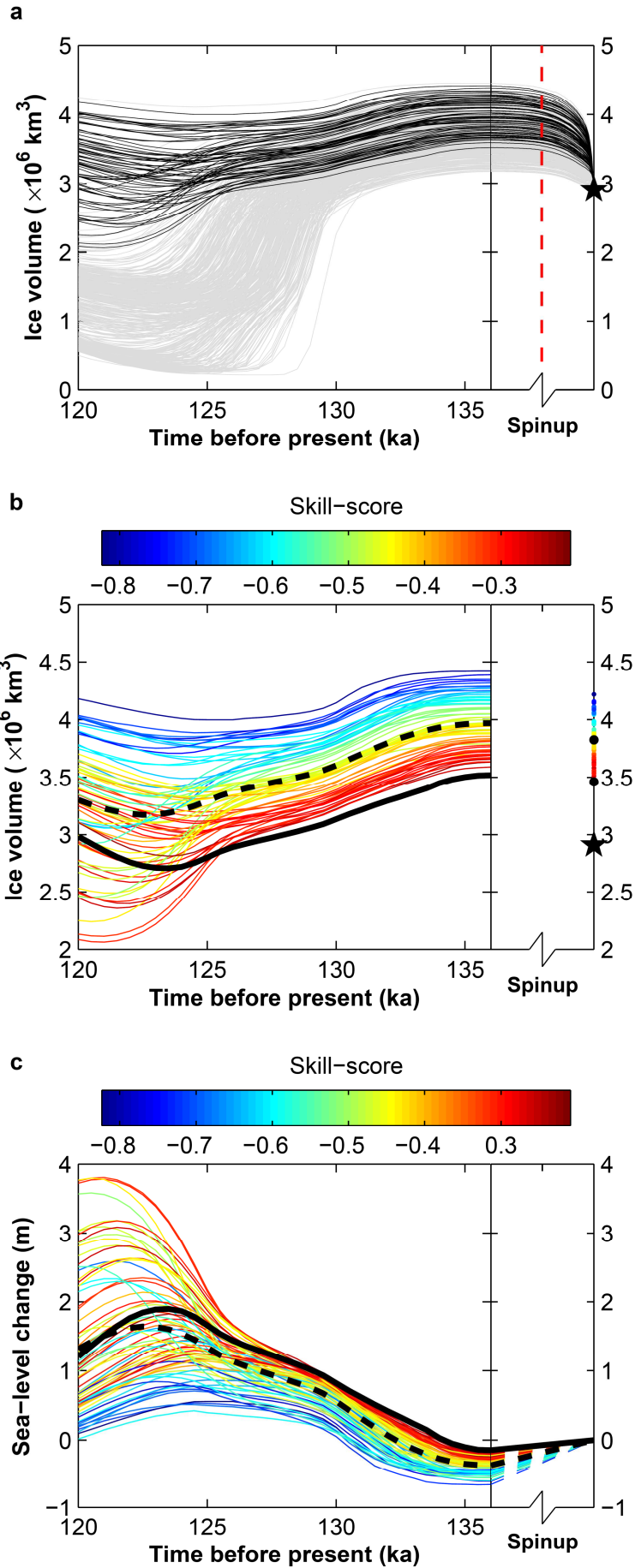
1272

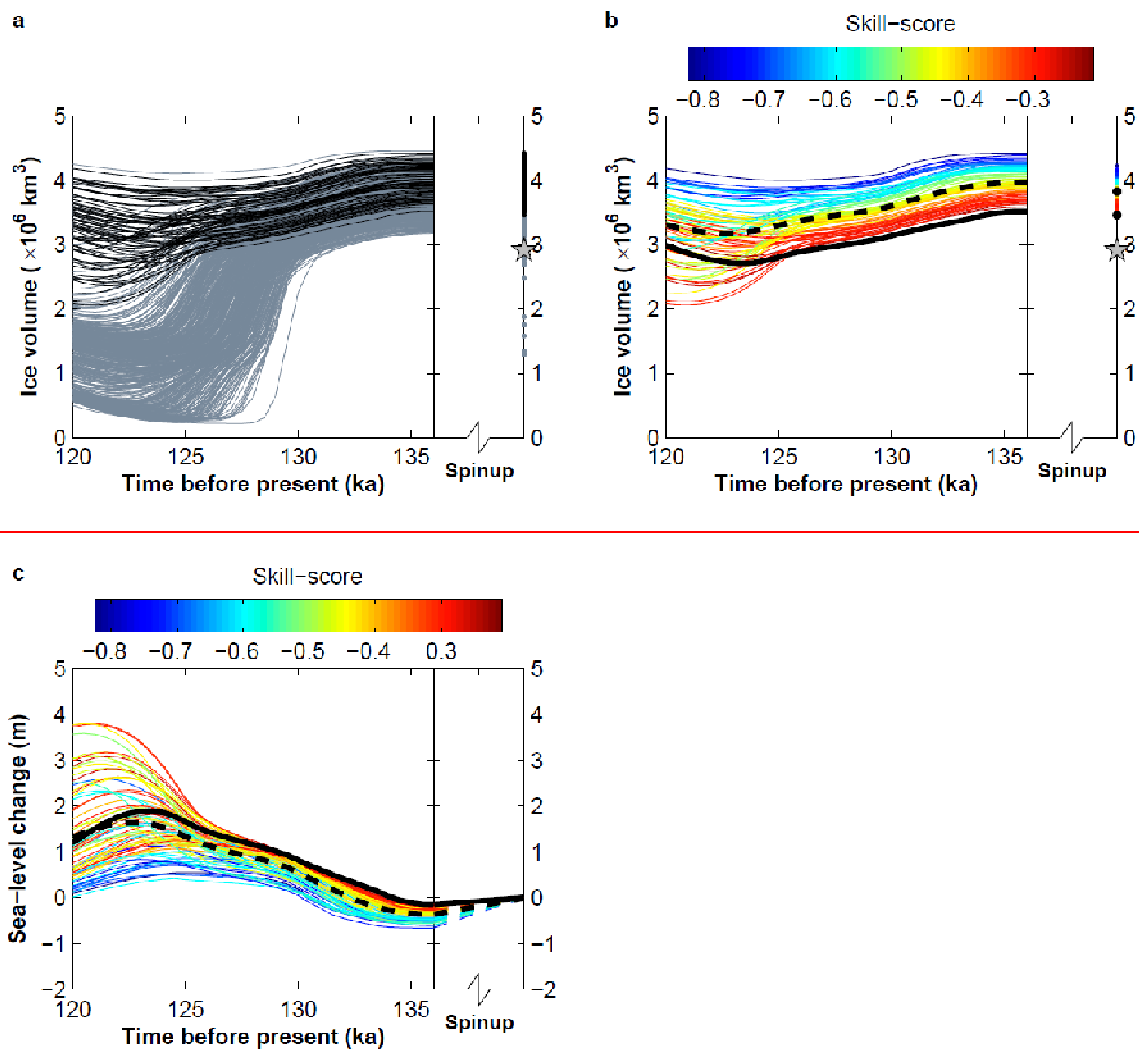
1273

1274

1275

1276





1278

1279 **Figure 6.** Simulated LIG GrIS evolution from the ensemble of simulations. (a) GrIS volume
 1280 evolution for all 500 configurations. Black lines show experiments where ice persisted at
 1281 NGRIP and Summit. (b) Ice volume change for 73 selected simulations according to
 1282 constraints at the Summit and NGRIP cores. (c) Change in GrIS sea-level contribution
 1283 relative to present day for the selected simulations. Also shown on (b) and (c) is the skill-
 1284 score for the simulated modern day GrIS (see equation (7)) on the right hand axis. The star
 1285 represents the modern day observed GrIS volume. The solid black line represents the
 1286 simulation with the highest skill score for the modern day GrIS. The dashed black line
 1287 represents the average for all accepted simulations. Simulated LIG GrIS evolution from the
 1288 ensemble of simulations. (a) GrIS volume evolution for all 500 configurations. Black lines
 1289 show experiments where ice persisted at NGRIP and Summit ice core locations. Also shown
 1290 is the modern day spin-up of 50,000 years followed by a further 50,000 years spin-up with a
 1291 136ka climatology (separated by red dashed line). (b) Ice volume change for 73 selected

1292 simulations according to constraints at the Summit and NGRIP cores. (c) Change in GrIS sea-
1293 level contribution relative to present day for the selected simulations. Also shown on (b) and
1294 (c) is the skill-score for the simulated modern day GrIS (see Eq. (7)) with the simulated
1295 modern day ice volume also shown on the right-hand axis of (b). The star represents the
1296 modern day observed GrIS volume (Bamber et al., 2001). The solid black line represents the
1297 simulation with the highest skill-score for the modern day GrIS. The dashed black line
1298 represents the average for all accepted simulations.

1299

1300

1301

1302

1303

1304

1305

1306

1307

1308

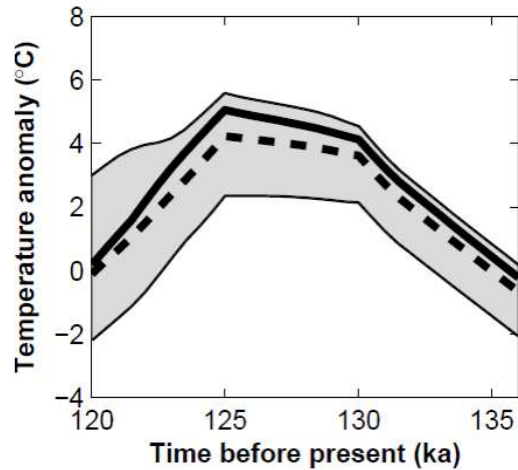
1309

1310

1311

1312

1313



1314

1315 **Figure 7.** LIG surface temperature anomaly (relative to pre-industrial) evolution, averaged
 1316 over the Glimmer model domain for the valid simulations. Included is the change in
 1317 temperature due to a lapse rate correction as a result of changing elevation as the ice sheet
 1318 changes in response to the climate forcing. The solid back line represents the accepted
 1319 simulation with the highest skill-score for the modern day GrIS. The dashed back line
 1320 represents the average for all accepted simulations.

1321

1322

1323

1324

1325

1326

1327

1328

1329

1330

1331

1332

1333

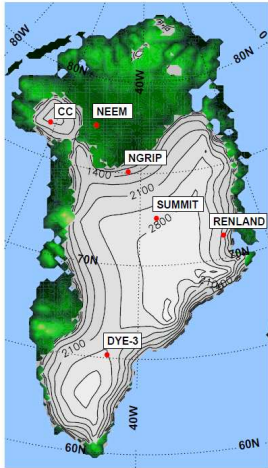
1334

1335

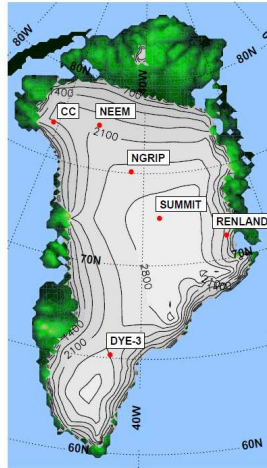
1336

1337

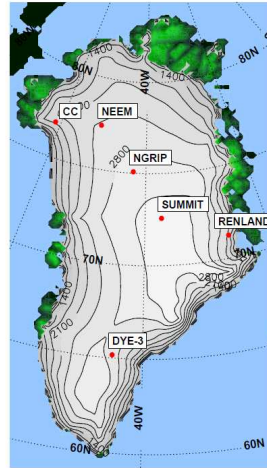
a



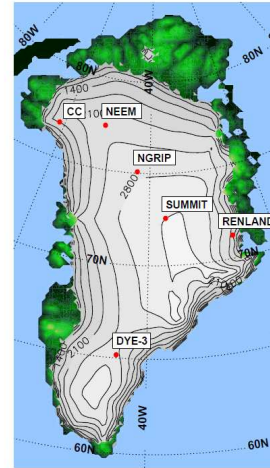
b



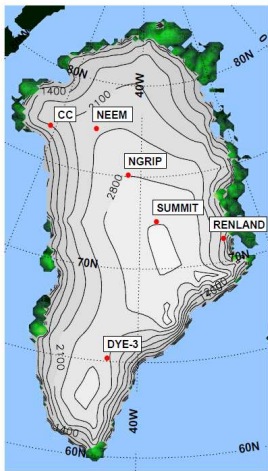
c



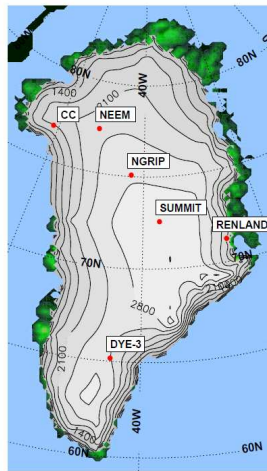
d



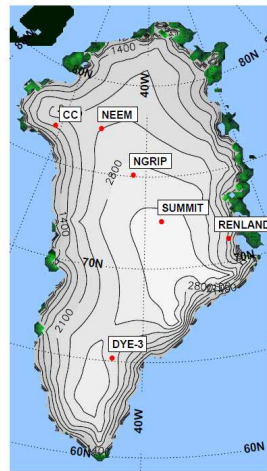
e



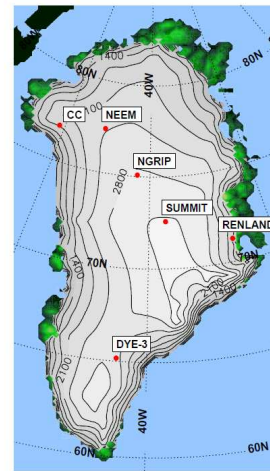
f

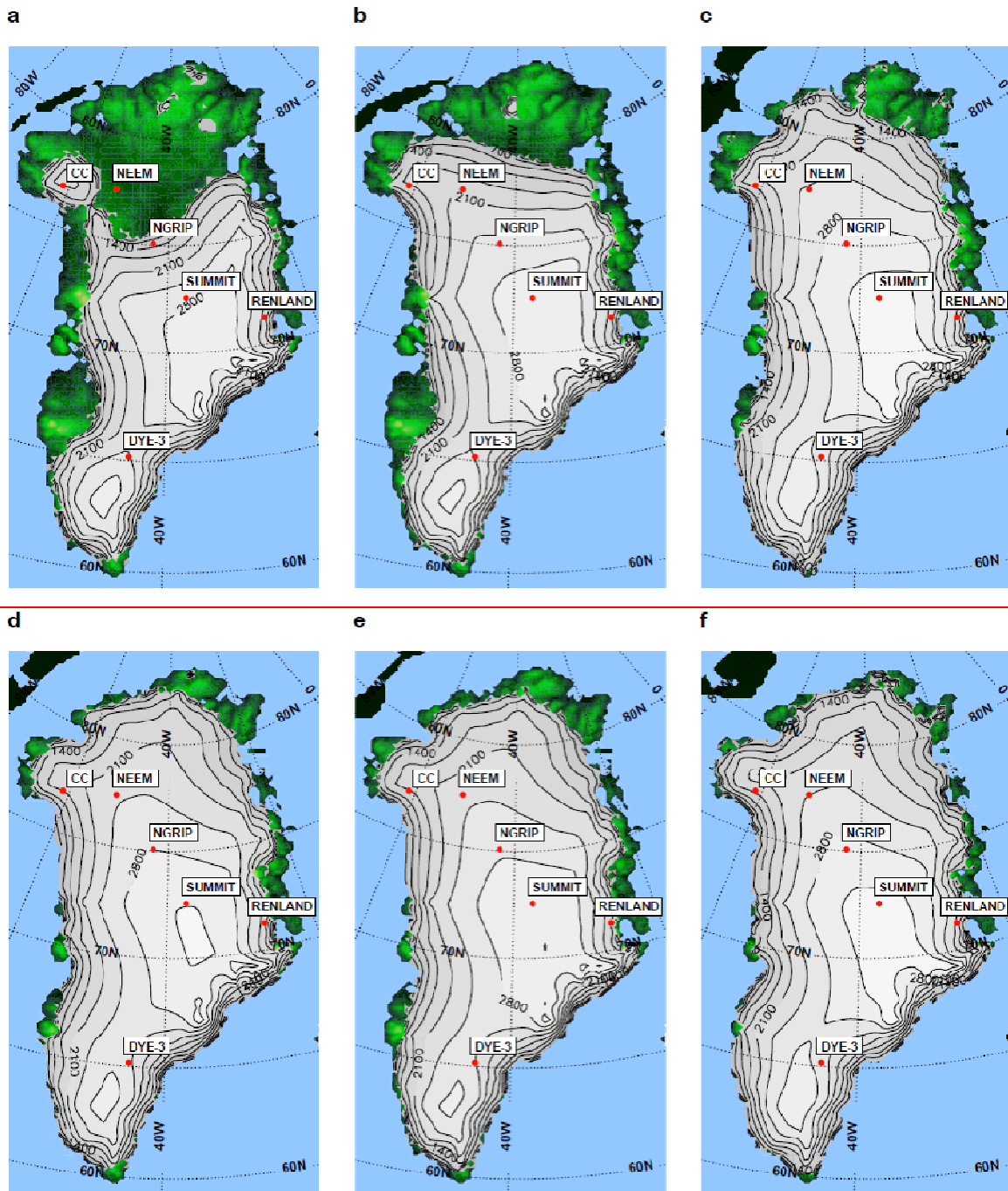


g



h





1339

1340

1341

1342

1343

1344

1345

1346

Figure 8. ~~Simulated range from the selected experiments for the minimum GrIS geometry during the LIG (a-c) and their respective modern day GrIS geometries (d-f). (a) Extent of the GrIS for the maximum contribution (at 121.0 ka) to LIG sea-level change (+3.8 m), (b) the extent of the most likely contribution (at 123.5 ka) to LIG sea-level change (+1.5 m) and (c) the extent of the minimum contribution (at 125ka) to LIG sea-level change (+0.4 m). Red spots show Greenland ice-core locations. Simulated range from the selected experiments for the minimum GrIS geometry during the LIG (a-d) and their respective modern day GrIS~~

1347 geometries (e-h). (a) Extent of the GrIS for the maximum contribution (at 121.0ka) to LIG
1348 sea-level change (+3.8 m), (b) the extent of the most likely contribution (at 123.5ka) to LIG
1349 sea-level change (+1.5 m), (c) the extent of the minimum contribution (at 125ka) to LIG sea-
1350 level change (+0.4 m) and (d) minimum extent for the ensemble member with a maximum
1351 GrIS contribution to LIG rise closest to the peak of the probability density plot in Fig. 10a
1352 (+1.5 m). Red spots show Greenland ice-core locations.

1353

1354

1355

1356

1357

1358

1359

1360

1361

1362

1363

1364

1365

1366

1367

1368

1369

1370

1371

1372

1373

1374

1375

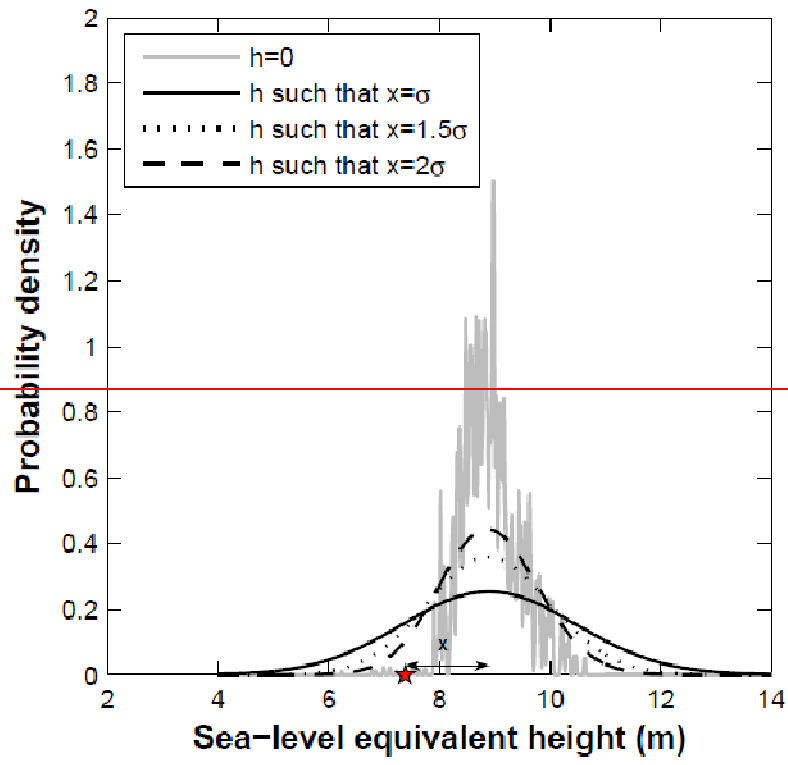
1376

1377

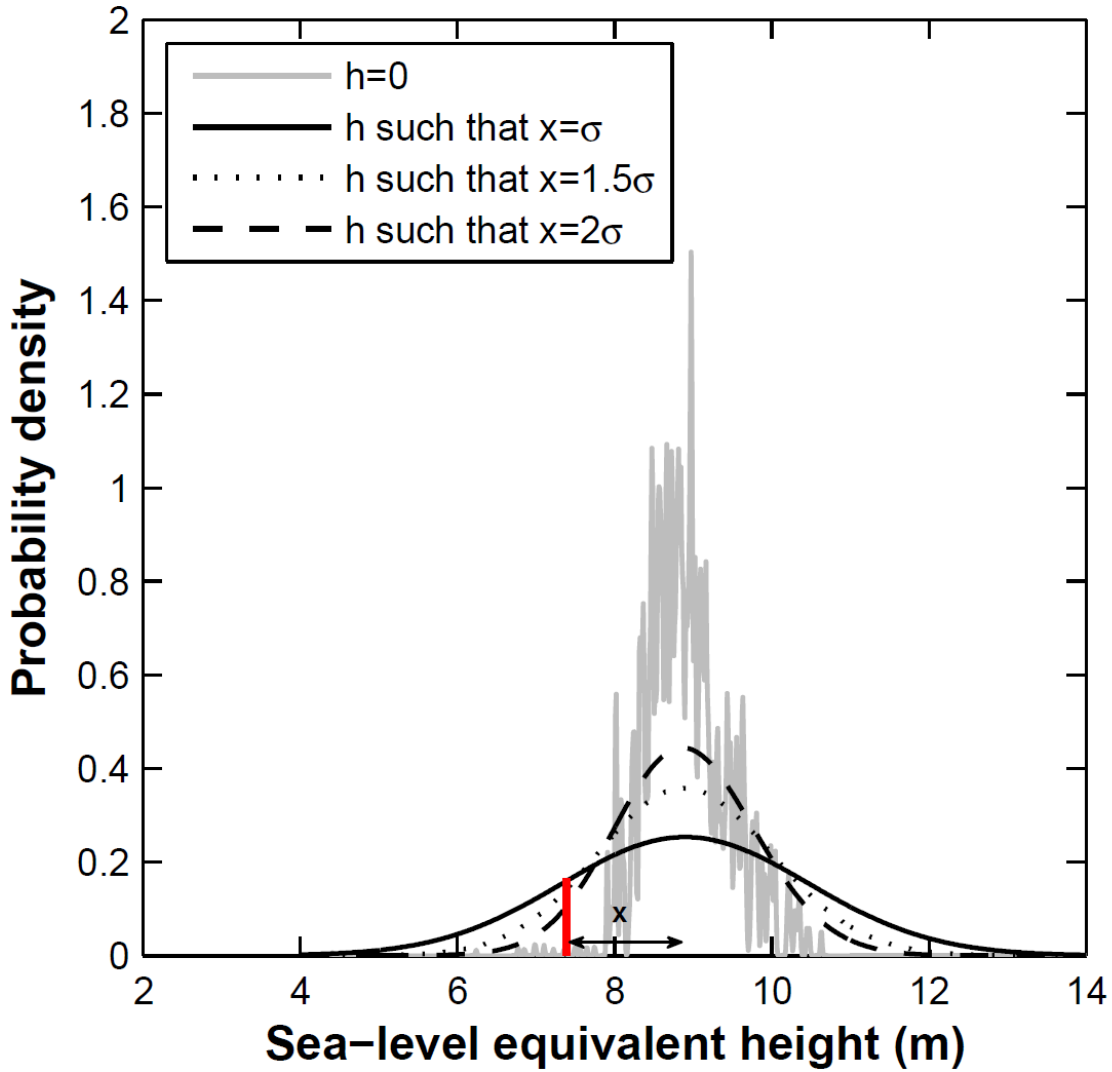
1378

1379

1380



1381



1382

1383 **Figure 9.** Probability density functions constructed from the 500 member ensemble of
 1384 modern day GrIS sea-level equivalent height. The red linestar denotes the observation from
 1385 Bamber et al. (2001). The distance x represents the difference between the mean of the
 1386 ensemble and the observation. The grey line shows the probability density function with no
 1387 smoothing. The black lines show the cases where the smoothing parameter, h , results in a
 1388 probability density function where $x=\sigma$ (dashed), $x=1.5\sigma$ (dotted) and $x=2\sigma$ (solid).

1389

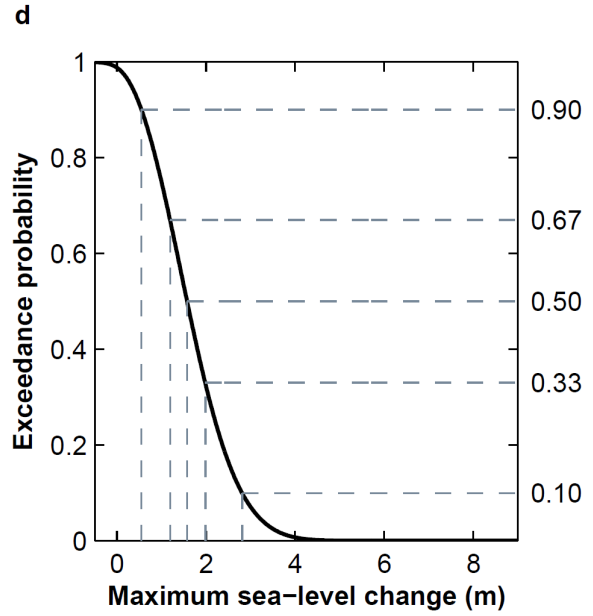
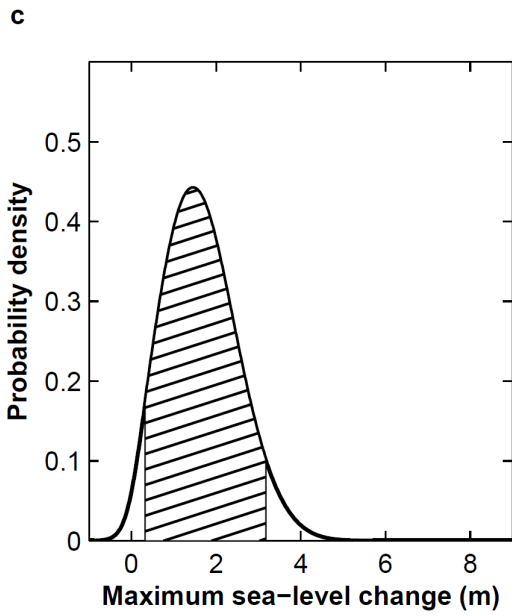
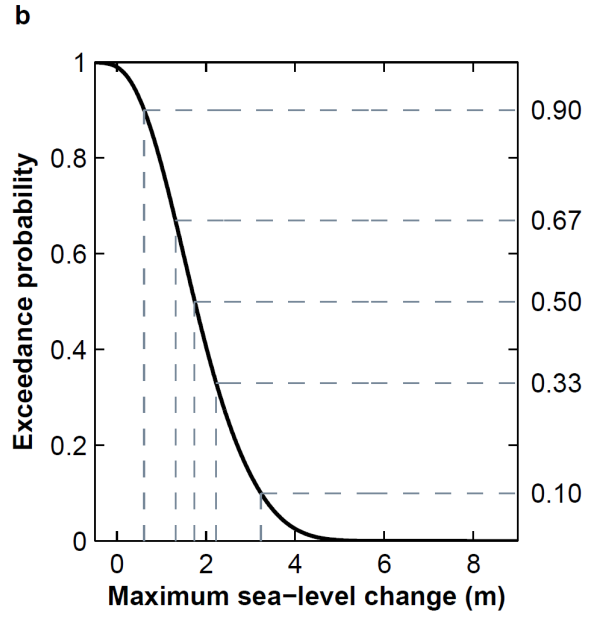
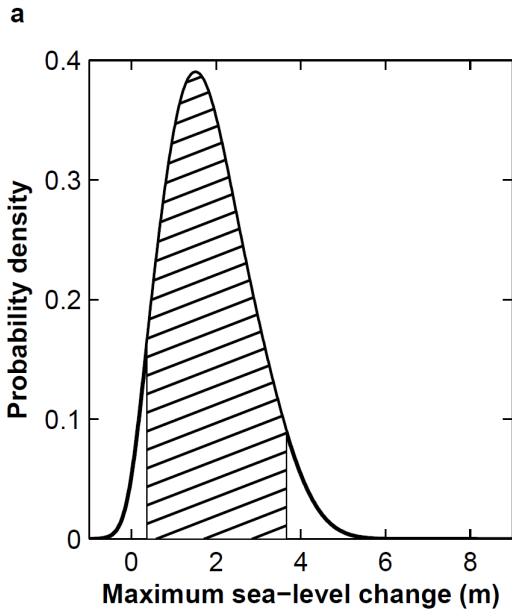
1390

1391

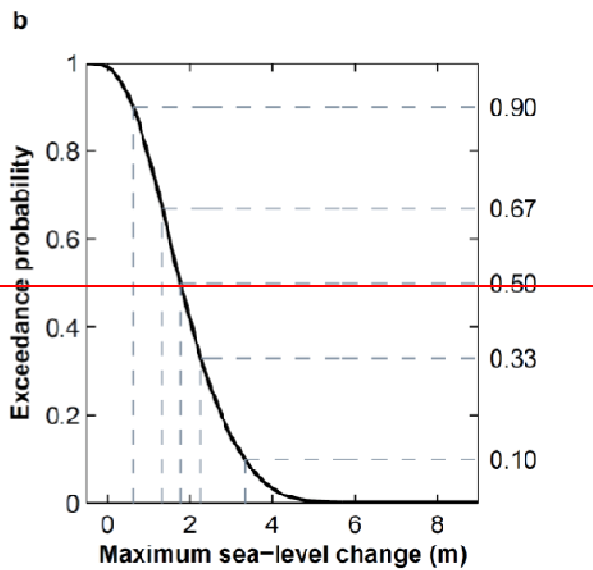
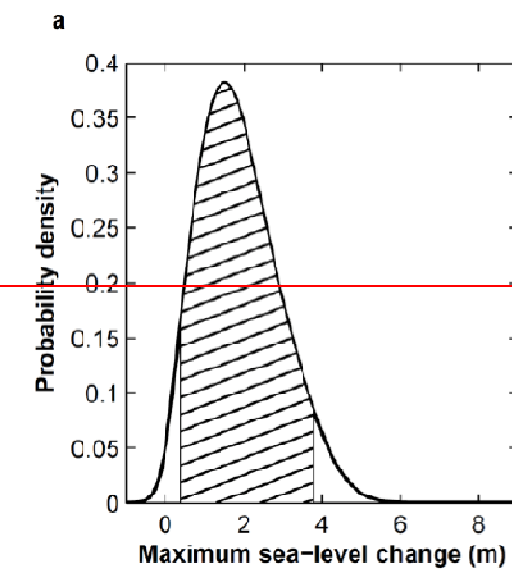
1392

1393

1394



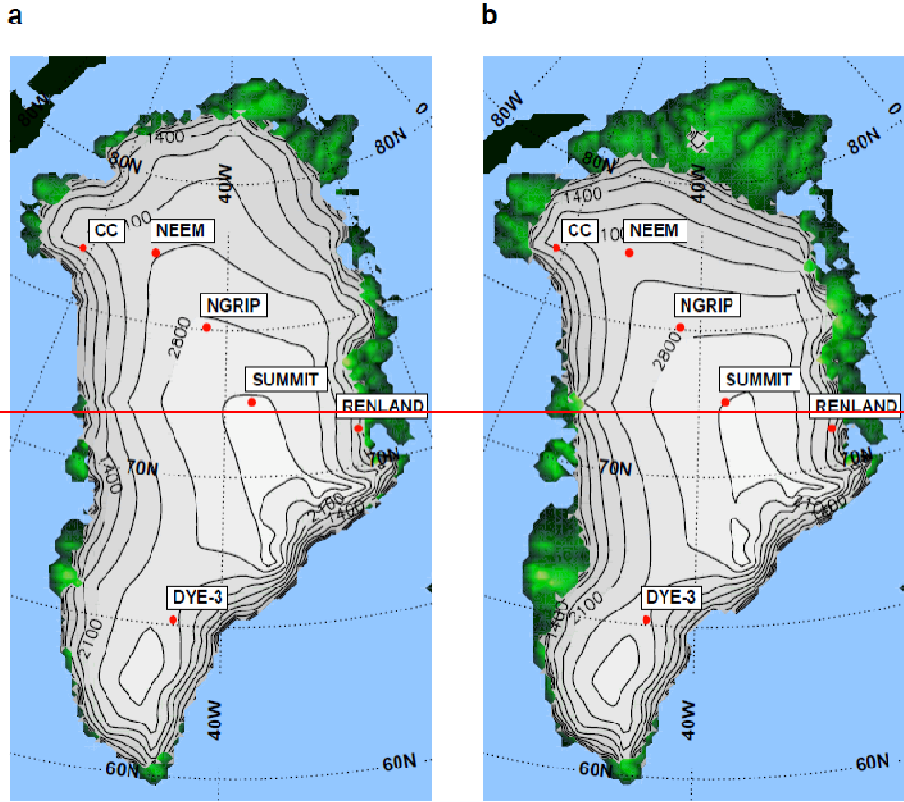
1395



1396

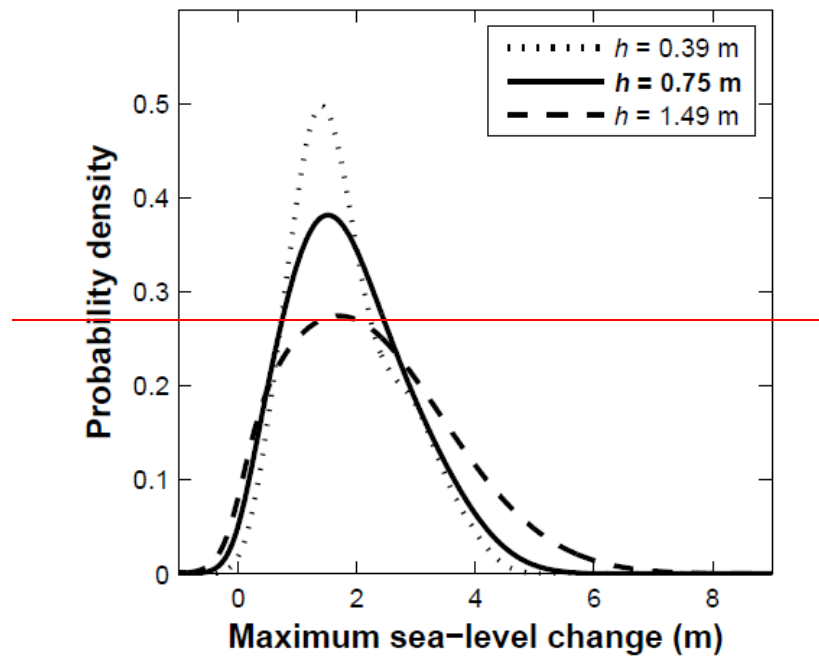
1397
1398
1399
1400
1401
1402
1403
1404
1405
1406
1407
1408
1409
1410
1411
1412
1413
1414
1415
1416
1417
1418
1419
1420
1421
1422
1423
1424
1425
1426
1427
1428
1429
1430

Figure 10. ~~GrIS maximum contribution to sea-level change during the LIG. (a) Probability density plot. The hashed region denotes the 90% confidence interval (0.3 to 3.6 m). (b) Exceedance values for the probability distribution. A probabilistic assessment of the GrIS maximum contribution to sea-level change during the LIG without the NEEM ice core constraint (a-b) and with the assumption ice is present throughout the LIG at the NEEM ice core (c-d). (a) Probability density plot. The hashed region denotes the 90% confidence interval (0.3 to 3.6 m). (b) Exceedance values for the probability distribution. (c) Probability density plot when the NEEM ice core data is included (90% confidence interval: 0.3 to 3.2 m). (d) Exceedance values for the probability distribution with the NEEM ice core data included. There is a 90% probability of a GrIS contribution exceeding 0.6 m during the LIG, a 67% probability of exceeding 1.2 m, a 50% probability of exceeding 1.6 m, a 33% probability the contribution exceeded 2.0 m and a 10% probability it exceeded 2.8 m.~~



1431
 1432
 1433
 1434
 1435
 1436
 1437
 1438
 1439
 1440
 1441
 1442
 1443
 1444
 1445
 1446
 1447
 1448
 1449

Figure 11. Simulated minimum GrIS extent for the ensemble member with a maximum GrIS contribution to LIG rise closest to the peak of the probability density plot in Fig. 10a. (a) Modern-day GrIS extent and (b) the minimum GrIS extent during the LIG for a contribution of 1.5 m to LIG sea level rise.



1450

1451

1452

1453

1454

1455

1456

1457

1458

1459

1460

1461

1462

1463

1464

1465

1466

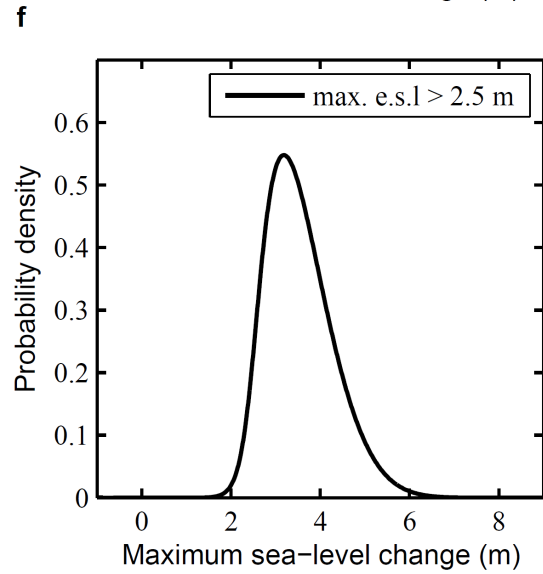
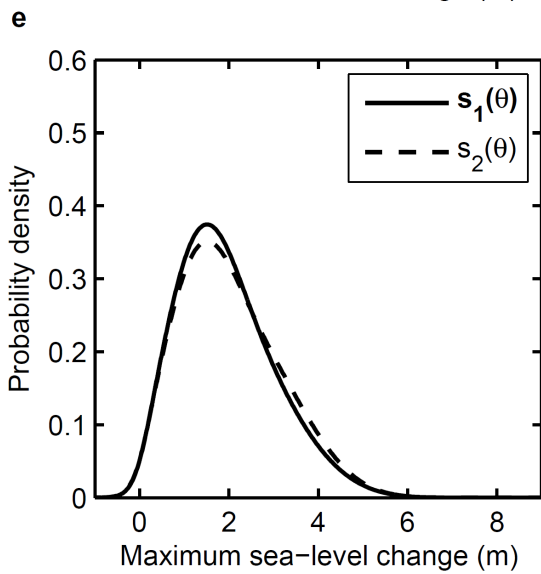
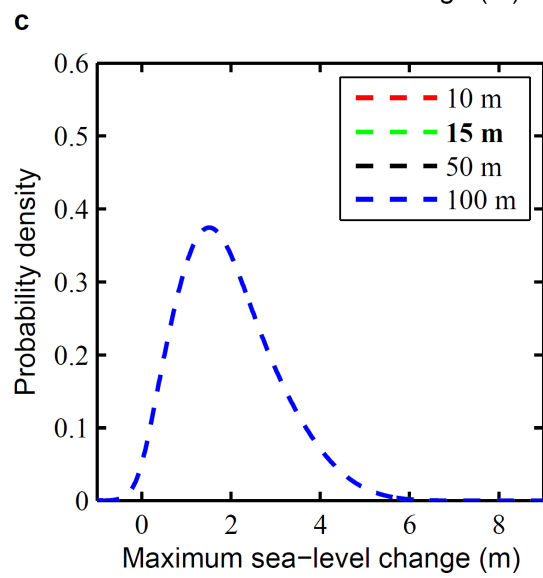
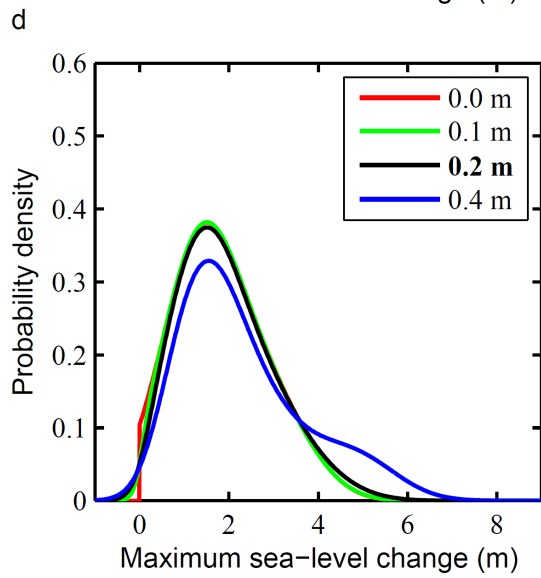
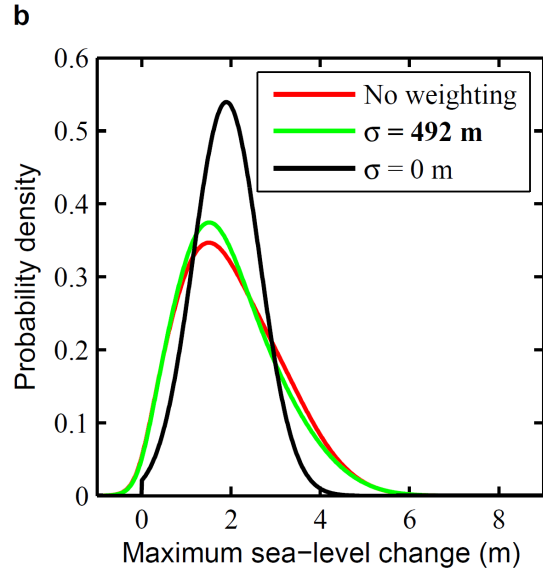
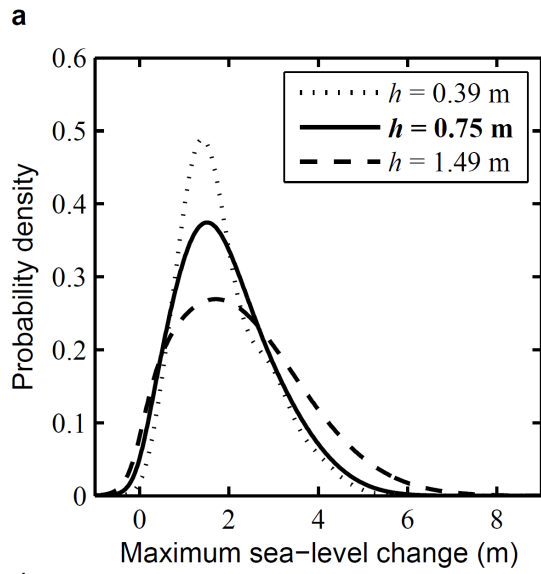
1467

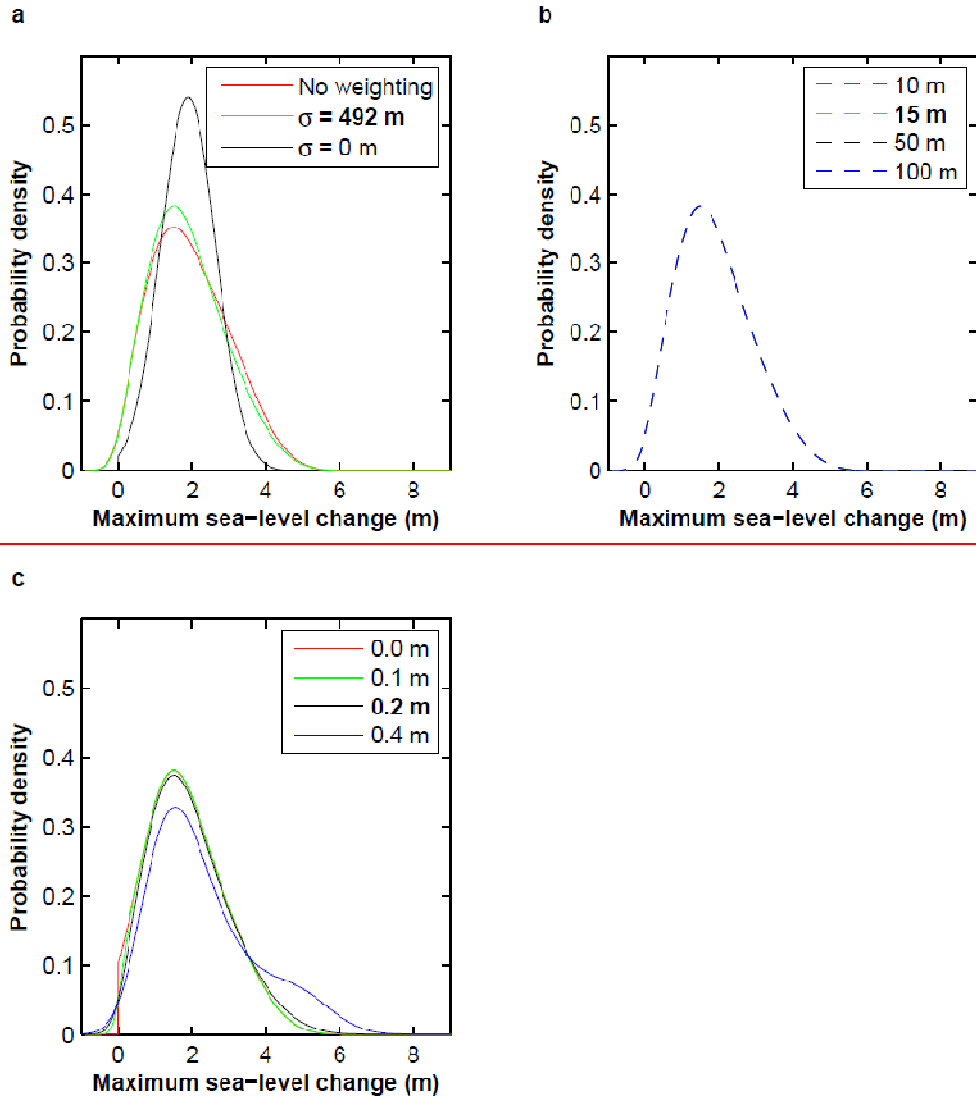
1468

1469

1470

Figure 12. Sensitivity of the LIG GrIS sea-level contribution probability density function to the Kernel smoothing parameter, h . Dotted line: optimal smoothing parameter according to equation (13), Solid line: smoothing parameter where modern day observation is 2σ from the ensemble mean (chosen as the most plausible case). Dashed line: smoothing parameter where modern day observation is 1σ from the ensemble mean.

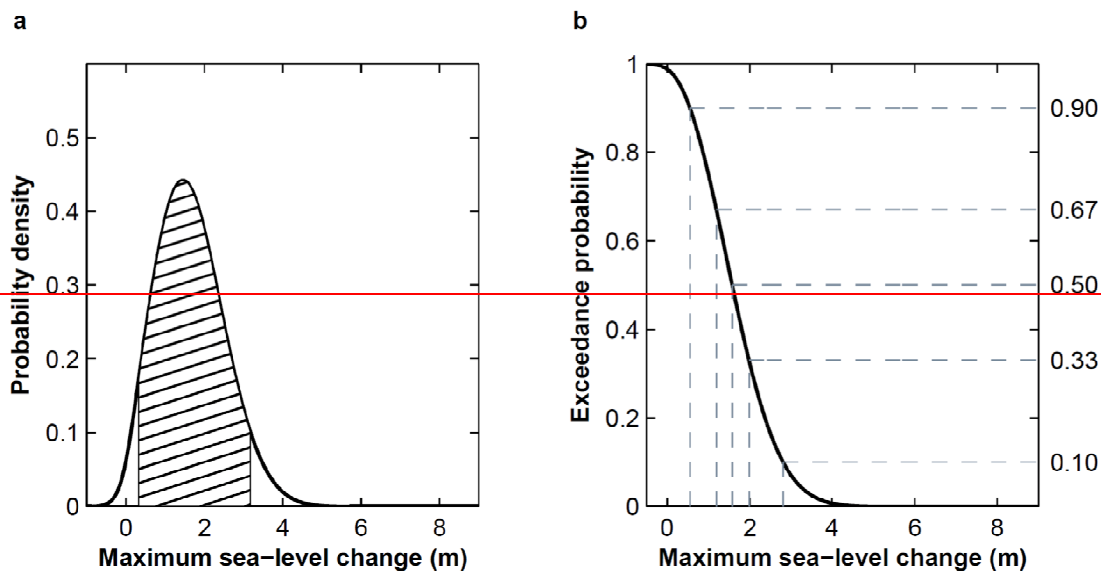




1472

1473 **Figure 11 Figure 13.** Sensitivity of the probability density function of the GrIS maximum
 1474 contribution to sea-level change during the LIG to (a) the model error, σ , in equation (7), (b)
 1475 observational ice thickness error ($\tau = 10, 15, 50$ and 100 m) from the Bamber et al. dataset
 1476 (2001) and (c) the logistic function given by equation (10) ($l_w = 0.0, 0.1, 0.2$ and 0.4 m). The
 1477 parameters highlighted in bold are those used for the most plausible case shown in Fig.
 1478 10. Sensitivity of the LIG GrIS sea-level contribution probability density function to (a) the
 1479 kernel smoothing parameter, h . Dotted line: optimal smoothing parameter according to Eq.
 1480 (13), Solid line: smoothing parameter where modern day observation is 2σ from the ensemble
 1481 mean (chosen as the most plausible case). Dashed line: smoothing parameter where modern
 1482 day observation is 1σ from the ensemble mean. (b) The model error, σ , in Eq. (7). (c)
 1483 Observational ice thickness error ($\tau = 10, 15, 50$ and 100 m) from the Bamber et al. dataset
 1484 (2001). (d) The logistic function given by Eq. (10) ($l_w = 0.0, 0.1, 0.2$ and 0.4 m). (e)

1485 Comparison of two different methods of calculating the skill-score such that $s_1(\theta)$ takes into
 1486 account the error in ice thickness at each grid-point while $s_2(\theta)$ uses the average ice thickness
 1487 of the whole ice sheet. The parameters highlighted in bold are those used for the most
 1488 plausible case shown in Fig. 10a. (f) The resultant probability density function (using the
 1489 default parameters) when the constraint that the GrIS contributed at least 2.5 m to global sea
 1490 level from Kopp et al. (2009) is taken into account.



1495
 1496
 1497 **Figure 14.** A probabilistic assessment of the GrIS maximum contribution to sea level change
 1498 during the LIG, assuming ice is present throughout the LIG at the NEEM ice core. (a)
 1499 Probability density plot. The hashed region denotes the probability of the contribution from
 1500 the GrIS being between 0.3 and 3.2 m (90% confidence interval). (b) Exceedance values for
 1501 the probability distribution. There is a 90% probability of a GrIS contribution exceeding 0.6
 1502 m during the LIG, a 67% probability of exceeding 1.2 m, a 50% probability of exceeding 1.6
 1503 m, a 33% probability the contribution exceeded 2.0 m and a 10% probability it exceeded 2.8
 1504 m. An ensemble of 500 simulations weighted according to their skill score for modern day
 1505 ice thickness and the presence of ice at NGRIP, Summit and NEEM core locations are used.
 1506 They are also weighted according to a five dimensional Gaussian fitted to the ice sheet model

1507 | ~~parameter distributions. The probability density function is constructed using a Kernel~~
1508 | ~~density estimator with a window width of 0.75 m.~~

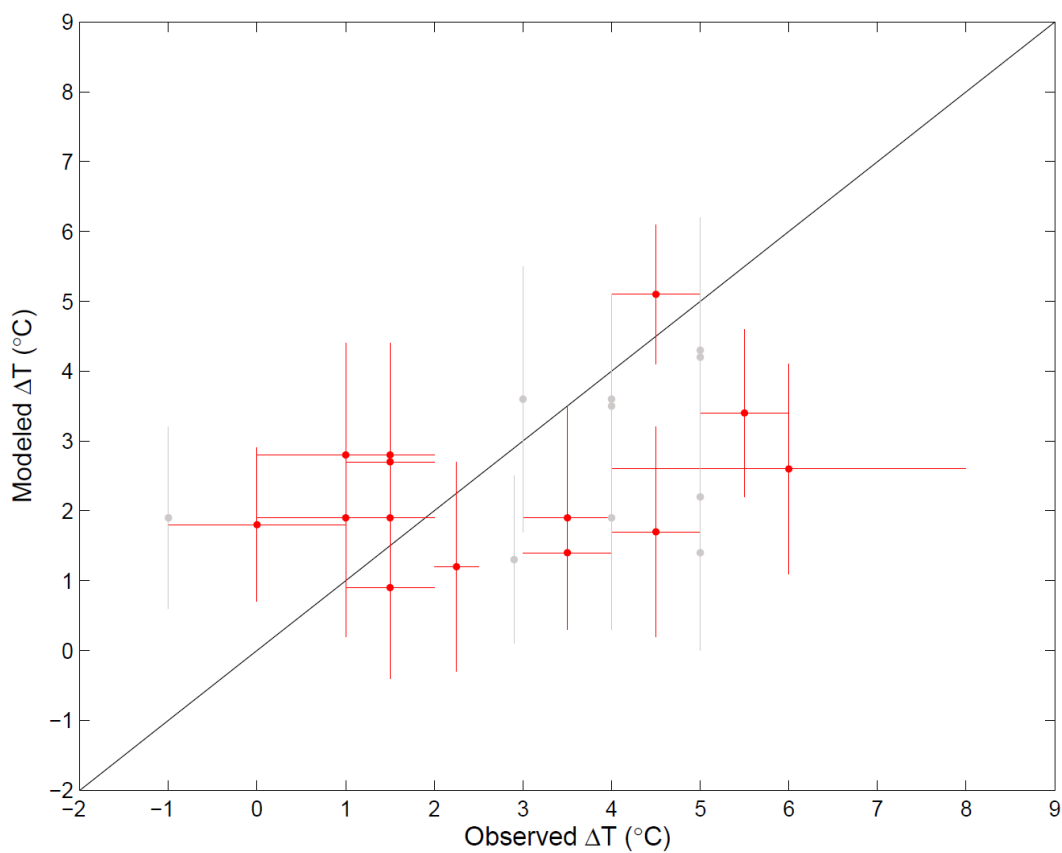
1509

1510 **Supplementary Information for: Quantification of the Greenland ice sheet**
1511 **contribution to Last Interglacial sea-level rise**

1512 **Emma J. Stone, Daniel J. Lunt, James D. Annan and Julia C. Hargreaves**

1513

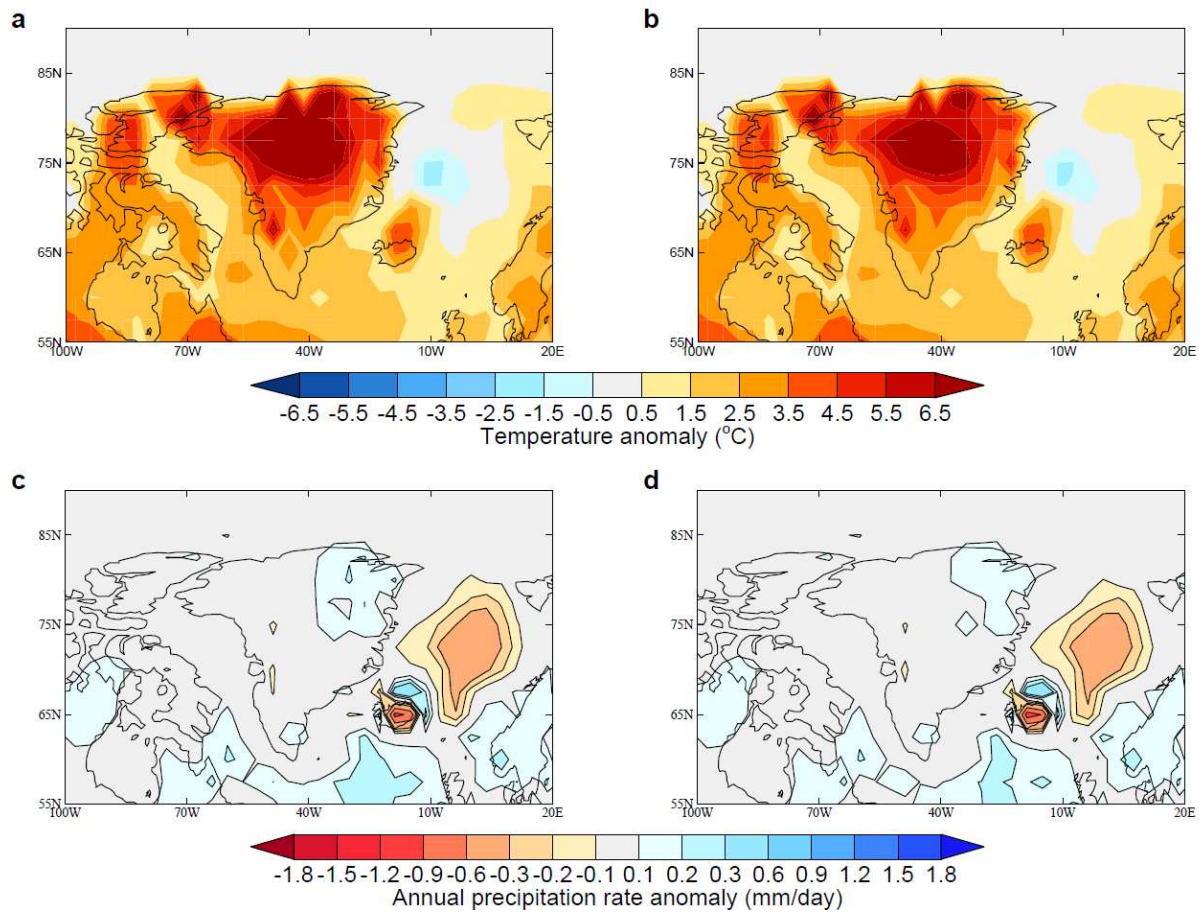
1514



1515

1516 **Figure S1.** LIG maximum summer high latitude Northern Hemisphere modelled temperature
1517 anomalies compared with temperature anomalies derived from palaeo-proxy reconstructions.
1518 The model simulation is the 130ka HadCM3 experiment with a fixed present day GrIS.
1519 Uncertainty is shown by the vertical and horizontal lines for each data point and in the case of
1520 the modelled temperature changes this is 2σ . Those data points which only included model
1521 uncertainty are coloured grey (see Table 3 for the location coordinates).

1522



1523

1524 **Figure S2.** Temperature and precipitation anomaly forcings derived from HadCM3
 1525 according to the coupling methodology described in Sect. 2.3 for the time at which minimum
 1526 ice volume is reached (a, c) and the time at which the average Greenland maximum
 1527 temperature anomaly is reached (b, d) for the palaeo-constrained simulation with the highest
 1528 skill-score.

1529

1530

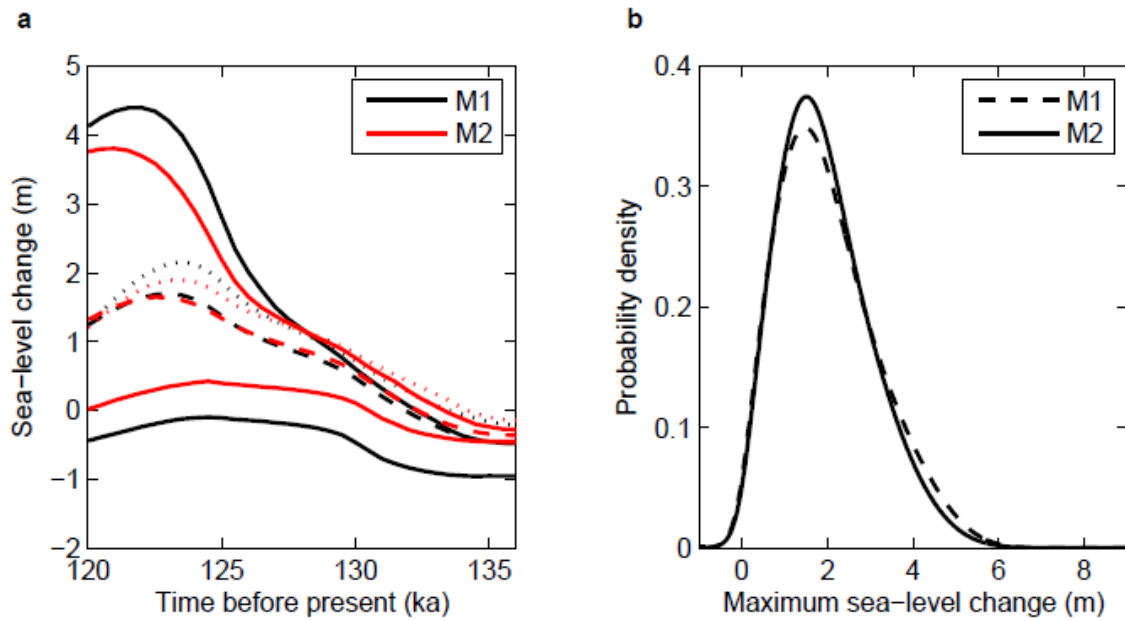
1531

1532

1533

1534

1535



1536

1537

1538 **Figure S3.** A comparison of LIG sea-level between coupling using two GrIS states (ice-
 1539 covered and ice-free: M1) and coupling with three GrIS states (ice-covered, partially covered
 1540 and ice-free: M2). a) Comparison of sea-level change between M1 and M2. The solid lines
 1541 are the minimum and maximum sea-level change from the ensemble. The dashed line refers
 1542 to the average of all accepted experiments and the dotted line shows the experiment with the
 1543 highest skill for modern day. b) Comparison of the probability density functions for
 1544 maximum LIG sea-level change for M1 and M2.